MTZ worldwide 9/2012
http://www.mtz-worldwide.com

www.MTZonline.com

MTZ WORLDWIDE

09 September 2012 | Volume 73

THREE-CYLINDER Diesel Engine by Hyundai

INJECTION System for Handheld Working Equipment

DEPOSITS in Exhaust Heat Exchangers

EFFICIENT REDUCTION OF EMISSIONS

Springer Vieweg

COVER STORY

EFFICIENT REDUCTION OF EMISSIONS

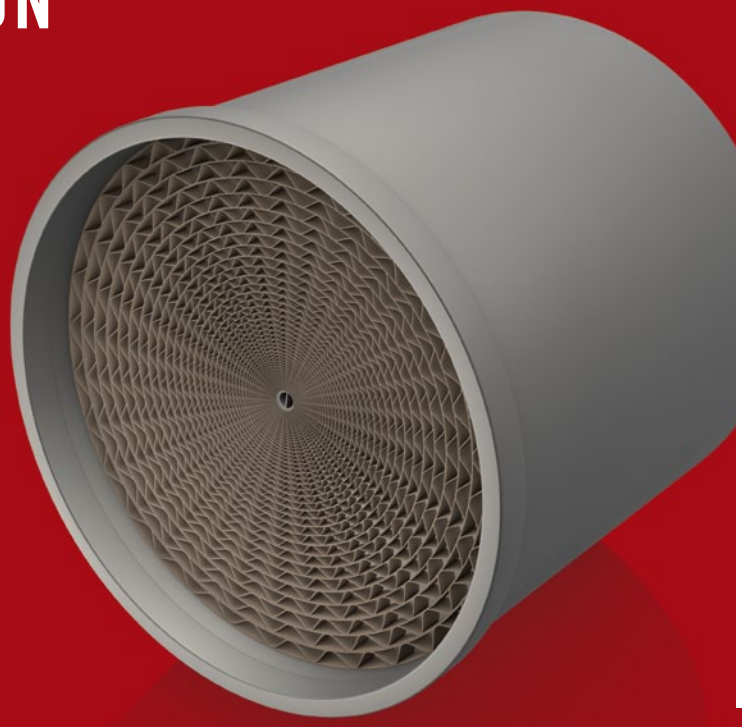

4, 10 | The main challenge in the further development of internal combustion engines is complying with future exhaust emissions standards while at the same time maintaining low CO_2 emissions. In the future, exhaust treatment systems that use selective catalytic reduction (SCR) will become more widespread. In this issue of MTZ, BASF presents a compact integrated catalytic converter that combines the functions of particulate filtration and NO_x reduction in a single component. Inside the engine, homogeneous charge compression-ignited combustion might offer an alternative to complex exhaust aftertreatment systems. However, this combustion process results in new challenges regarding combustion control and engine load. The advance development department of MTU, in cooperation with the Institute of Reciprocating Engines at Karlsruhe Institute of Technology (KIT), has developed a research prototype that allows partially homogeneous charge combustion with controlled self-ignition to take place over the entire engine map.

MODULAR STRATEGY

Dear Reader,

It is a well-known fact that engines have become increasingly complex over the past few decades, and it is a process that is still ongoing today. Further reductions in CO_2 emissions through downsizing and electrification as well as the introduction of the Euro 6 standard for diesel engines are just some of the current technical challenges. And in spite of all this innovative technology, the main focus is still on costs and product quality.

Whenever I talk to experts about these issues, they soon mention the term "modular strategy" as a key approach. Modules that can be flexibly combined to create space for a wide range of technical implementations – freely scalable, from minimum to maximum, from a basic engine to a high-tech powertrain. Of course, these concepts require huge initial investment, as modularisation usually requires a complete redesign of the powertrain platform, or at least the complex and cost-intensive adaptation of all systems and components. The cost-saving potential then becomes apparent over the production period. In addition to greater flexibility, modularity also means high production volumes, in other words low-cost, high-quality mass production of innovative products.

It comes as no surprise, therefore, that it is the big, multi-brand car makers like Volkswagen or General Motors who are pushing ahead with this strategy. The losers are likely to be smaller manufacturers who do not have sufficient capital for a complete implementation of a modular concept or, even if they have a modular strategy, do not have enough purchasing power to benefit from the fundamental advantages of this concept. Even selective cooperation on individual projects, as is currently being advanced by some car makers for cost reasons, will, in my opinion, be made much more difficult in the future if a modular strategy is consistently implemented – manufacturers would have to deviate too far from their in-house standards in order to be compatible with the products of their cooperation partner.

One solution for smaller market players might be modular strategies that include several manufacturers, as these would result in a corresponding purchasing volume. I recommend considering this option with an open mind and going beyond hierarchical in-company thinking. What is your opinion? Please send your comments to me by email at Richard.Backhaus@rb-communications.de or use the blog at www.ATZonline.de.

Best regards,

RICHARD BACKHAUS,
Vice-Editor in Chief
Wiesbaden, 12 July 2012

MTU HCCI ENGINE WITH LOW RAW EMISSIONS

The main challenge when developing off-highway engines is to keep emissions within the limits to apply in the future while maintaining low fuel consumption and low CO_2 output. Homogeneous charge compression ignition or HCCI provides an alternative to complex exhaust aftertreatment systems. The predevelopment department of MTU Friedrichshafen worked with the Institute of Internal Combustion Engines at the Karlsruhe Institute of Technology (KIT) to devise a research prototype for an industrial application which would allow semi-homogeneous combustion with controlled self-ignition over the full engine map.

DIESEL ENGINE REQUIREMENTS

Due to their wide application scope, off-highway diesel engines are subject to an array of design criteria. On the water, they can be found propelling workboats, military vessels and yachts. On land, their repertoire is much broader and ranges from agricultural machinery and special vehicles such as cranes, to construction, mining and rail vehicles. Furthermore, diesel engines play a leading role in power generation and in oil and natural gas production on land and at deep-sea sites. High cost-efficiency, an outstandingly long service life, top reliability at high loads, low space requirements, low power-to-weight ratios and wide engine performance maps are the key criteria in the field of high-speed diesel engines. Which factor takes priority varies greatly according to application. On machines with high capacity utilisation for example, fuel consumption primarily determines life-cycle costs and is therefore highly rated. In applications where only emergency situations are to be covered, fuel consumption is of secondary importance. Even within a single application, requirements may vary depending on the customer and final use. A summary of requirements is given in ❶. Along with the stringent emissions limits, these demands have paved the way to the very high cylinder peak pressures possible on modern diesel engines, and to sophisticated injection systems and their high injection pressures. In the USA in particular, diesel engines in the

AUTHORS

DR.-ING. CHRISTOPH TEETZ
is Head of Predevelopment and Analytic at MTU Friedrichshafen GmbH (Germany).

DR.-ING. DIRK BERGMANN
is Head of Corporate Liaison Management at MTU Friedrichshafen GmbH (Germany).

DR.-ING. ARNE SCHNEEMANN
is Head of Thermodynamics at MTU Friedrichshafen GmbH (Germany).

DIPL.-ING. JOHANNES EICHMEIER
is Scientific Assistant at the Institute for Reciprocating Engines (IFKM) of Karlsruhe Institute of Technology (KIT) (Germany).

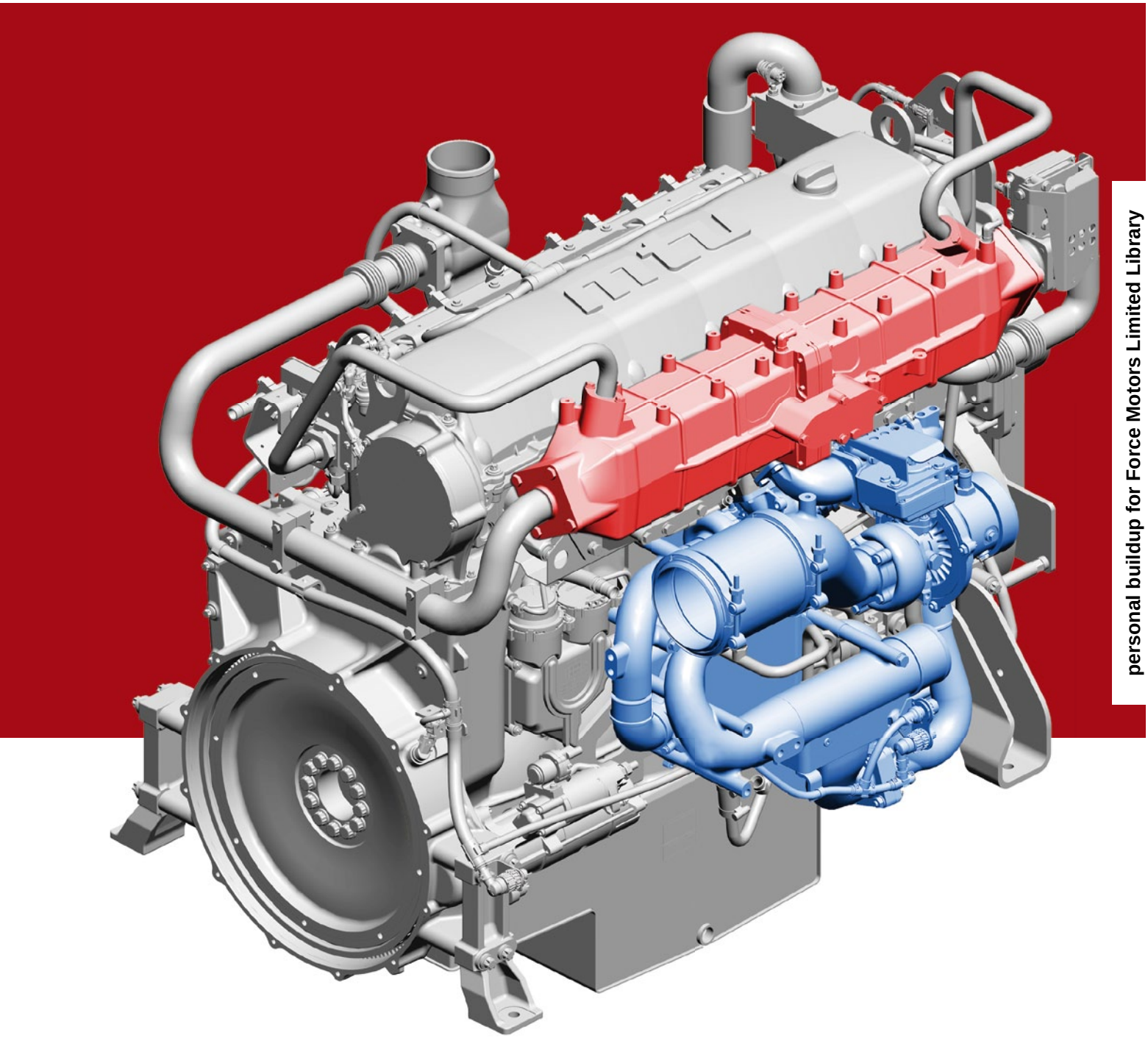

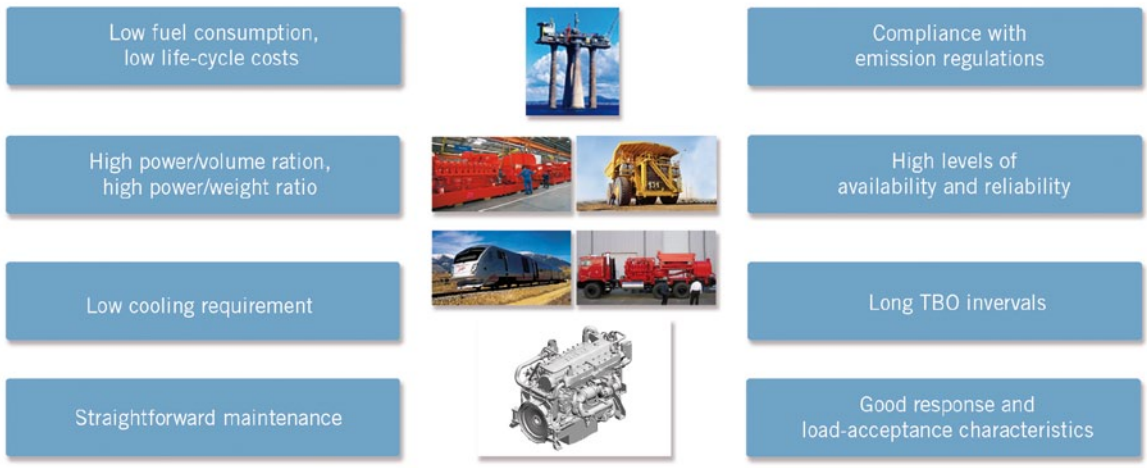

❶ Requirement profile for off-highway applications [1] (relative priorities between the criteria and priority levels within each criterion differ according to application)

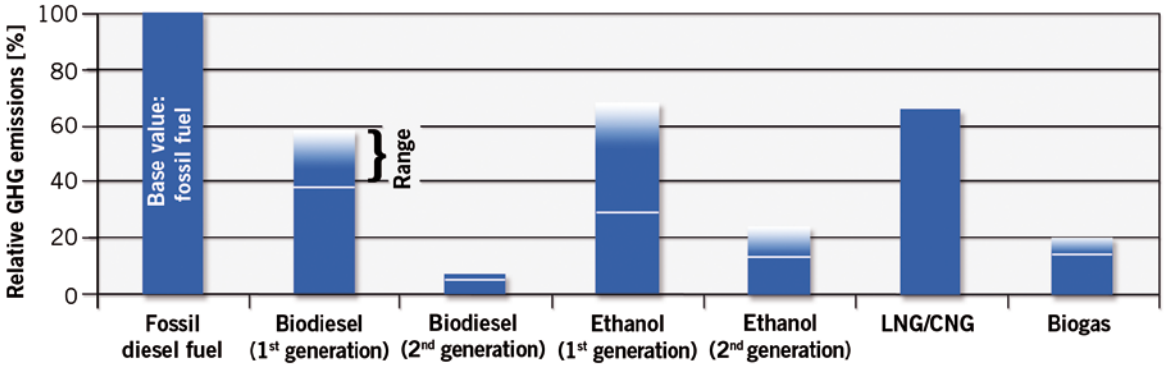

❷ Typical values for greenhouse gas emission (GHG) reduction through use of alternative fuels (source: Directive 2009/30/EG of European Parliament and Council of 23. April 2009)

130 to 560 kW power range are to be subject from 2014 to EPA Tier 4 legislation, which imposes limits of 0.4 g/kWh for NO_x and 0.02 g/kWh for particulate matter. Diesel units can only satisfy those requirements using a combination of in-engine measures and exhaust aftertreatment systems (SCR, particulate filters), which makes them a good deal more complex and expensive.

Against this background, MTU Friedrichshafen set itself the goal of developing an alternative to the diesel engine, whose widespread use in the off-highway sector will continue to ensure its prevalence there. The plan was to build a combustion engine able to satisfy the strictest emissions dictates, but of sufficiently low complexity to assure top reliability and cost-efficiency. This paper describes the current status of research work being performed jointly by MTU Friedrichshafen and the Institute of Internal Combustion Engines at the Karlsruhe Institute of Technology (KIT).

FUEL SCENARIOS

Ever-stricter emissions regulations governing off-highway engines also have an impact on diesel fuel specifications. For example, to ensure the smooth functioning of components in exhaust aftertreatment systems and to reduce SO_x emissions, the sulphur content of EN 590 (the diesel fuel sold at gasoline stations) has been continually reduced in recent years, and is now down to < 10 ppm. In the marine sector, where permissible sulphur levels can still be relatively high, these have been and continue to be reduced. In sensitive areas, particularly that of inland shipping, marine distillate fuels have even been replaced by sulphur-free diesel fuels in individual cases. The general trend is therefore a growing demand for sulphur-free diesel fuels or higher-quality distillates similar to diesel fuel.

Since diesel and gasoline are produced in relatively equal quantities at the refining stage, the increase in demand for diesel fuel will lead, in the short or long term, to a worldwide gasoline glut [2, 3]. Taking into account the large quantities of ethanol-based fuels available in some regions of the world, as well as recently discovered large reserves of natural gas, it can be expected that next to diesel fuels, gasoline will likewise be commercially attractive in the off-highway sector.

Another aspect of the fuel scenario in the off-highway sector is environmental protection measures aimed at reducing CO_2 emissions. Next to the higher fuel efficiencies associated with lower fuel consumption and the use of regenerative raw materials in fuels, another effective way of lowering relative CO_2 emissions is to use fuels with higher hydrogen content, ❷. That paves the way for the entry of gasolines with shorter chains and higher hydrogen contents into off-highway applications. This scenario prompted MTU Friedrichshafen to evaluate gasoline for its use in off-highway engines. An approach based on homogeneous combustion was selected. The target was to meet Tier 4 emissions regulations using in-engine measures while achieving high cost-effectiveness.

HOMOGENEOUS CHARGE COMPRESSION IGNITION

The major advantage of homogeneous charge compression ignition or HCCI is avoidance of soot and NO_x with simultaneously high efficiency. Hence its deployment in gasoline and diesel engines in automobile and utility vehicles has been the subject of investigation in recent years.

In the HCCI process, a lean, homogeneous air/fuel mixture is ignited by means of compression. Since the moment of self-ignition depends on the composition of the mixture and thermodynamic charge conditions, it cannot be directly influenced. Self-ignition starts at various places in the combustion chamber at once, causing very short combustion lengths which enhance efficiency. Thanks to the homogeneity of the mixture, local zones of heat or richness do not form, so the generation of particulate matter and nitrous oxides is avoided.

Compared to conventional gasoline combustion, HCCI allows a substantial reduction in fuel consumption in the partial load zone, allowing the continued use of low-priced three-way catalysts. Used in a diesel engine, HCCI makes it possible to dispense with complicated exhaust aftertreatment systems without detriment to efficiency. Due to the different properties of gasoline and diesel fuel, the peripheral conditions and requirements for implementation of HCCI vary according to the engine. The difference between the fuels lies in their evaporation and ignition behaviours. Gasoline already begins to evaporate at a low temperature, making the creation of a homogeneous fuel mixture unproblematic. The mixture can be formed using both traditional intake ports and gasoline direct injection. At the same time, its poor ignition performance necessitates higher temperatures during compression, and these must be made available – for example by having high residual gas rates in the combustion chamber [4, 5, 6]. Diesel fuel on the other hand has a high ignition performance, but much poorer evaporation characteristics. That means that fuel

pre-mixing using conventional injection valves is not feasible. Likewise direct injection can only take place within a narrow range towards the end of compression, otherwise wall deposits and oil thinning will result. To still achieve a fuel mixture which is largely homogeneous, ignition delay must be lengthened by means of high external exhaust return rates (≥50 %) [7].

The use of HCCI is limited to the part load range in both gasoline and diesel engines, since the rapid release of heat which typically occurs as the load increases results in high pressure gradients which cause the permissible load limits to be exceeded. On automobiles, emission test cycles are only carried out in the part load range, so despite the limitations on its use, HCCI allows future emission limits to be respected without elaborate exhaust gas aftertreatment systems and while still exploiting the advantages of low consumption on gasoline engines. On industrial engines, emissions test cycles also cover full load on account of the load collective, and therefore the engine map must be considerably extended [8].

In view of their contrasting characteristics, an obvious approach is to exploit the respective advantages of diesel and gasoline fuels with the aim of facilitating higher loads and controlling self-ignition. Several promising studies have already been carried out, although these have so far been limited to research at universities, since the need for a second tank and injection system on automobiles and commercial vehicles considerably pushes up expenditure [9, 10, 11].

The predevelopment department of MTU Friedrichshafen worked with the Institute of Internal Combustion Engines at the Karlsruhe Institute of Technology (KIT) to devise a research prototype for an industrial application which would allow semi-homogeneous charge compression combustion with controlled self-ignition over the full engine map. The fuels – gasoline or ethanol and diesel – are combined in such a way as to avoid the disadvantages associated with most HCCI combustion processes. The next chapter deals with the dual-fuel HCCI engine and the results achieved.

RESULTS

In dual-fuel HCCI, a lean, homogeneous mix of gasoline or ethanol with air is ignited by injecting a small quantity of diesel fuel. The homogeneous basic mixture is produced externally in the intake port, while the diesel fuel is injected during compression. Injection of the diesel fuel is designed to ensure that it likewise burns as homogeneously as possible. Timing of the start of injection has a decisive influence on subsequent combustion and can be used to control combustion timing [12]. As in all HCCI combustion processes, heat is released very rapidly, meaning that the cylinder charge must be lean enough to avoid the formation of excessively high pressure gradients. Up to medium loads, a lean basic mixture is theoretically sufficient, but for reaching full load, high exhaust gas return rates are needed. As the load increases, lower diesel fuel volumes are required to prompt self-ignition.

From these findings, which were initially obtained on a single-cylinder Series 1600 unit, the requirements for the full engine prototype could be derived. The full engine is based on a six-cylinder version of an MTU Series 1600 unit with 10.5 l cylinder displacement and a rated output of 300 kW at 2100 rpm. At its optimum operating point, the prototype achieves 42 % efficiency. The main differences between the prototype and the standard engine unit are:

: cooled high pressure exhaust gas return
: two-stage charging with intercooling
: gasoline injection in the inlet duct
: reduced compression ratio (ε=11.75).

The full-load curve attainable on this engine is shown in ❸. The curve in relation to speed is typical for a diesel-mechanical application which requires high torque at medium speeds in order to counteract speed dips. By comparison with the Series 1600 diesel engine, the dual-fuel HCCI prototype, when powered with gasoline, achieves 17 % lower maximum torque and 14 % lower power output at full load. Notwithstanding, the engine map range is perfectly acceptable for a diesel-mechanical application. If ethanol is used instead of gasoline, the engine almost achieves the full-load plot of a diesel engine. Due to ethanol's higher octane count, the basic mixture has a lower ignition performance and combustion proceeds more slowly. Higher loads are therefore possible on the one hand, with less charge dilution required over large areas of the engine map on the other. The benefit is a reduction in charge-changing losses, which translates into higher efficiency.

❹ shows the percentage of diesel fuel in the overall fuel mass and the rate of exhaust gas return in the engine map for gasoline operation. Over most of the engine map, the homogeneous basic mixture can be ignited using very small quantities of diesel fuel. Only when the load is very low does the proportion of

❸ Comparison of full load curves for dual-fuel HCCI prototype and diesel engine

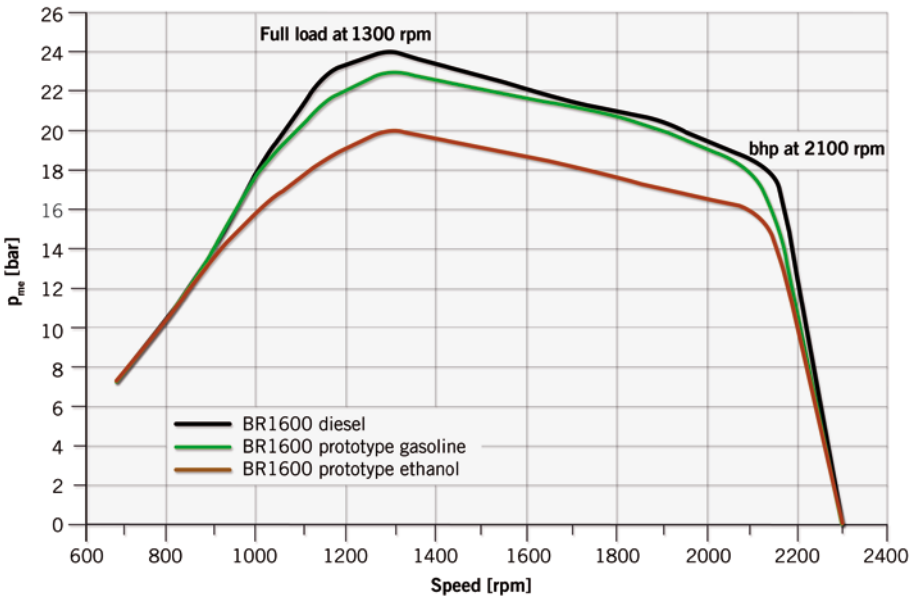

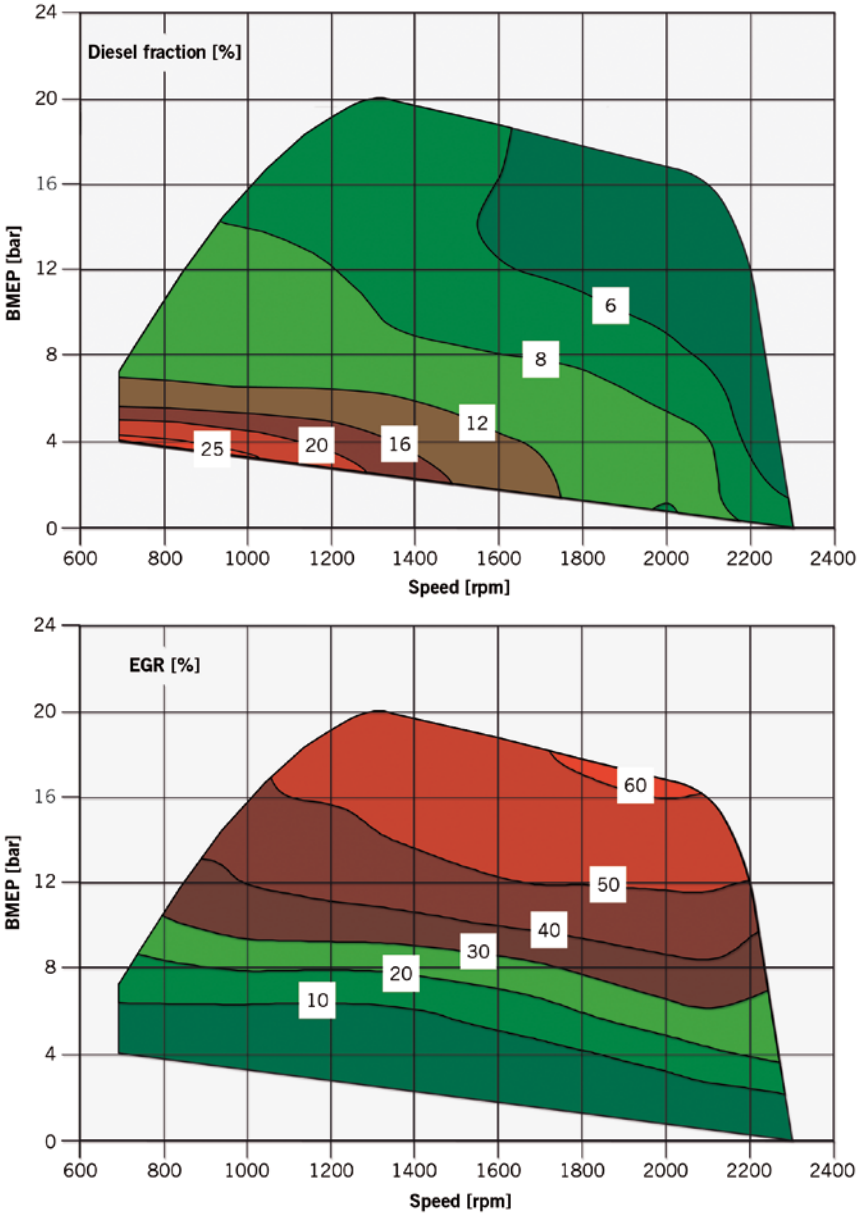

❹ Percentage of diesel fuel in overall fuel mass (top) and exhaust gas return rate (below) in engine map

diesel fuel increase more sharply, since the charge temperatures are very low at these points. The need for EGR increases continually in relation to load, with exhaust gas return rates of > 50 % needed in the upper third of the engine map where excessively steep pressure gradients are to be avoided. The maximum permissible pressure gradient is 100 bar/ms.

Over the whole engine map, the dual-fuel HCCI engine displays exceptionally low particulate and nitrous oxide emissions falling far below the thresholds set for 2014 by emission standards in Europe (Euro Stage IV: 0.4 g/kWh NO_x, 0.025 g/kWh PM) and the US (EPA-Tier 4: 0.4 g/kWh NO_x, 0.02 g/kWh PM). The exhaust gas values measured in the C1 test cycle as per ISO 8178, Part 4, demonstrate that fact impressively. ❺ lists the cycle-dependent operating points of the dual-fuel HCCI engine. With the exception of no-load, the engine runs in HCCI mode at all operating points using gasoline as fuel in the homogeneous basic mixture. At no-load, engine operation takes place in diesel mode, since with HCCI, the HC and CO emissions rise dramatically when loads are very low.

❻ shows the values determined for particulates and NO_x in relation to EPA Tier 4 limits. Based on the given limit, the dual-fuel HCCI engine emits 93 % less NO_x and 40 % fewer particulates.

SPEED [rpm]	BMEP [bar]	WEIGHTING
2100	16	0.15
2100	12	0.15
2100	8	0.15
2100	1.6	0.10
1300	20	0.10
1300	15	0.10
1300	10	0.10
700	Idle	0.15

❺ C1-cycle points for a dual-fuel HCCI engine in gasoline mode

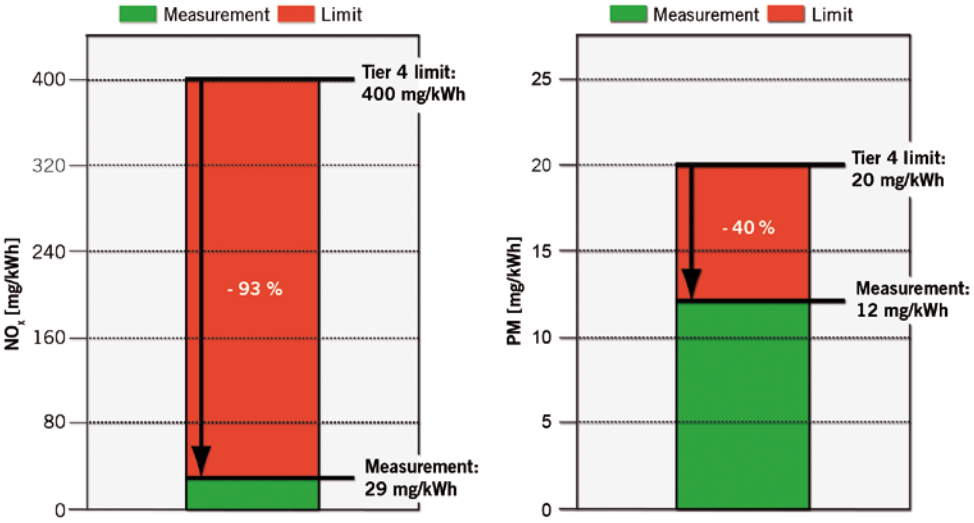

❻ Nitrous oxide (left) and particulate emissions (right) from the dual-fuel HCCI engine in the C1-cycle (particulate matters calculated from filter smoke number (FSN) according to MTU internal correlation)

With these emissions levels, exhaust aftertreatment can be safely dispensed with. As in all HCCI processes, HC and CO emissions are higher than for diesel combustion. However, these are easy to eliminate using a simple oxidation catalyst, as initial investigation at the engine test stand has shown. Nevertheless, the low exhaust gas temperatures call for further optimisation measures, and these are currently being researched.

SUMMARY AND PERSPECTIVES

The predevelopment section of MTU Friedrichshafen worked with the Institute of Internal Combustion Engines at the Karlsruhe Institute of Technology (KIT) to devise a homogeneous combustion process (HCCI). This process enables emissions limits as per EPA Tier 4 standards in the US and Stage IV standards in Europe to be respected, even leaving room to spare. With this method, a gasoline fuel introduced into the combustion chamber homogeneously is ignited by means of a semi-homogeneous diesel fuel. The process is controlled with the support of cooled exhaust gas return which is variable over the entire engine map. As opposed to conventional HCCI processes, this process can be used over the entire engine map. Future research will serve to optimise the combustion process with respect to efficiency, applications scope and emissions and prepare it for operation in the field.

REFERENCES

[1] Dohle, U.; Schneemann, A.; Teetz, C.; Wintruff, I.: Erfüllung künftiger Abgasemissionsvorschriften – Lösungen der MTU Friedrichshafen. 31. Vienna Motor Symposium 2010
[2] Gasoline Glut will Create Dilema for Oil Industry & Government. JPC press release, Vienna, 20.02.2008
[3] N.N.: Zu viel Benzin: Probleme für Raffinerien. In: Die Presse, print issue, 15.02.2008
[4] Pritze, S.; Königstein, A.; Rayl, A.; Chang, C-F.; Najt, P.; Grebe, U. D.: GM's HCCI-Erfahrungen mit einem zukünftigen Verbrennungssystem im Fahrzeugeinsatz. 31. Vienna Motor Symposium 2010
[5] Herrmann, H.-O.; Herweg, R.; Karl, G.; Pfau, M.; Stelter, M.: Homogene Selbstzündung am Ottomotor – ein vielversprechendes Teillastbrennverfahren. 14. Aachen Colloquium Automobile and Engine Technology 2005
[6] Sauer, C.: Steuerung der ottomotorischen Selbstzündung. Dissertation, Stuttgart University, 2010
[7] Otte, R.; Raatz, T.; Wintrich, T.: Homogene Dieselverbrennung – Herausforderung für System, Komponenten und Kraftstoff. In: MTZ 69 (2008) No. 12
[8] Teetz, C.: Wie MTU künftige Emissionsrichtlinien meistert. In: MTZ Extra 100 Jahre MTU (2009), pp. 64 – 71
[9] Olsson, J.-O.; Tunestål, P.; Johansson, B.: Closed-Loop Control of an HCCI Engine. SAE 2001-01-1031, 2001
[10] Johansson, B.: Homogeneous charge compression ignition: the future of IC engines. In: Int. J. Vehicle Design 44 (2007) No. 1/2, pp. 1 – 19
[11] Curran, S.; Prikhodko, V.; Cho, K.; Sluder, C.; Parks, J.; Wagner, R.; Kokjohn, S.; Reitz, R.: In-Cylinder Fuel Blending of Gasoline/Diesel for Improved Efficiency and Lowest Possible Emissions on a Multi-Cylinder Light-Duty Diesel Engine. SAE 2010-01-2206, 2010
[12] Eichmeier, J.; Wagner, U.; Spicher, U.: Controlling Gasoline Low Temperatur Combustion by Diesel Micropilot Injektion. ICEF2011-60042, ASME 2011 Fall Technical Conference

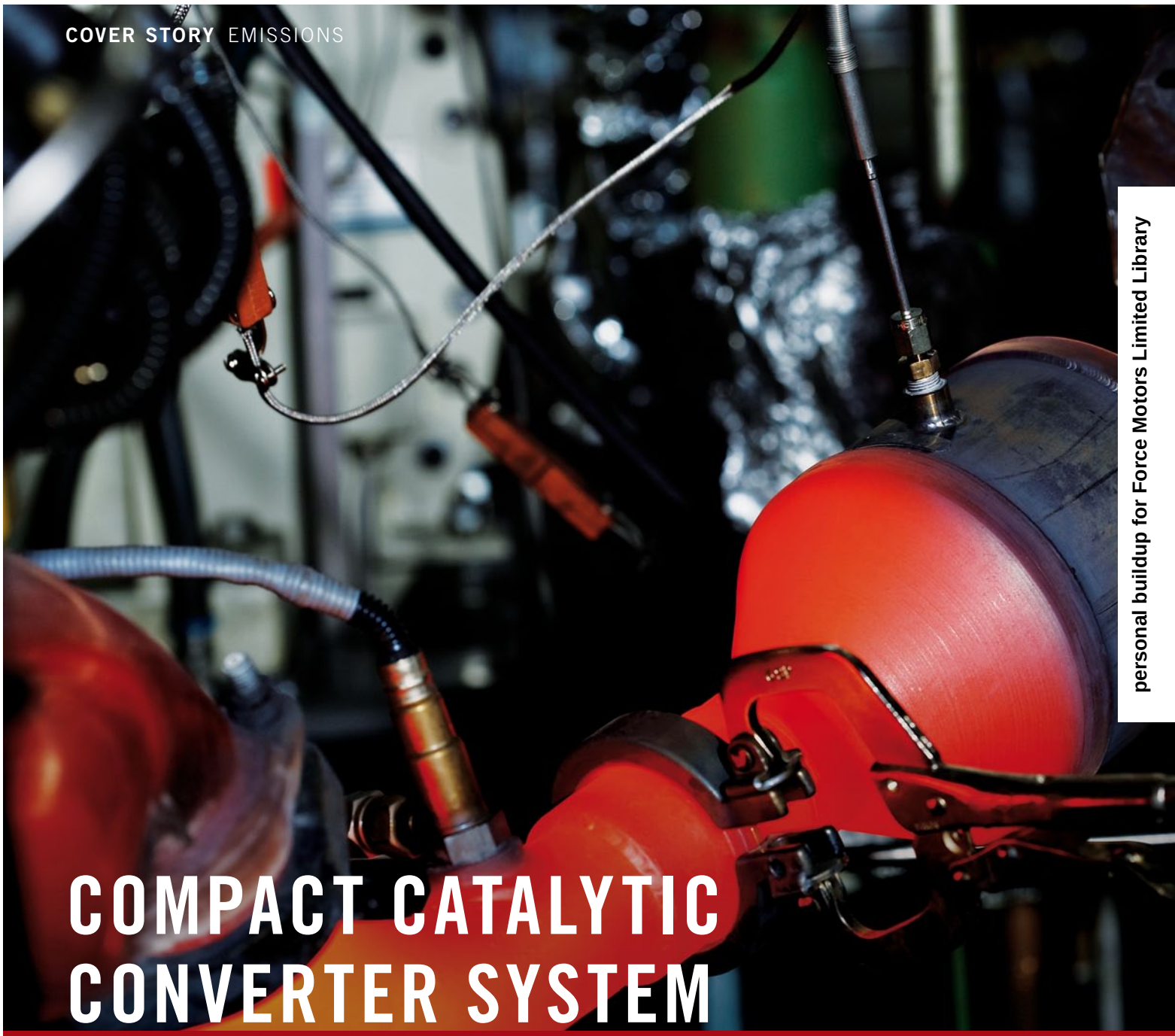

COMPACT CATALYTIC CONVERTER SYSTEM FOR FUTURE DIESEL EMISSIONS STANDARDS

The Euro 6 emissions standard for diesel passenger cars will broaden the application of exhaust aftertreatment systems that use selective catalytic reduction. This will mean a further increase in the volume and complexity of the exhaust aftertreatment system. BASF has developed a compact integrated catalytic converter that combines the functions of particulate filtration and NO_x reduction in a single unit.

AUTHOR

DR. KLAUS HARTH
is Vice President Environmental Catalysis Research at the BASF Corporation in Iselin (USA).

INCREASING REQUIREMENTS FOR THE CATALYTIC CONVERTER SYSTEM

Over the last several decades, advances in environmental catalyst technologies have contributed significantly to reducing tailpipe emissions from combustion engines. At present, a modern catalytic system is capable of converting more than 95 % of the carbon monoxide (CO), hydrocarbons (HC), nitrogen oxides (NO_x) and soot present in the exhaust gas to carbon dioxide, water and nitrogen gas. While future environmental regulations will require further reductions of these harmful emissions, combustion engine development is driven by the need for higher fuel efficiency and less production of carbon dioxide. These trends will demand further continuous performance improvements of the catalytic exhaust gas treatment system. In this article, the development of catalytic systems is explained by the example of diesel passenger cars.

CATALYTIC COMPONENTS FOR DIESEL EXHAUST GAS TREATMENT

The primary function of the diesel oxidation catalyst (DOC), ❶, is to completely oxidise hydrocarbons and carbon monoxide in the exhaust gas to carbon dioxide and water. In specific applications, the DOC is also expected to partially convert nitrogen oxide (NO) to nitrogen dioxide (NO_2). A stable concentration of NO_2 can be used to oxidise soot on a catalytic soot filter (CSF) or to promote NO_x

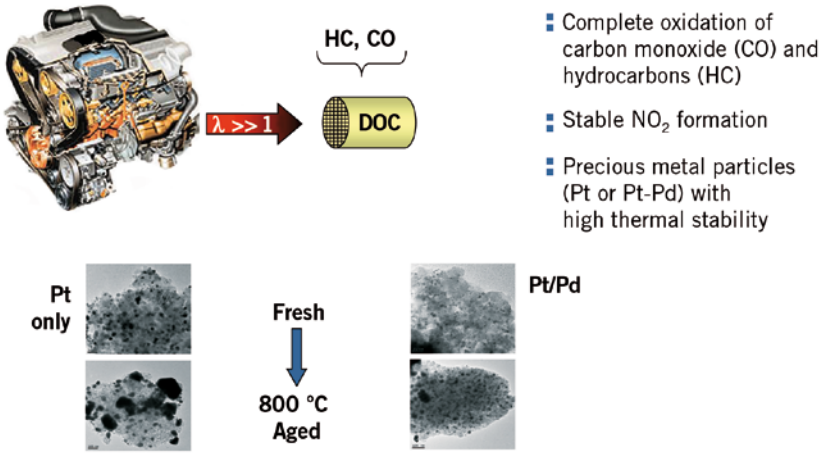

❶ Diesel oxidation catalyst (DOC)

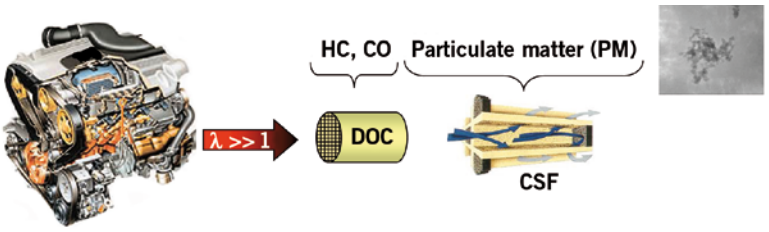

- Filtration of particulate matter
- Active or passive regeneration
- Complete oxidation of CO and HC
- Stable NO_2 formation

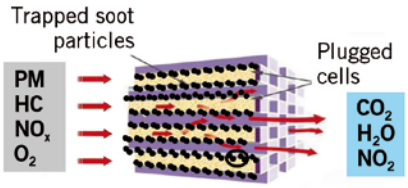

❷ System of DOC and CSF

conversion over the selective catalytic reduction (SCR).

The active components of a DOC coating are small precious metal particles of Pt and Pd supported on high surface area inorganic oxides (e.g. alumina). The DOC washcoat may also contain components like zeolites to better manage the conversion of hydrocarbons during cold start.

In addition to the architecture of the washcoat, the size, composition and matrix of the precious metal particles play a crucial role in reliable DOC performance under real driving conditions. Utilising the broad experience in catalysis and material science, BASF has developed a broad portfolio of high performance DOCs for different applications. These DOCs can be further tailored to specific customer applications.

Early emission regulations for light duty diesel vehicles could be met with a single DOC plus engine control adjustments. At that time, the volume of the DOC was comparable to the engine displacement volume. Recently, filter elements (CSF) have been added to diesel vehicles to prevent soot-particles from getting to the atmosphere, ❷. In contrast to flow-through substrates of conventional vehicle catalysts, the channels of a filter substrate are blocked at alternating ends. This forces the exhaust gas to flow through the porous wall of the monolith. Soot particles are retained and accumulated in the filter until a critical pressure drop across the filter element triggers an active regeneration. Regeneration occurs when extra fuel is combusted over the DOC and the resultant heat ignites of soot in the filter. This extra fuel is injected either into the combustion chamber or directly into the exhaust gas upstream of the DOC.

In addition to this active regeneration principle, passive regeneration systems can currently be found in heavy duty diesel vehicles. The soot retained in passive systems undergoes continuous oxidation by the NO_2 produced by the upstream DOC. In addition, the filter itself may contain catalytic components. Common coatings comprise precious metals, which – in analogy to DOC – ensure complete oxidation of CO and HC as well as a stable formation of NO_2.

The two leading technologies for controlling NO_x emissions are lean NO_x traps (LNT) or selective catalytic reduction catalysts (SCR), ❸. Each uses a reducing agent for the conversion of NO_x to nitrogen gas. The LNT uses partially combusted diesel fuel and the SCR uses ammonia as the reducing agent. Ammonia is usually produced by the decomposition of urea on board the vehicle. Incorporation of these NO_x abatement components into the exhaust gas treatment system adds significant volume and complexity to the emission control system.

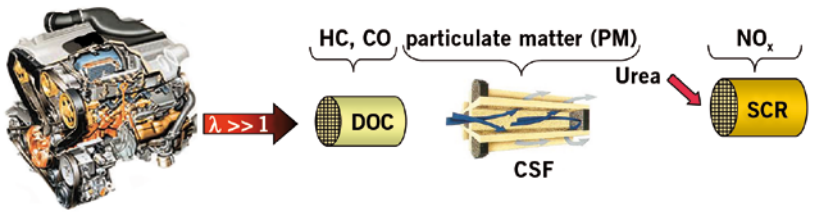

- Reduction of NO_x by ammonia (NH_3): $NO + NO_2 + 2NH_3 \rightarrow 2N_2 + 3H_2O$
- Ammonia produced by on-board hydrolysis of urea
- Metal-zeolites (e.g. Cu-chabazite) with high activity and stability

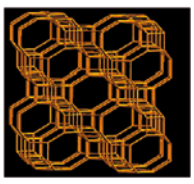

❸ System of DOC, CSF and SCR

❹ $DeNO_x$ performance and dependence of back-pressure on filter-porosity and SCR material loading

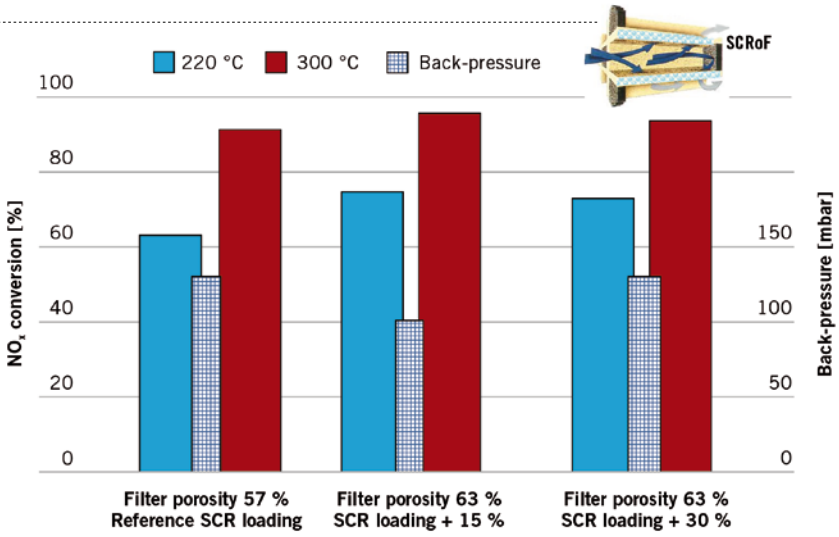

For light duty diesel applications the SCR catalyst consists of a Cu or Fe containing zeolite. Typical zeolites are Fe-beta and Cu-chabazite. Cu-chabazite exhibits an excellent low temperature activity, a broad temperature window of activity and superior high temperature stability. In addition, an ammonia oxidation catalyst may be used downstream of the SCR to prevent ammonia slip. Systems of this type are already in use for heavy duty applications. They require sophisticated control of timing of CSF regeneration cycles and an active urea dosing strategy. For light duty applications, systems with smaller volume requirements and less complexity are highly desired.

INTEGRATED CATALYST

The increasing complexity of catalytic systems for vehicles with diesel engines is a driving force to develop smart and less complex systems for the future. Here, the trade-off between complexity and cost reduction on one side and the requirements to meet current and future emission regulations on the other side must be balanced.

A possible approach to simplification is to integrate CSF and SCR function in one component and place the active mass of the SCR catalyst on the filter substrate of the CSF. This integrated catalyst is in the following called SCR on Filter or just SCRoF. For such an SCRoF component there are complex requirements. To achieve on the one hand a high NO_x conversion level, particularly in the aged state, SCR-active materials with very high intrinsic activity are required. At the same time it is desirable to accommodate the highest possible amount of these active compositions in the pores of the filter substrate. However, here limits are set by the maximum pressure loss, a filter component may have. On the other hand, filters with low porosity are preferred for the safe control of all particulate matter emissions and the compliance of small so-called soot mass limits.

Therefore SCRoF applications require filter substrates with tailor-made porosities which overcome this conflict. In addition to the filter porosity, the catalytic material and the coating process are of critical importance. For use as an integrated system, such as a close coupled position, the dosage and the thermolysis of urea and the regeneration concept must also be addressed.

❹ shows the possibilities that open up the use of filters with optimised porosity. Shown are the measured NO_x conversion levels in stationary engine tests for catalysts with different porosity and active mass loading. This evaluation was carried out at BASF's engine laboratory in Hanover. A filter substrate with a medium porosity of 57 % and a standard SCR catalyst loading served as reference. The use of filters with higher porosity (63 %) leads to a lower initial back-pressure and enables to increase the SCR loading by 15 %. This results in an increase of at least 10 % points versus the reference. A further increase of SCR catalyst mass on the high porosity filter does not lead to an additional increase in NO_x conversion under the chosen stationary conditions.

The filtration efficiency was also evaluated. Because of the close-coupled design of the system, there was no significant adverse effect observed with the SCRoF. Even with the higher porosity of the filter, the soot-mass regulation (4.5 mg/km in the Euro cycle) and the limit for the soot particle number ($6*10^{11}$/km in the Euro cycle) could be met.

An important method for evaluation of catalyst systems remains the transient evaluation on the vehicle. Several transient cycles were studied for SCRoF. The performance in the European Driving Cycle (NEDC), the U.S. light duty cycle (FTP72 and US06), and other cycles (e.g. WLTP) was evaluated. It turns out that the exact system design is an important element for performance optimisation. It is important that a high-performance DOC has a very fast light-off and ensures complete oxidation of CO and HC as well as stable oxidation of NO. In addition, because of the extremely close-coupled location of the DOC, it has to be thermally stable. The DOC developed by BASF met the limit for CO (500 mg/km in the Euro cycle) after aging for 16 h at 800 °C. A significant improvement was achieved for the NO oxidation behaviour as well. The deterioration of the NO oxidation could be significantly reduced.

The Euro 6 limit values for NO_x (80 mg/km in the Euro driving cycle) can be met with a SCRoF system on a vehicle even under difficult testing conditions, ❺. In this example, the average NO to NO_2 ratio was 25 % (as opposed to the optimum of about 50 %). This

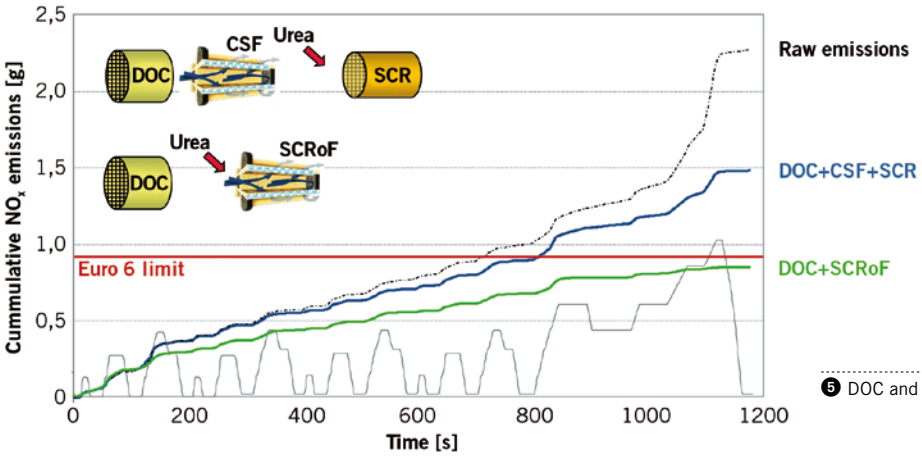

❺ DOC and SCRoF system can meet Euro 6 NO_x limit

constraint was deliberately chosen to push the boundaries of the system and also to differentiate the ability of next generation DOC to work with SCRoF catalysts. Only an optimised DOC and an optimised SCRoF were able to meet these limits. With this optimised system, a significant improvement was observed compared to the classical system composed of DOC, CSF and SCR.

The new generation DOC and SCRoF catalyst system was also evaluated on the U.S. cycle. The NO_x conversion observed was > 85 % and the requirements of Tier2 Bin5 were met. Additional performance improvement can be achieved when a small SCR catalytic converter is used under the floor (downstream of the SCRoF). The catalyst volume of this SCR part was 50 % of the SCRoF component. This additional SCR increased NO_x conversion to more than 90 %.

DURABILITY

An important and crucial development goal for SCRoF catalyst systems is the durability, ❻. The U.S. test cycle (FTP72) was chosen. Similar results were obtained under steady-state and in other transient cycles (e.g. NEDC). In this test, the components were loaded with soot and regenerated under engine conditions. This process was repeated more than 220 times to mimic realistic end-of-life conditions for the catalysts. Over an equivalent mileage of 180,000 km, no significant deterioration of the NO_x conversion was observed. This result clearly underlines the robustness of the SCRoF system developed by BASF.

CONCLUSION

BASF has developed a new smart catalyst technology based on the broad know-how in catalysis and materials research. This new compact system comprising an SCRoF is able to meet stringent emission requirements.

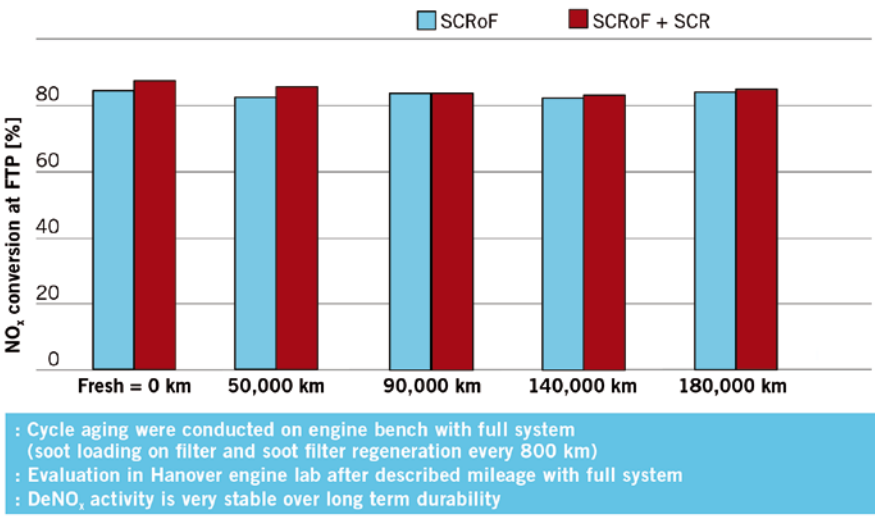

❻ DOC and SCRoF thermal durability

STOP LOOKING. START FINDING.

ATZ ONLINE. KNOW MORE. GO FURTHER.

Information that inspires is the root of innovation. Staying up to date helps accelerate development. And substance is what makes knowledge valuable. ATZonline is the place to go when you want to know what's happening in our industry and to get information that is unique in its depth. ATZ, MTZ, ATZelektronik, ATZproduktion subscribers get access to a complimentary archive of industry articles as well as specials and whitepapers. All articles are well researched, with background and insider information.

No need to look any further – get your competitive advantage on **www.ATZonline.com**

ATZ online

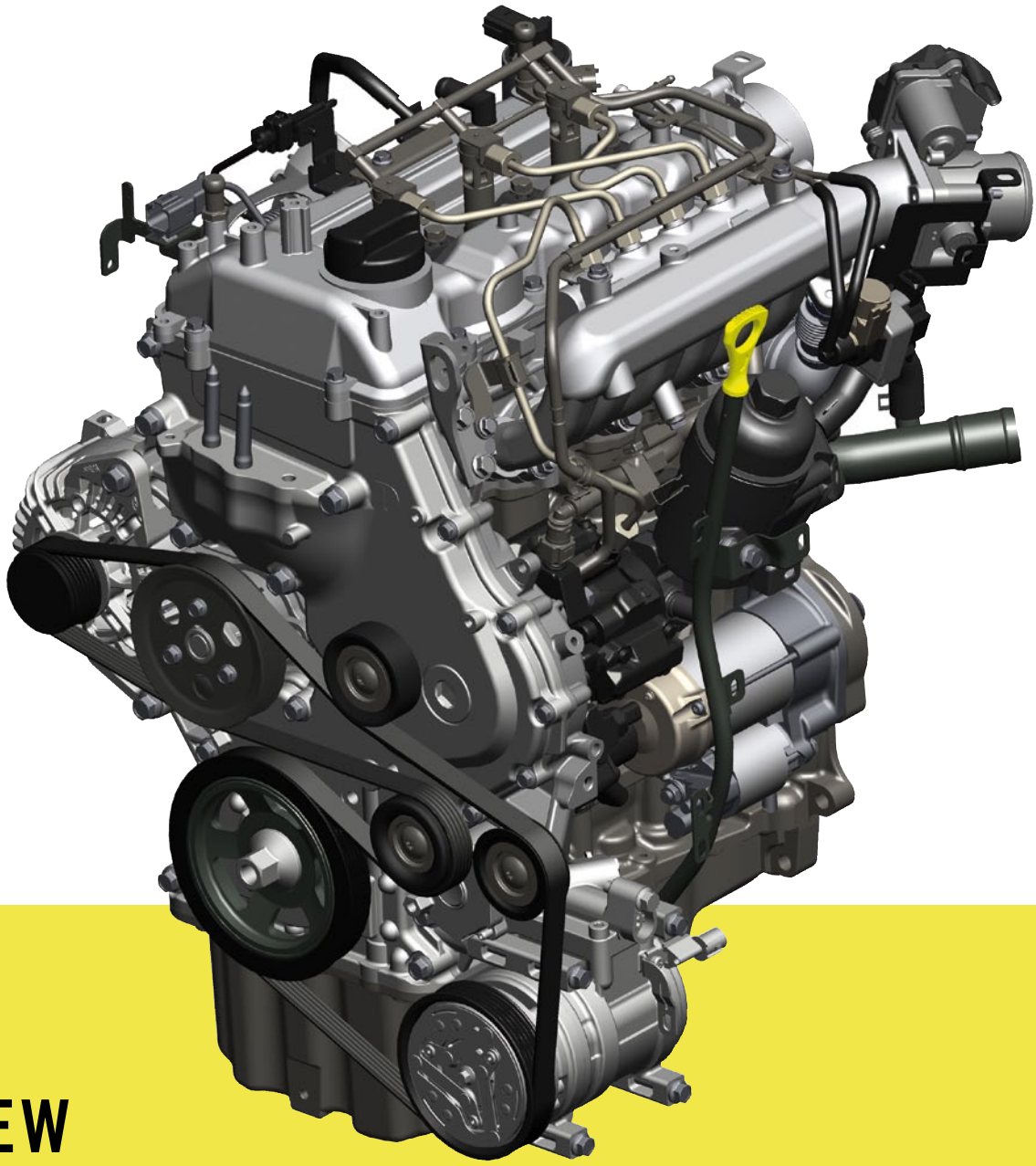

THE NEW HYUNDAI/KIA 1.1-L THREE-CYLINDER DIESEL ENGINE

To achieve low CO_2 emission with the recently launched B-segment vehicle Kia Rio, Hyundai has introduced the second-generation U2 1.1-l three-cylinder diesel engine. This engine and further vehicle features allow a class-leading CO_2 emission of 85 g/km achieved by state-of-the-art technologies including an idle start/stop (ISS) system as well as weight and friction reductions. In addition, the combustion system was optimised to provide sufficient power output and to enable appropriate drivability for B-segment vehicles.

AUTHORS

KYUNG WON LEE
is Part Manager for Passenger Car Diesel Engines in the Engineering Design Team at Hyundai Motor Company in Seoul (South Korea).

KYOUNG IK JANG
is Senior Research Engineer for Passenger Car Diesel Engines in the Engineering Design Team at Hyundai Motor Company in Seoul (South Korea).

JEONG JUN LEE
is Senior Research Engineer for Passenger Car Diesel Engines in the Test Team at Hyundai Motor Company in Seoul (South Korea).

DONG HAN HUR
is Research Engineer for Passenger Car Diesel Engine in the Test Team at Hyundai Motor Company in Seoul (South Korea).

COMPETITIVE POWER OF FUTURE DIESEL ENGINES

It is acknowledged that improving fuel economy and complying with increasingly stringent emission standards are major concerns in the automotive world. Recent sharp increases in oil prices triggered by the recovery from global economic crisis and political instability in oil-producing countries have forced automakers to pursue the development of more efficient and energy saving powertrains and vehicle technologies.

Compliance with upcoming emission standards while maintaining fuel economy is another challenge, especially for diesel engines. Current diesel engines with Euro 5 certification are proved to retain their competitive power against gasoline engines from the viewpoint of total cost of ownership. The engineering targets of emissions can still be reached by a refined combustion system combined with a diesel particulate filter (DPF) and without expensive and complicated reduction of nitrogen oxide ($DeNO_x$ aftertreatment). The amount of fuel economy penalty that has to be paid in the process of the NO_x emission reduction by about 30 % from the Euro 4 level is not significant.

However, considering the engineering requirements and market acceptance issues, a highly expensive $DeNO_x$ aftertreatment system might be considered as a standard device for the upcoming Euro 6 emission standard. In addition, it will eliminate a substantial portion of the overall competitive power of the diesel engine. Meanwhile, the enforcement of highly challenging CO_2 and fuel economy standards combined with greenhouse-gas-based tax systems under discussion on a global scale is expected to be an important turning point for the competitiveness of diesel engines. The additional cost for CO_2 reduction devices or hybridisation of gasoline engines required to reach the CO_2 standards will significantly reduce the price gap between diesel and gasoline vehicles. Hence, the definition of most cost-efficient systems and refined calibration that allows full utilisation of system potential will decide on the competitive power of future diesel engines.

DEVELOPMENT CONCEPT

The development of the new generation 1.1-l engine aimed to enhance the appeal of Hyundai/Kia B-segment vehicles by achieving the lowest CO_2 emission in the segment while providing enough power output for a fun-to-drive feel and driver comfort.

The main concepts of development were:

- to reach a class leading CO_2 emission level
- to optimise NVH (Noise, Vibration, Harshness) characteristics by refined calibration and structural analysis
- to deliver satisfactory power output and retain a fun-to-drive feel for B-segment vehicles
- to define a most cost-efficient system for upcoming emission standards.

With the Kia Rio, the new engine has achieved a class leading CO_2 homologation value of 85 g/km with affordable drivability. With a high potential in combustion efficiency as well as emission and power output, this engine will play a key role in Hyundai's future strategy in eco-friendly vehicle development.

ENGINE SPECIFICATION

Although the U2 1.1-l engine is boosted by a wastegate turbocharger (WGT), it delivers the same maximum power output as its predecessor boosted by a turbocharger with a variable geometry turbine (VGT), ❶. The development of the

Engine	U 1.1-l diesel (predecessor)	U2 1.1-l diesel
Type	In-line three-cylinder engine	
Valvetrain	Dual-overhead camshaft, four-valve design	
Displacement	1120 cm^3	
Bore x stroke	75 mm x 84.5 mm	
Maximum power	55 kW at 4000 rpm	
Maximum torque	152 Nm at 2000 rpm	180 Nm at 1750 to 2500 rpm
Compression ratio	17.8 : 1	16.0 : 1
Charger	Variable geometry turbine turbocharger	Wastegate turbocharger
Injection system	Common rail injection (Bosch)	Common rail injection (Delphi)
System pressure	1600 bar	1800 bar
Emission	Euro 4	Euro 5

❶ Specification of the new 1.1-l three-cylinder diesel engine in comparison to its predecessor

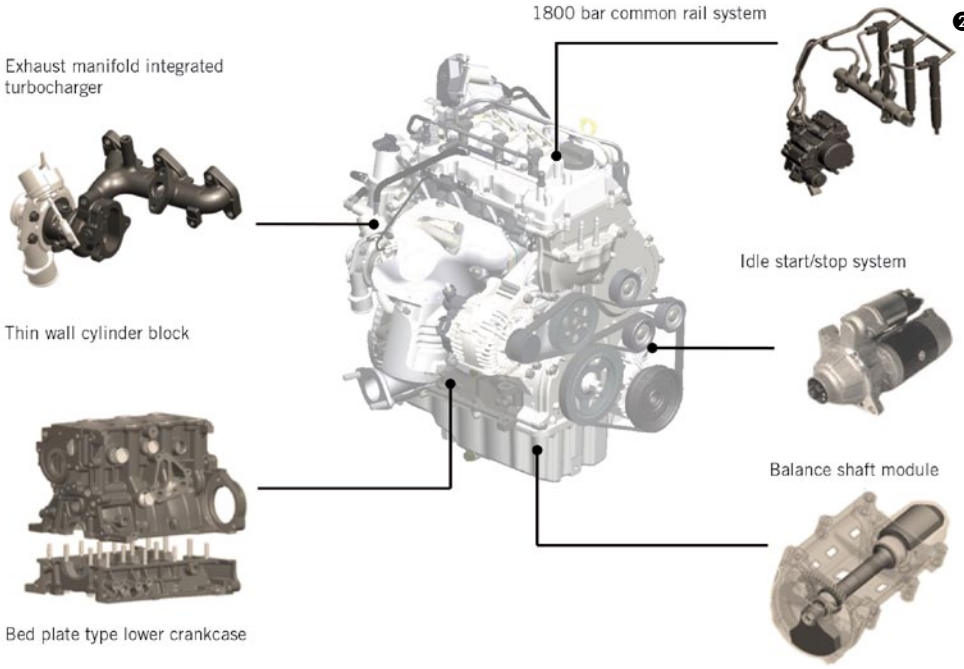

❷ Significant design features

new combustion system focused on enhancing low-end torque which is essential for the drivability of a B-segment vehicle powered by a downsized engine. The maximum torque has been improved from 152 Nm at 2000 rpm in its predecessor to 180 Nm and this maximum torque is delivered within the wide range between 1750 and 2500 rpm.

A common rail fuel injection system supplied by Delphi was introduced and maximum injection pressure was increased from 1600 to 1800 bar to allow higher performance and emission potential. The compression ratio was reduced from 17.8:1 to 16.0:1. This figure is an optimal compromise between two opposing requirements towards better emission potential against start ability and combustion stability, especially under cold atmospheric conditions. A diesel oxidation catalyst (DOC) is located at a close-coupled position for faster light-off and a DPF is located in the under-floor position.

ENGINE HARDWARE FEATURES

Some important design features were implemented to achieve enough potential for minimising CO_2 emissions, achieving Euro 5 compliance, maximising power output and reaching a comfortable acoustic behaviour, ❷. Combining an 1800 bar common rail system with an optimised WGT leads to a high engine potential. Furthermore, a cooled exhaust gas recirculation (EGR) system with enhanced cooling capacity actuated by a linear solenoid valve with position sensor generally accepted as standard NO_x reduction package was also introduced.

A substantial portion of the fuel consumption reduction is achieved by the ISS system, which automatically shuts down the engine when the vehicle comes to a stop. In addition, the intelligent braking energy recuperation system minimises electricity generation during acceleration and converts the kinetic energy of the vehicle into electric energy during braking.

The so-called bed plate structure of the engine block was already introduced for the existing U engine series to enhance stiffness and thereby acoustic behaviour. Especially for the three-cylinder engine a gear driven mass balancer shaft was installed which completely offset the 1st unbalanced moment. Another feature incorporated is a turbocharger integrated with the exhaust manifold which is beneficial for performance and fuel economy by reducing flow losses together with weight and cost reduction.

Significant weight reduction is achieved by an optimised structure and thickness of the cylinder block. The dimensions and clearances of important moving parts and the piston ring preload considering the peak firing pressure and oil consumption were optimised for friction reduction.

The timing system is driven by a maintenance-free two-step chain system where the primary chain drives a high-pressure pump. The layouts and configurations of both chains have been optimised by finite element method (FEM) and multi-body simulation.

COMBUSTION CHAMBER

For enhanced fuel economy and emission potential the engine compression ratio was reduced from 17.8:1 in the predecessor engine to 16.0:1 in the U2 engine. A wider and shallower combustion chamber shape was introduced to optimally match the fuel injection system with higher pressure.

As a lower compression ratio has demonstrated an advantage in NO_x emission due to lower combustion temperatures and a higher power output under the same peak firing pressure, the carbon monoxide (CO) and unburned hydrocarbon (UHC) emission, especially during the warm-up phase and under cold ambient atmosphere, may be deteriorated. Refined calibration is applied for the pilot, main injection and EGR especially during warm-up to guarantee stable combustion and thereby reduce CO and UHC.

The combustion chamber shape was optimised based on computational simulation and an experimental approach to improve fuel economy and emissions by maximising air utilisation and promoting the air-fuel mixture, ❸.

FUEL INJECTION SYSTEM

The common rail fuel injection system with its maximum injection pressure of 1800 bar, ❹, leads to shorter injection duration and an enhanced performance. The number of injector holes is increased from seven to eight and the flow area of each hole is reduced by about 5 %, which allows improved emission potential by enhanced atomisation of injected fuel and air mixing. Although the hole diameter is reduced, coking robustness is secured by a shorter injector hole length of 0.65 mm.

These changes provide more precise control of small injection amounts and shorter intervals between the injections.

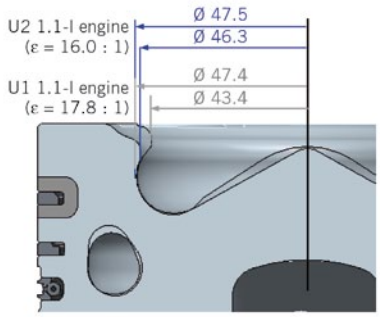

❸ Combustion chamber shape (dimension data in mm)

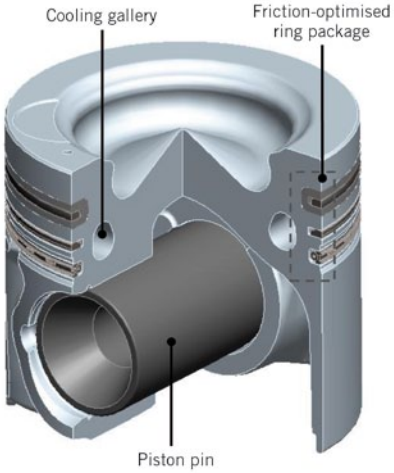

The best combination of single- and double-pilot injections with improved calibration of other control parameters enables an optimal compromise between emission, fuel economy and acoustic behaviour within the system reliability limit.

EGR AND AFTERTREATMENT SYSTEMS

To comply with stringent emission standards, it is important to control NO_x emission especially at the relatively high brake mean effective pressure (BMEP) operating range. For the small U2 engine an electronically controlled cooled EGR system with enhanced cooling capacity was adopted to reduce NO_x emissions by lowering combustion temperature, ❺.

A diesel oxidation catalyst is located at a close-coupled position just downstream the turbocharger to assure faster light-off of the catalyst, thereby minimising CO and UHC emissions. Meanwhile, due to the limited space in the engine room, the DPF is located at the underfloor position. The DPF substrate is made of aluminium-titanate. To enhance the soot and ash storage capacity, a novel asymmetric design of the substrate with a larger inlet channel volume than that of the outer channel was introduced. This ensures a lifetime ash maintenance-free DPF system, ❻.

One important issue for DPF development is an accurate estimation of the soot mass accumulated inside the particle filter. The simplest way to do that is to measure the pressure drop across the DPF and calculate the accumulated soot and ash mass. However, it turned out that the accuracy is limited under certain operating conditions, which led the engineers to devise a new scheme to extend the reliability of soot mass estimation to a wider operating range. Estimation of accumulated soot mass was updated by applying correction factors depending on the vehicle driving conditions. To reflect the effect of ash accumulation on soot estimation, several DPF samples were collected from fleet vehicles operating in a variety of driving modes and intensive investigations have been carried out.

ENGINE PERFORMANCE

Supported by the described technical features, the U2 1.1-l engine provides improved power output compared to its predecessor. A balance between maximum power output and low-end torque is essential for the drivability of the vehicle and has been another aspect in focus. As a result, the maximum torque is available throughout a wide engine-speed range. The comparison of power output with its predecessor shows the advantage of the new engine, ❼.

NVH DEVELOPMENT

In parallel with improved calibration of the injection and air management relevant parameters, engine hardware was optimised for improved acoustic behaviour. Main sources of noise emission have been identified and appropriate measures were implemented.

Since the timing device of the small U2 engine is driven by a chain system, the chain and the chain case are main sources of noise. Structural analysis was carried out for design improvement and, based on this modal analysis, reinforcement was made by applying ribs to the chains and covers. As the oil pan is another signifi-

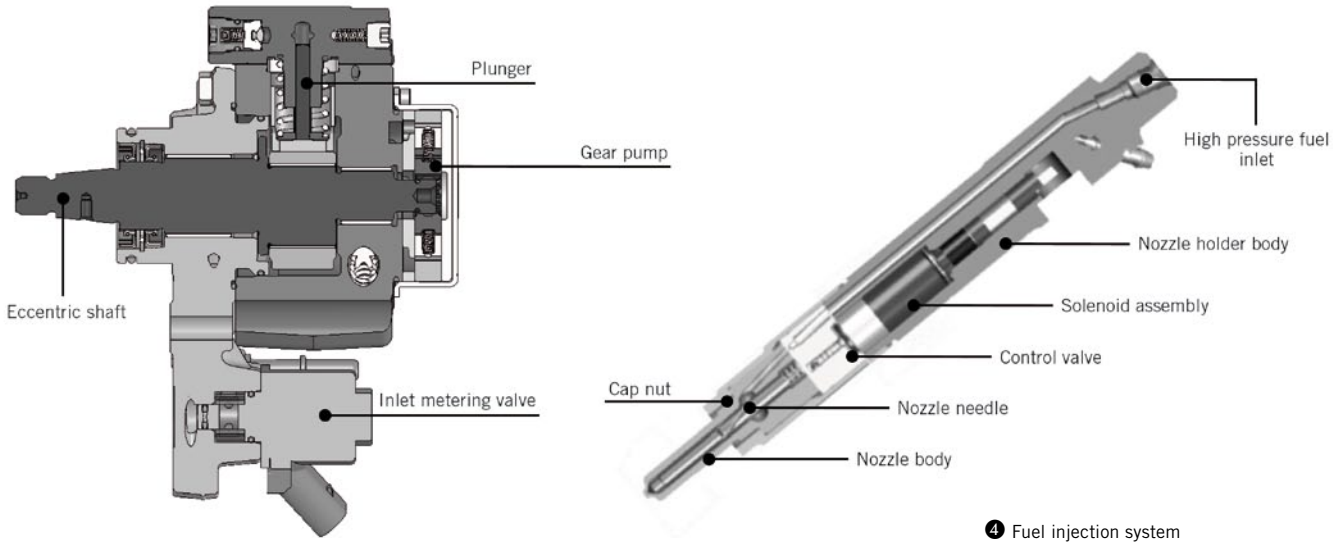

❹ Fuel injection system

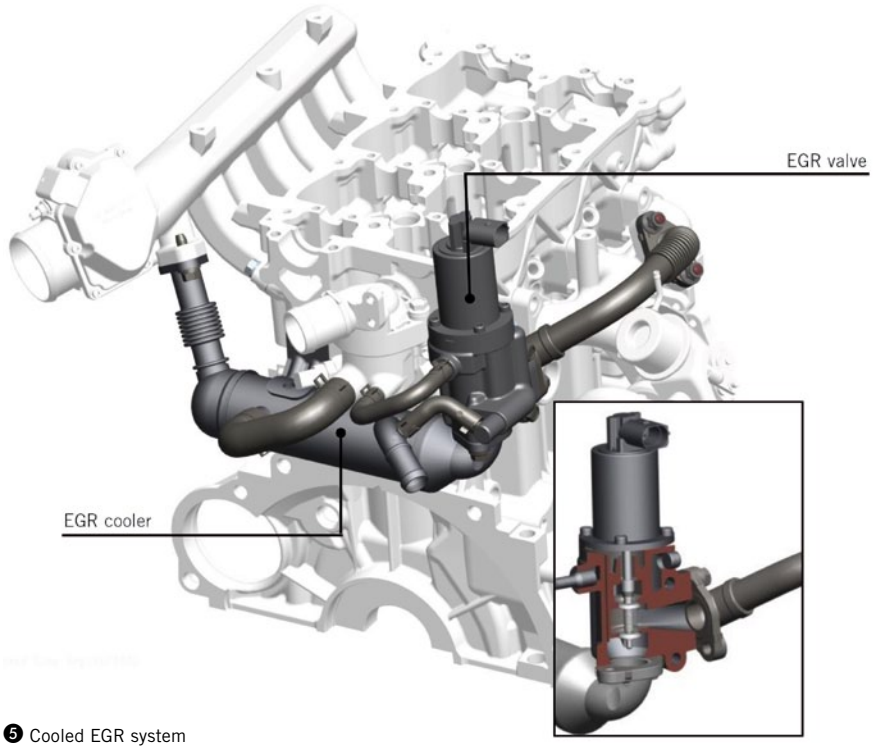

❺ Cooled EGR system

cant source of noise emission, its shape and structure were also improved. With structural analysis the effect of shape and location of ribs on noise characteristics has been investigated to find the optimal shape of the oil pan.

The sound pressure level inside the cabin was also measured, ❽, following the dynamic stiffening of the power-train. This has been realised by the introduction of the bed plate engine block structure and bell-shaped matching plane between the engine and gear box. The combination of all these measures improves the NVH behaviour significantly.

VEHICLE PERFORMANCE AND ECO MANAGEMENT

The result of the enhanced engine torque and power is an affordable acceleration performance for a B segment vehicle like the Rio, ❾. Spurred by improved power output combined with a refined selection of gear-step ratio of the matched six-speed manual gear box, drivability and fuel consumption are improved. The elapsed time for acceleration from standing to 130 km/h and from 120 to 140 km/h are 30.1 and 14.9 s, respectively. These are highly competitive values, considering that the engine achieves a very low CO_2 emission.

For improving fuel economy from the vehicle point of view, additional functions such as a battery management sys-

❻ Aftertreatment systems

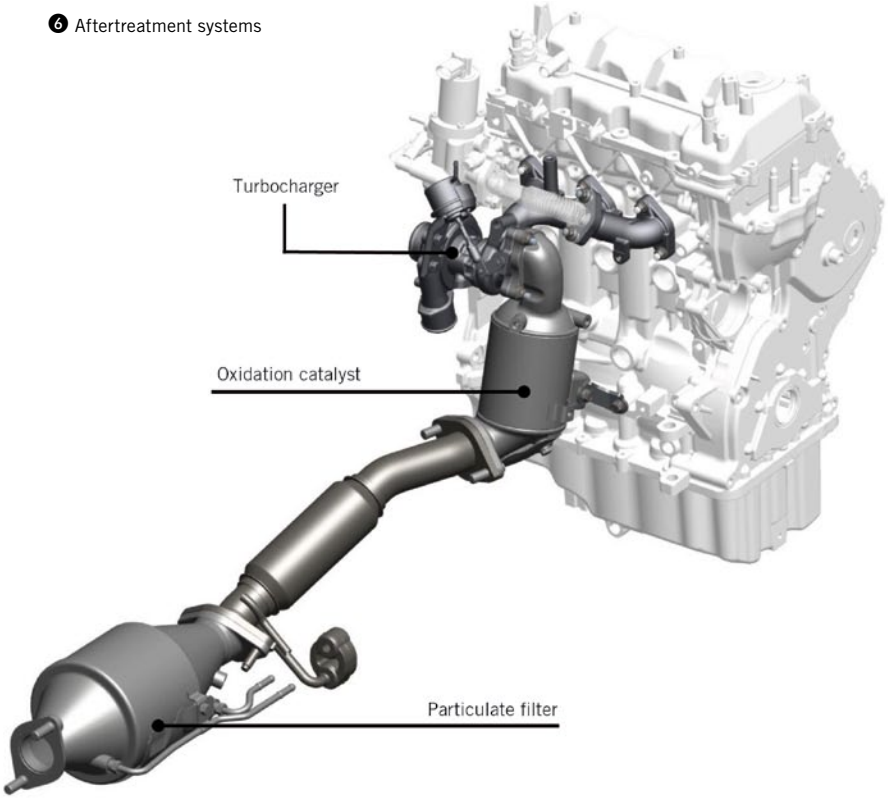

Asymmetric cell geometry of the particulate filter

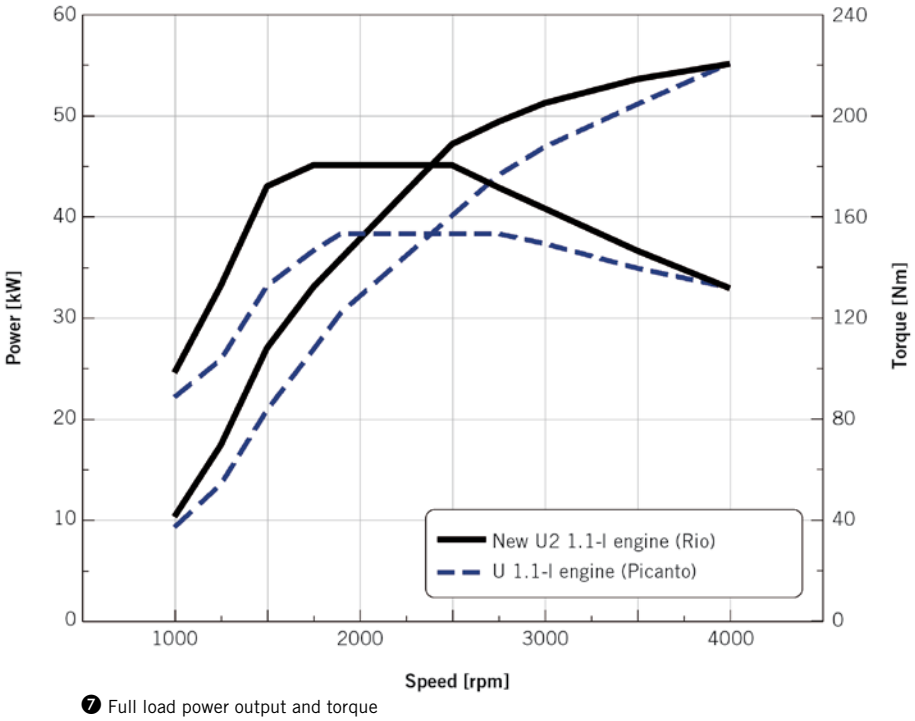

❼ Full load power output and torque

❽ Sound pressure level inside the cabin

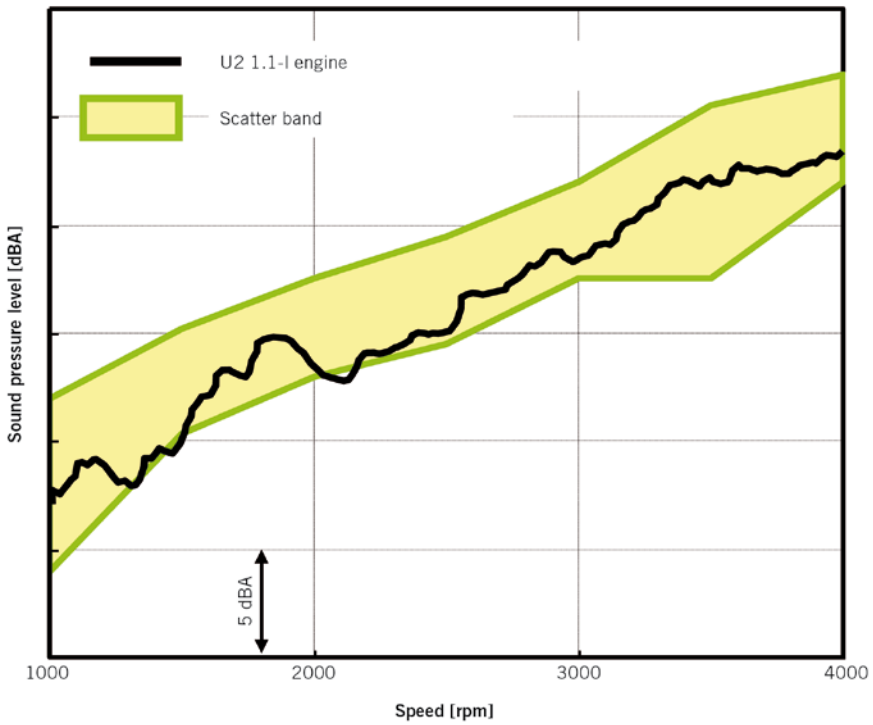

Test weight		1308 kg
Maximum speed		160 km/h
Acceleration	0 to 130 km/h	30.1 s
	120 to 140 km/h	14.9 s
CO_2 emissions		85 g/km

❾ Vehicle performance of the Kia Rio with the 1.1-l U2 engine

tem and ISS were implemented. With such technologies the fuel consumption becomes more competitive and the CO_2 level is reduced with a faster dynamic response of the vehicle compared to the current version of the engine.

SUMMARY

Hyundai developed the new U2 1.1-l three-cylinder engine to enhance the performance of B-segment vehicles by achieving a class-leading CO_2 emission of 85 g/km and complying with the stringent Euro 5 emission standard with a highly cost-effective system.

To achieve these challenging targets, various state-of-the-art technologies have been implemented to the engine and vehicle. Improvements made in the combustion system include a novel proprietary design of a combustion bowl for maximising air utilisation and reduced compression ratio. This was matched with a refined injector configuration with higher system pressure, increased number of holes and reduced hole diameter compared with the preceding system. The ISS function, combined with a braking-energy recovery system, reduces CO_2 emissions significantly. Optimisation of gear-step ratio and reduction of drag force with an active air flap and aerodynamic design are the main contributors from the vehicle side.

Thanks to the improvements in the combustion system, the diesel engine delivers maximum power output of 55 kW, which is comparable to other engines boosted by VGT, and a maximum torque of 180 Nm in the range from 1750 to 2500 rpm. With only three cylinders the engine provides comfortable NVH characteristics owing to the balance shaft module and bed plate type lower crankcase.

Based on its potential in fuel economy, power output and NVH characteristics, the small U2 diesel engine will enhance the competitive power of Hyundai/Kia B-segment vehicles by complying with tough upcoming emission legislation while maintaining its fun-to-drive performance.

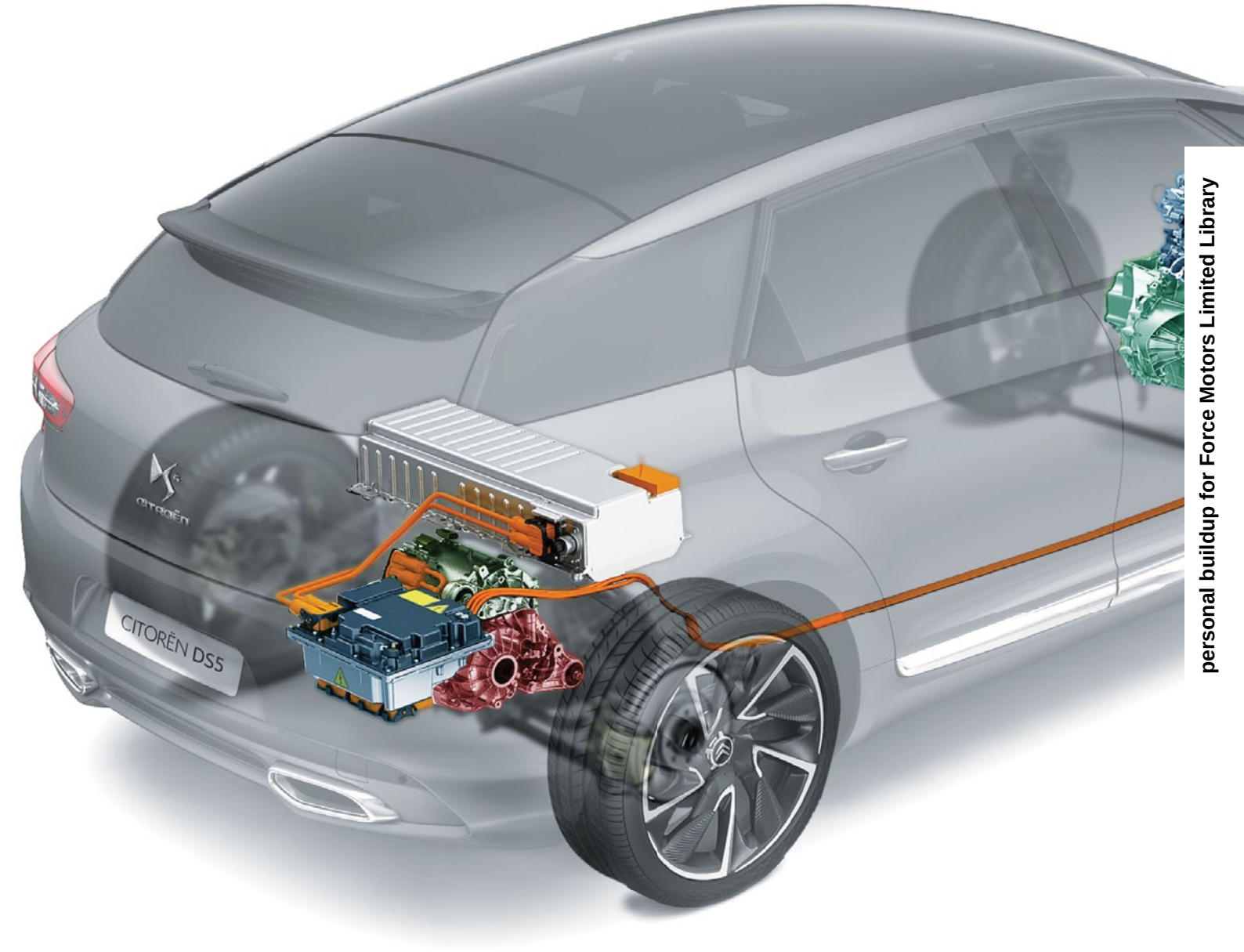

THE NEW HYBRID DIESEL POWERTRAIN BY PSA

Currently, there is a whole variety of hybrid vehicle architectures in development. Specifically, so called axle-split hybrid vehicles containing an electric drive at one axle and a combustion engine drivetrain at the other, provide not only excellent fuel efficiency but also a considerable benefit in vehicle performance. The new hybrid powertrain from Peugeot and Citroën combines an electric axle drive with a diesel engine. In the following, the axle-split system advantages, design components and its impact on CO_2 reduction will be presented.

AUTHORS

YVAN AGLIANY
is Hybrid4 Powertrain Project Manager at PSA Peugeot Citroën in La Garenne Colombes (France).

VINCENT MULOT
is Hybrid4 Powertrain System Design Leader at PSA Peugeot Citroën in La Garenne Colombes (France).

WILLIAM MAILLE
is Hybrid4 Powertrain Project Manager Deputy at PSA Peugeot Citroën in La Garenne Colombes (France).

ZAHIR BALIT
is Hybrid4 Electric Electronic Project Manager at PSA Peugeot Citroën in La Garenne Colombes (France).

AXLE-SPLIT DIESEL HYBRID

Following intensive work on hybridisation in the past decade, PSA Peugeot Citroën has developed the Hybrid4 technology. Its release on Peugeot 3008 early 2012 have been seen as a major technical breakthrough, as it is the first diesel hybrid worldwide. Hybrid4 is a highly innovative technology, and a good illustration of PSA Peugeot Citroën know how on hybrid powertrain design, ❶. The powertrain architecture is based on an original dual axle architecture which minimises the impacts on the front axle and allows the carry over of conventional engine and gearbox, concentrating the efforts on the design and the integration of a dedicated rear axle comprising battery, power electronic and rear e-motor.

The choice of the hybridisation of a diesel engine ensures drastic performances, including unrivaled fuel economy for a compact SUV as well as a high level of dynamic performances. Taking advantage of the dual axle architecture the design team decided to offer to the client four differentiated driving modes, ❷. The automatic mode is dedicated to fuel economy, emissions reduction and offers to the driver an exceptional drivability and comfort. In this fuel-saving mode, thanks to hybrid technology, the Peugeot 3008 reaches 99 g CO_2/km on MVEG cycle. In ZEV mode, the driver will enjoy the capability of the system to run on pure electric driving for urban usage. Compared with automatic mode, the pure electrical capability is improved in terms of acceleration and engine start is avoided unless the driver needs higher power. In sport mode, the design team emphasised

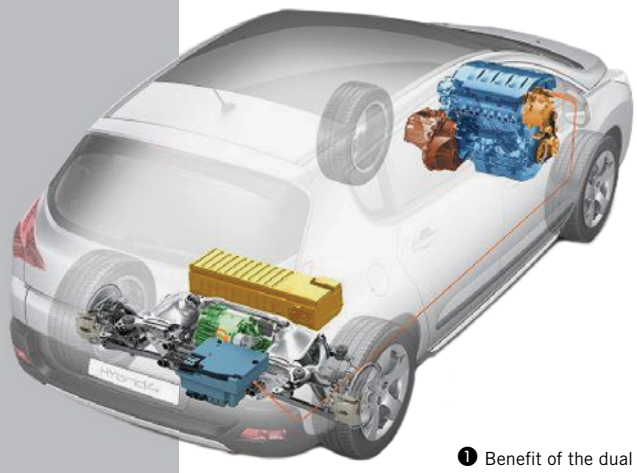

: A step change in terms of fuel economy by using the efficiency of the diesel engine, used over its optimum operating range, with an electric motor on the rear axle suited to urban driving

: Improved driveability and original eAWD features offered by dual axle architecture

: Minimal impact on front axle: ability for PSA to carry over conventional engine and gearbox

❶ Benefit of the dual axle hybrid topology

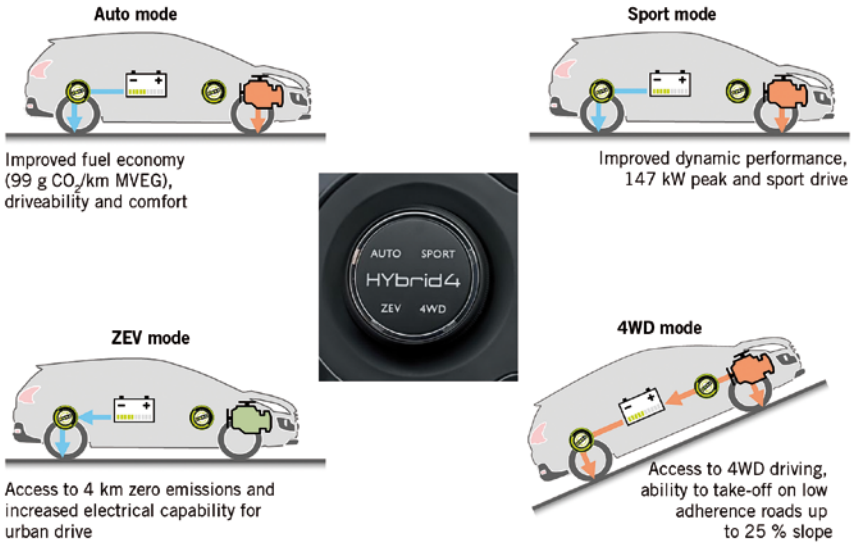

❷ Dual axle hybrid topology with four driving modes

the dynamic behaviour of the vehicle, and the simultaneous use of power from the internal combustion engine on the front axle and the 27 kW electrical boost on the rear axle, offering to the client a highly dynamic vehicle with a grand total performance of 147 kW. In 4WD mode, power is released from the engine through two paths: while engine power is supplied to the front axle for vehicle traction, a fraction of it is derived from the front 8.5 kW motor to the rear motor, offering a unique 4WD feature through hybridisation. With this innovative feature, the client is able to take-off on low adherences grounds for slopes up to 25 %.

POWERTRAIN SYSTEM DESIGN

Such complementary modes offered by the powertrain are made possible by the combination of key functionalities, ❸. Some of them are standard for parallel hybrid architecture, others are new features developed to use all the potential offered by Hybrid4 topology.

Start/stop is the first key functionality adapted to Hybrid4 technology. This functionality enables to stop the engine, at vehicle stop or when electrical drive is required, to improve efficiency. In case of high torque request from the driver, the restart must be performed in a very short time in order to deliver the requested traction. Design of the components and adaptation of the diesel engine calibrations lead to a best in class start/stop functionality.

The design team developed a coupling/decoupling function for the rear e-motor. To achieve good electrical accelerations in urban usage, a high value for rear gearbox ratio should be chosen but with a direct impact on e-motor losses on highway usage. The coupling/decoupling functionality allows to overcome this constraint. The rear e-motor decouples automatically above 120 km/h and, when vehicle speed decreases below 120 km/h, the rear machine couples again automatically to re-activate rear axle. This function is also activated below 120 km/h, to improve fuel economy and minimise losses, when traction is performed by front axle on stabilised speed with no need for electrical torque, ❹. Coupling is performed in a very short time (approximately 500 ms) when electrical drive is needed.

Drivability improvements are also obtained with the chosen architecture by using the rear electric axle to compensate the front torque reduction during automated manual transmission (AMT) gear shifting, ❺. This compensation needs a good torque precision and coordination between the front clutch and the rear

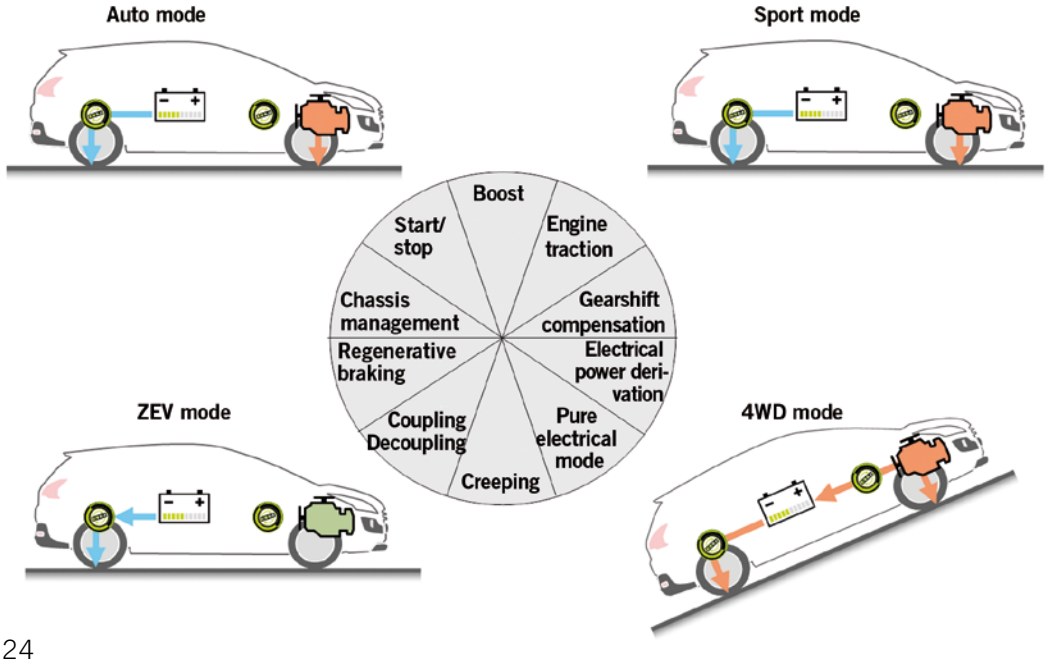

❸ Hybrid4 powertrain system functionalities

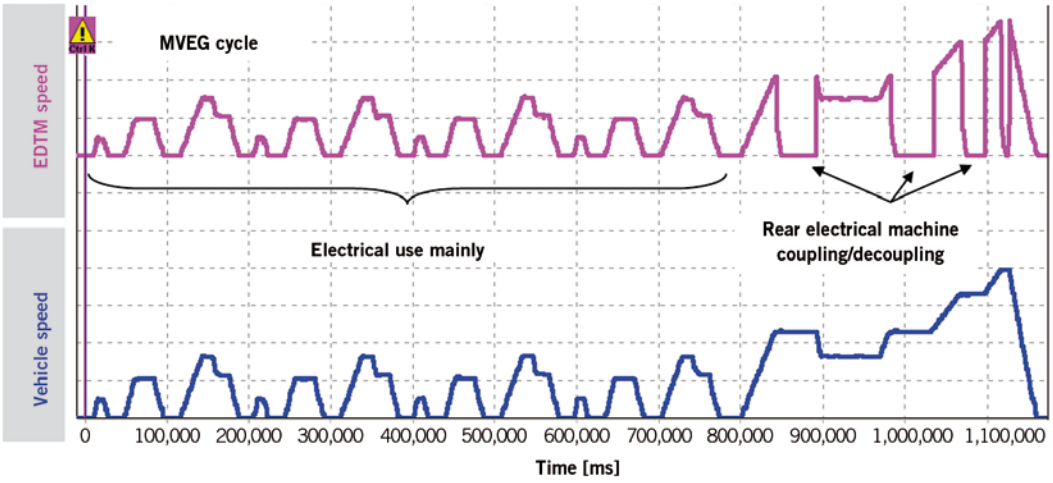

❹ Rear electrical machine coupling/decoupling functionality (schematic view)

e-motor. The coordination is adapted to the gearshift profile of each mode (dynamic, smooth, etc). This compensation allows to keep a constant acceleration during gear shifting, equivalent to a conventional automatic transmission, for a wide range of vehicle acceleration.

Regenerative braking is one of the key features of parallel hybrid. This functionality brings a 16 % fuel reduction on MVEG cycle. The driver can control the vehicle deceleration with the gas pedal in a range up to 1 ms². At low speed this deceleration is reduced slowly to ensure a smooth transition with electrical creeping around 15 km/h. Another functionality is the electrical boost when rear axle and front axle are combined to maximise power delivered at wheel. Powertrain can then deliver 147 kW as peak power. Thanks to Hybrid4 topology, the additional power is supplied on the rear axle of the vehicle that enables to limit the mass transfer during acceleration and improves power capability at wheels.

The teams of chassis and powertrain design also took advantage of the dual axle architecture to propose an original 4WD feature. When using the 4WD mode the powertrain determines a static torque split and supplies torque to the two axles. When the electronic stability programme (ESP) detects a slip on one of the wheel, an traction control (ASR) request is sent from the chassis to the powertrain which then reduces the applied torque on the slipping wheel and modifies the torque split to transfer the desired torque to the second axle. Thus the grip is ensured at all time and the torque transfer function allows the driver to takeoff on slopes up to 25 %, ❻.

Electrical energy available from the battery being limited to 1.1 kWh, an additional functionality was developed to ensure continuous 4WD mode. While engine power is supplied to the front axle for vehicle traction, a fraction of it is derived from the front 8.5 kW motor to the rear motor. In such mode, the high voltage battery supports peak power need whereas energy derived from front axle supports a continuous power that maintains the state of charge of the battery. The front e-motor was designed to continuously supply power for mountain usage with slipping surface.

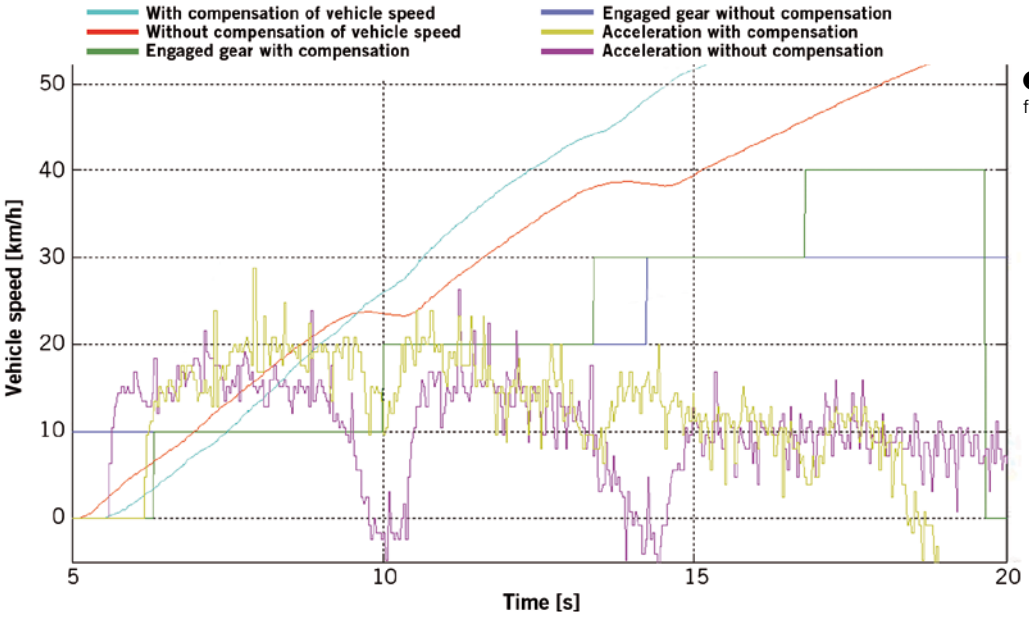

❺ Gear shift compensation functionality

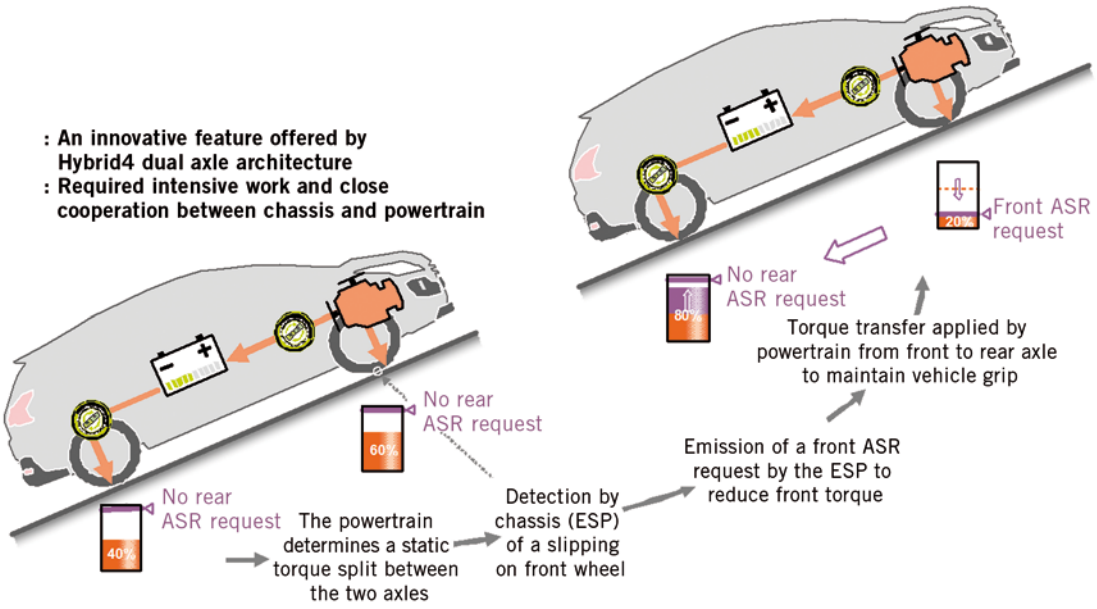

❻ 4WD powertrain mode

A pure electrical function ensured by rear e-motor and high voltage battery was designed. In automatic mode, this function is selected automatically by powertrain management to optimise fuel economy. In real time, depending on speed and acceleration, the system control compares the efficiency of thermal engine with the efficiency of electrical system. If a benefit is determined, the engine stops and the pure electrical mode is used. This optimisation is also related to high voltage battery state of charge to ensure the robustness of this function and avoid very low state of charge. Using this functionality alternatively with recharging mode (regenerative braking or recharge derived from engine), the powertrain can offer a range up to 300 km of cumulative electrical drive on a total range of 900 km. When the driver selects ZEV mode, priority is given to electrical acceleration down to low state of charge of the high voltage battery. Then the driver can easily run in pure electrical mode up to 60 km/h and for a range of 4 km.

In addition, Hybrid4 also offers some pure thermal engine traction phases. This function is used to ensure vehicle drive at middle to high power when power needs is above electrical capabilities (or low state of charge of the battery). In this phase, six-speed AMT is controlled to optimise engine operating points and front e-motor to support high voltage battery state of charge if natural regenerative braking is not sufficient.

Creeping was not included in AMT transmission basic features. The design team also took advantage of the architecture to develop such functionality through the support of the rear e-motor. It is simply activated at zero speed when the driver releases brake pedal and deactivated after 2 s with pushed brake pedal. With this function, the vehicle can drive up to 12 km/h and maintain vehicle in slope up to 5 % in forward and reverse direction. This function is a key feature to move vehicle silently and smoothly for parking drive or in heavy traffic jam.

All described functionalities are combined in order to offer to the driver the maximum range of capabilities of Hybrid4 architecture in the different modes. In order to reduce fuel consumption and improve driveability, automatic mode is the result of the combination of pure electrical mode, start/stop, regenerative braking, coupling/decoupling, thermal engine traction, gearshift compensation and creeping. Sport mode disables pure electrical mode and activates more boost in order to maximise dynamic response of the powertrain. In 4WD mode, specific chassis management and power derivation are activated whereas start/stop and pure electrical mode are disabled to optimise 4WD traction at low speed and keep state of charge of the high voltage battery even at vehicle stop.

SUB-SYSTEMS AND COMPONENTS DESIGN

Based on system design, the project team worked intensively to develop new subsystems and components or to adapt existing ones so that the hybrid architecture, ❼, can fulfil all expected performances. This development was made jointly with key suppliers, bringing their great expertise in this highly challenging and innovative project.

The hybrid power control unit (HPCU), developed by Bosch, is the overall control unit of the electric system of the Hybrid4. It comprises two processors that control and supervise both electric motors, the powertrain management unit (PTMU) and auxiliary devices like cooling water pump and dog clutch. The DC-DC converter that had to be integrated needed to have a continuous power output of 2.5 kW. Since such a device was not available for the necessary design space, Bosch decided to launch an in-house development of that DC-DC converter. The double-inverter features second generation insulated gate bipolar transistor (IGBT) power modules that provide a maximum phase current of respectively 340 A in case of the electric drive traction machine (EDTM) and 120 A in case of the belt alternator starter machine (BASM). Contrary to a conventional inverter, which Bosch uses in an earlier series project, the new double-inverter features double functionality within a hardware design space comparable to a single inverter.

During the development process of the EDTM traction machine, primary focus from the design team, was on a reduced moment of inertia, low bearing friction and little overall weight. The liquid cooled, permanent excited synchronous

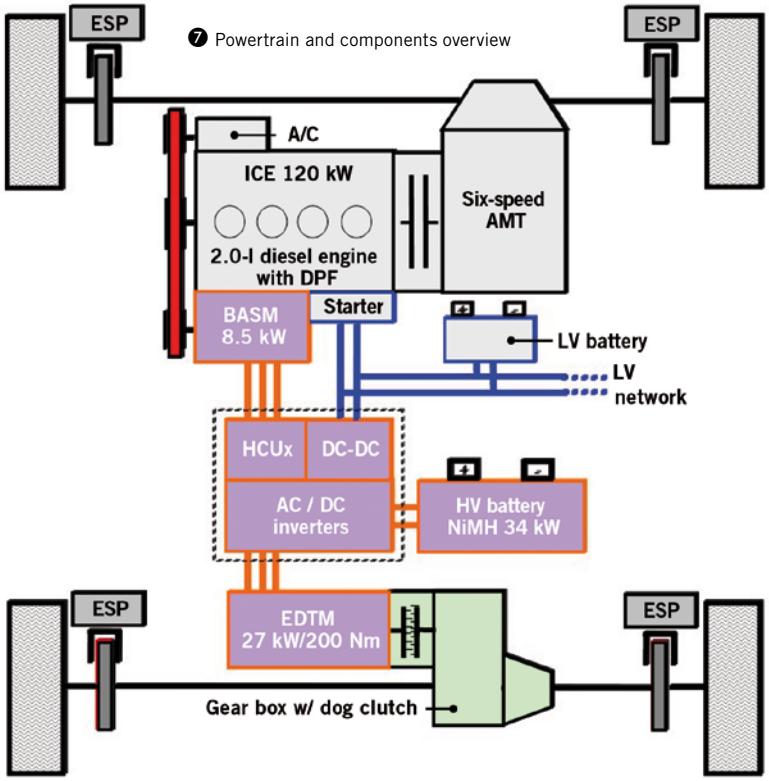

❼ Powertrain and components overview

machine features distributed stator windings and an iron length of 120 mm. Sensing the electric motor position angle is done by using a resolver. This device provides – contrary to digital positioning sensors – an analog sensor signal which is directly related to the position angle of the electric machine. The power electronics uses this position signal to provide a dynamic and robust EDTM control under all vehicle operations.

Main requirement for the BASM, which is mounted in the diesel engine's belt drive, is to replace the traditional low-voltage alternator. The BASM has to fit in the available design space of the formerly used alternator. With a continuous power output of 8.5 kW the BASM can directly support the EDTM during 4WD vehicle operation leading to maintaining the charge of the high voltage battery. Additionally, the BASM offers a start/stop mode to the combustion engine. The necessary torque output is 52 Nm which is supplied by an iron length of 80 mm and features single-tooth stator windings. The crankshaft torque to start the combustion engine is applied via a specifically designed belt pulley.

The high voltage (HV) battery, key component of the hybrid system, is developed from Sanyo. Ni-MH technology was chosen by considering the trade-off between cost, technology maturity and performances. Based on proved unitary cells, the system design of the battery had to meet strong requirements regarding efficiency, power, energy capability and packaging. The assembly of 168 cells offers a range of 150 to 270 V to maximise high voltage efficiency of electric system. It offers a maximum peak power of 31 kW to ensure regenerative braking or boost functions. 5.5 Ah (1.1 kWh) is also available to give a 4 km range autonomy in pure electrical mode.

The design team decided to carry over the so-called BMP6 six-speed automatic manual transmission (AMT) on the front axle. First requirement was to contribute to high efficiency of the powertrain when front axle is used in the different modes. Thus a new high efficiency oil was developed and validated for the AMT. In addition, the gearshift management was tuned to improve engine setpoints regarding fuel economy. The PSA AMT was also reinforced to provide 300 Nm maximum torque to take advantage of the 120 kW engine power.

The new rear gear box developed by GKN was a high technical challenge in regard of compacity to allow the integration into rear axle. The solution was the addition of a compact actuation and a good integration with the e-machine. Its 7.46 ratio was defined in association with 200 Nm e-motor to ensure acceleration in pure electrical mode. In order to decouple rear machine at 120 km/h, a dog clutch with actuator was part of the design. Actuator and sensor were designed to ensure precision of the control and transparent coupling/decoupling phases. The contribution to fuel economy was a key requirement. It was fulfilled with dog clutch technology that minimise mechanical losses and with a high efficiency mechanical design.

The design team also decided to carry over the 120 kW 2.0-l HDi diesel engine on the front axle. High torque delivered by front e-motor and high number of start/stop phase lead to develop a new front end accessory drive (FEAD) with reinforced belt. The quick startup of the 2.0-l engine was a high requirement to ensure quick torque response during transition from electrical drive mode to thermal engine traction. Fuel and emissions reduction was also a main requirement that lead to adapt the calibration to hybrid usage setpoints.

The powertrain management developed by PSA coordinates all powertrain sub-systems. This manager was developed to synchronise all hybrid functionalities described above. To manage smooth transitions between modes, the control unit is based on a global torque control of the different torque generators (clutch, engine, e-motors). Torque requests are adapted in real time to fullfill permanently torque driver demand. Powertrain also takes into account in real time all torque limitations information sent by components in case of functional or dysfunctional limits. The powertrain management also controls the activation and deactivation of the powertrain, to fulfil the strong safety requirements regarding torque and high voltage.

FUEL ECONOMY

❽ depicts an overview on how various facts and measures affect fuel consumption. In the Hybrid4 the additional penalties are estimated to be around 3 % for the extra weight of components such as

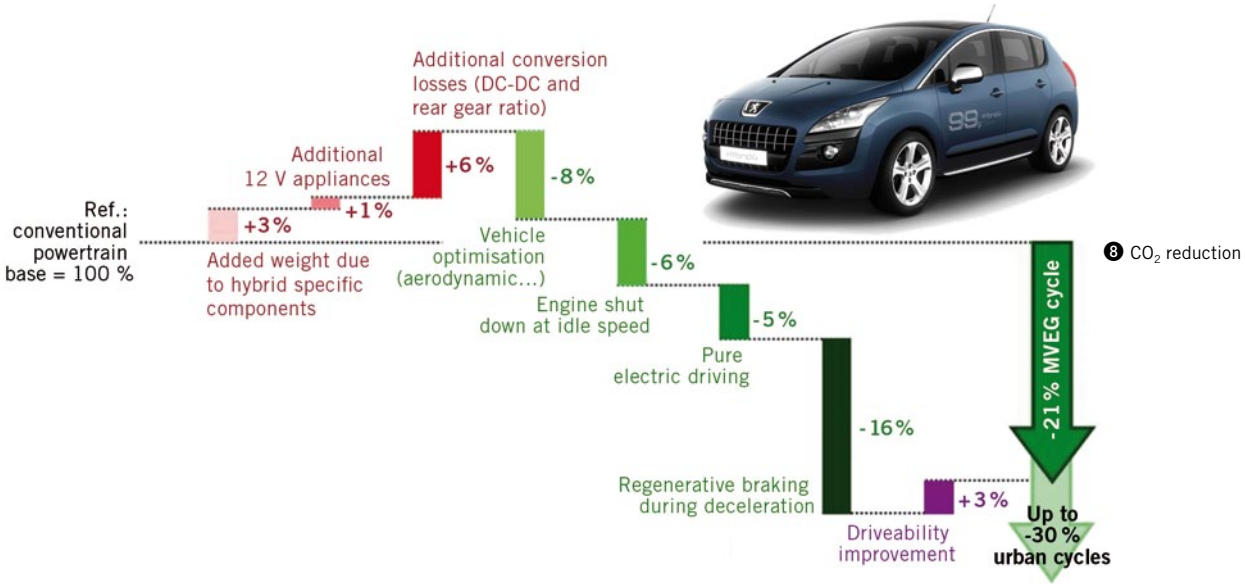

battery or power electronic, 1 % for extra additional 12 V consumption and 6 % for conversion losses (either mechanical or electrical). To cope with these negative consequences of hybridisation, the design team worked on vehicle body optimisation (e.g. aerodynamic drag reduction) for a benefit of 8 %, benefits from engine shut down at idle speed (6 %), pure electric driving (5 %) and regenerative braking during deceleration to benefit from vehicle kinetic energy (16 %).

The trade-off made between fuel economy, dynamic performances and drivability (e.g. boost function or torque compensation during gear shifting) are estimated to be worth 3 % in the total result. As a result the Peugeot 3008 Hybrid4 emits only 99 g CO_2/km on MVEG cycle which represent a gain of 21 % compared to an equivalent conventional vehicle. For urban cycles fuel economy might reach gains up to 30 to 35 % as the effect of hybridisation will be more important for low speed cycles.

CONCLUSIONS

The axle-split hybrid vehicle topology presented in this article introduces a sophisticated 4WD capable hybrid vehicle unveiled from Peugeot Citroën in their Peugeot 3008, 508 RXH and Citroën DS5 models early 2012. Bosch, Delphi. GKN, Magneti Marelli and Sanyo are the key suppliers to develop or adapt components to support Peugeot Citroën launching the first diesel hybrid vehicle worldwide.

BOOSTING CIRCUITS WITH THE NEWEST KNOWLEDGE.

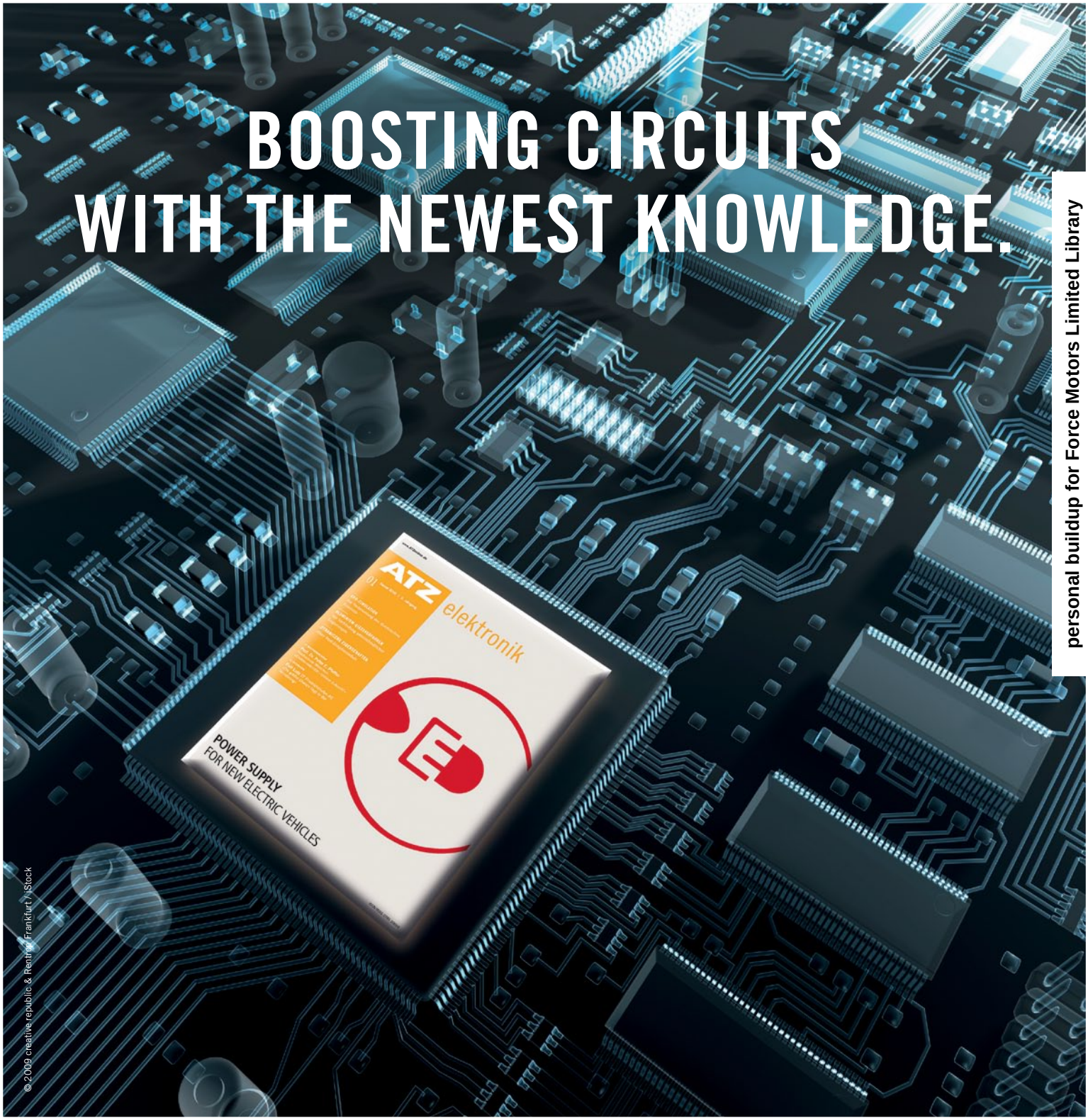

LEADING TECHNICAL KNOWLEDGE, WHICH PUTS AUTOMOTIVE ELECTRONICS INTO GEAR.

Electronics are the motor for innovation in automotive engineering. **ATZ elektronik** delivers the newest findings on electric mobility, high performance electronics, energy management, testing, human-machine interaction, consumer automotive electronics, and anything else that would electrify automobile developers. Geared for professionals who seek unique in-depth information.

More information at: www.ATZonline.de/leseprobe/atze

ATZ elektronik

ELECTRONIC FUEL INJECTION SYSTEM FOR HANDHELD WORKING EQUIPMENT

Stihl has developed an electronically controlled fuel injection system for hand-held working equipment and has introduced it on the market with the TS 500i cut-off machine. As a batteryless concept, the system can be restarted without special maintenance even after long periods out of use.

AUTHORS

DIPL.-ING. WOLFGANG ZAHN
is Member of the Board of Management, responsible for Research and Product Development worldwide, at the Andreas Stihl AG in Waiblingen (Germany).

DIPL.-ING. HEIKO DÄSCHNER
is Manager for Integrated Electronic Systems in the Research Division at the Andreas Stihl AG in Waiblingen (Germany).

DIPL.-ING. WOLFGANG LAYHER
is Manager for Mechatronic Systems in the Research Division at the Andreas Stihl AG in Waiblingen (Germany).

DIPL.-ING. ARNO KINNEN
is Manager for Advanced Research in the Division Power Tools at the Andreas Stihl AG in Waiblingen (Germany).

MOTIVATION

The two-stroke internal combustion engine with carburetor remains the preferred drive system for hand-held working equipment. Proven thousands of times over, and continually optimised over several decades, the carburetor of today is a highly perfected product, both as engine component and in the technology used for its production, but it is now also close to the absolute limits of its development. This article describes the construction and operating principle of an electronically controlled batteryless fuel injection system for two-stroke engines, breaking free of the constraints of the Venturi principle that underpins the carburetor and thereby providing the means for meeting the requirements of the future.

COMPONENTS OF THE BATTERYLESS FUEL INJECTION SYSTEM

The central component of the injection system, ❶, is the electronic control unit, which controls ignition and injection without requiring a battery. The electrical energy for the fuel injection system is obtained from a generator (alternator) connected to the crankshaft. This system delivers an alternating voltage with its frequency and amplitude modulated as a function of the engine speed. In the lower engine speed range, a boost converter in the control unit increases the rectified alternator voltage to a defined level, thereby providing electrical energy for the continuous loads, even at the starting engine speed.

Detection of the crank angle is indispensable as an input variable for fully electronic engine management. This angle is determined from the induction voltage curve of the generator signal. The points where the generator voltage crosses the zero level are without electrical load and therefore represent known fixed-position angle marks in the crank circle. Consequently, no additional sensor for the crank angle or top dead centre is required.

As soon as the user pulls the starter rope and the engine speed has passed a given threshold, the initialisation and synchronisation process of the control unit is started. During initialisation, the control unit starts with a system test to check that all the measurable variables have plausible values. If this test is successfully completed, synchronisation of the generator signal with the crankshaft position is started, ❷. At the latest after a crank angle of 315° the control unit recognises the position of the crankshaft and starts the functions that are synchronised with the crank angle, such as ignition and fuel injection.

The available sensor inputs are fed in at regular timed intervals, and sometimes several times per operating cycle. Both the load signal, via crankcase pressure and temperature measurement, and the position of the stop switch are recorded as analog variables over the full engine speed range. As output variable, a valve output stage is implemented, operating as an independent closed-loop control circuit that holds the voltage for the injector valve at a setpoint value. Consequently, the controller requires only timer-controlled discrete signals in order to implement fuel injection. This system reduces the worlkload of the microcontroller, so that, despite limited resources, computing time is available for other control tasks. The control unit also integrates high voltage generation, including the ignition coil. This module forms a coil ignition system with freely selectable ignition timing and variably adjustable dwell angle.

The control unit comprises a 16-bit microcontroller with 64 kB flash ROM and 8 kB RAM. The microcontroller operating system has been developed in-house specifically for this application, in order to perform the fast real-time calculations required for basic operation of the engine. The adaptive software controllers that run on the operating system are individually developed for specific models and are ported to the target processor by automatic code generation.

To detect the operating point of the two-stroke engine, a pressure/temperature sensor is fitted at the crankcase. The pressure sensor is a piezo-resistive absolute pressure sensor with analog pressure measuring circuit for signal conditioning. The pressure is applied at the front, and a layer of gel protects the circuitry from aggressive media in the crankcase. The temperature sensor is a standard NTC element.

The injector valve is designed as a pure metering valve. Unlike conventional fuel injection systems, there is no primary atomisation at the valve. The rotation of the crankshaft in combination with the inflow and outflow processes in the crankcase generate a highly turbulent air flow. Mixture preparation takes place during the secondary stage, i.e. during the transfer process in the crankcase, transfer ports and combustion chamber. Fuel injection is triggered once per revolution in synchronism with the combustion cycle. The injection frequencies vary from 0 to 170 Hz, with injected fuel quantities between minimal 1 mg and maximal 45 mg per injection.

The injection pump provides a reliable supply of fuel under all operating conditions and in all engine positions. The diaphragm pump and pressure reducer are housed in a single component. In addition, a manual fuel pump ensures that if the system has been run until empty it can be easily vented and restarted with only a small number of pulls of the starter rope. The concept of the diaphragm pump is characterised in particular by its simple construction, robust operating characteristics and insensitivity to air and vapor. The pump is driven by means of the crankcase pressure. The pressure reducer is designed as a spring-loaded diaphragm pressure reducer and regulates the operating pressure to 100 mbar above atmospheric pressure. On the intake side, a fuel filter, complete with magnetic separator, is installed upstream of the injection pump.

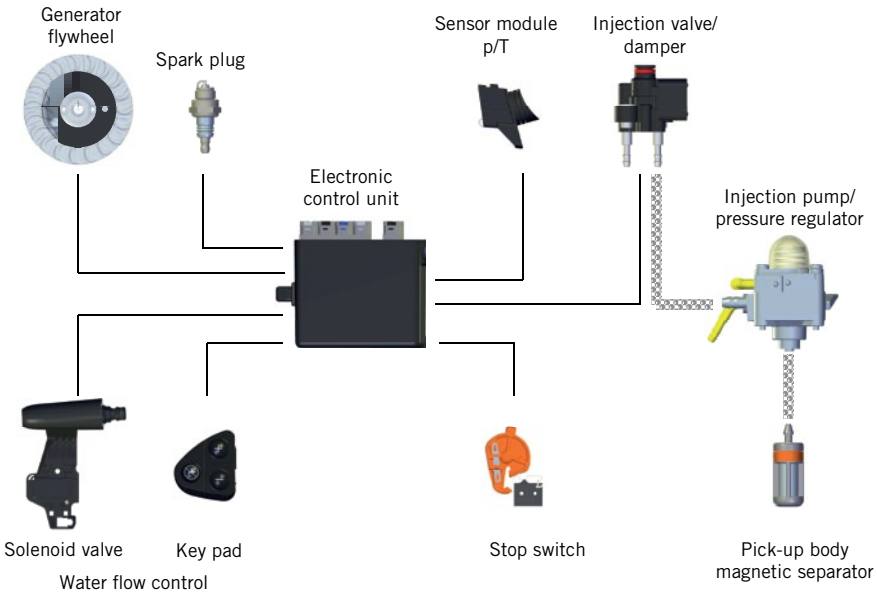

❶ Injection system by Stihl

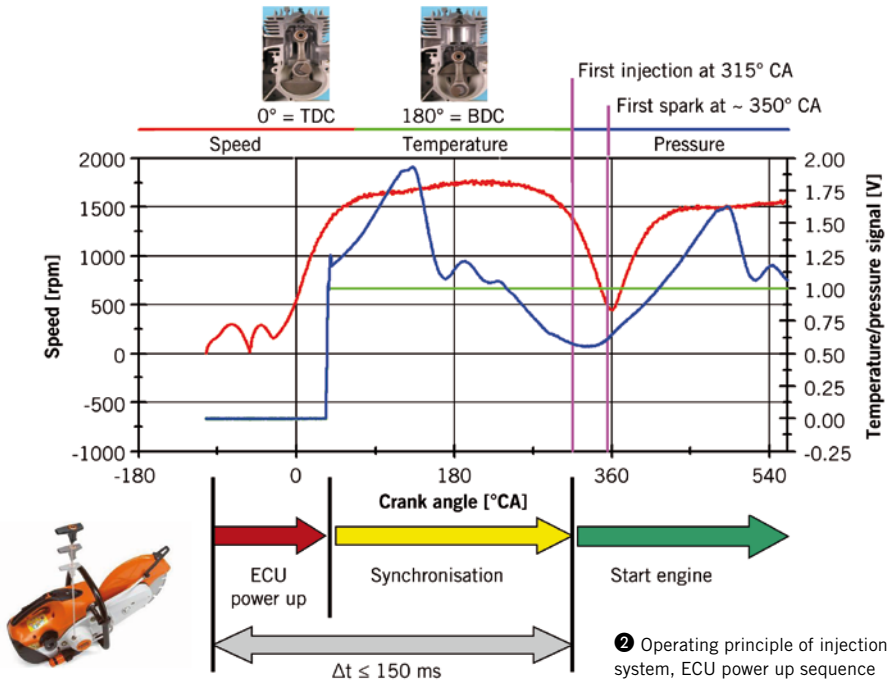

❷ Operating principle of injection system, ECU power up sequence

INTEGRATION IN THE CONSTRUCTION OF A HAND-HELD WORKING MACHINE

The injection system was introduced on the market with the TS 500i cut-off machine. ❸ shows the technical data of the TS 500i. The core engine uses the 2-Mix system from Stihl, which delivers optimised fuel efficiency and low emissions. The cross-sections and lengths of the transfer ports and the engine control timing have been specially adjusted to create internal stratified fuel charging by advancing the exhaust, thereby minimising scavenging losses during the load change in the gas cycle. In addition to the low exhaust emissions, the engine has high combustion efficiency, which

	TS 420 A	TS 500i	TS 700
FUEL SYSTEM	Carburetor	Stihl injection	Carburetor
ENGINE TECHNOLOGY	Stihl 2-Mix	Stihl 2-Mix	Stihl 2-Mix
WATER CONTROL	Electronic	Electronic	Manual
DISPLACEMENT [cm³]	66.7 cm³	72.2 cm³	98.5 cm³
POWER	3.2 kW at 9000 rpm	3.9 kW at 9500 rpm	5.0 kW at 9300 rpm
TORQUE	3.8 Nm at 7000 rpm	4.6 Nm at 6000 rpm	5.8 Nm at 6500 rpm
WEIGHT	10.1 kg	10.2 kg	11.6 kg
SPEC. FUEL CONSUMPTION	500 g/kWh	420 g/kWh	450 g/kWh
VIBRATION LEVEL $a_{hv,eq}$ LEFT/RIGHT	3.9 m/s² / 3.9 m/s²	2.4 m/s² / 2.0 m/s²	6.6 m/s² / 4.5 m/s²
NOISE LEVEL $L_{p,eq}$	98 dB(A)	98 dB(A)	101 dB(A)

❸ Technical data TS 500i in comparison to other Stihl cut-off machines

leads to a combination of low fuel consumption and high power output power.

The design of the TS 500i is based on the proven top-handle concept of compact cut-off machines. The control unit is located on the tank housing directly underneath the rear handle. For servicing and maintenance, there is the added advantage that all connectors, including the diagnostic connector, are easily accessible via the service cover. The technical control features eliminate the need for a separate throttle shutter start position, which is normally required for machines powered by a carburetor engine. Consequently, the presented system has only two switch positions: "0" for machine stop (OFF) and "1" for both engine start and machine operation.

In the presented system, the carburetor of conventional machines is reduced to a throttle shutter body with a throttle shutter actuated by the throttle cable. The injector valve and sensor module are located underneath the throttle shutter, directly on the crankcase, ❹. The control unit also controls the integral water system of the cut-off machine. When cutting concrete, the control unit automatically activates the water flow required to bind the generated dust and sets the volumetric flow rate to the user-selected quantity by means of a solenoid valve.

KEY FUNCTIONS OF THE FUEL INJECTION SYSTEM

Load control in the gasoline engine is quantitative, by means of the variable adjustment of the throttle shutter by the user. If the crankcase of the single-cylinder two-stroke engine is considered as a port-controlled piston pump, the air mass passing through the unit can be determined by measuring the pressure and temperature in the crankcase. A measuring and analysis algorithm specially adapted to the engine can then be used to determine the air mass flow at the operating point.

In the two-stroke engine, the fuel is fed into the crankcase. For this purpose, fuel is injected at a system pressure of 100 mbar above atmospheric pressure during the upwards movement of the piston. Since at this point in the cycle the pressure in the crankcase is negative (vacuum), the pressure drop available for fuel transfer is higher than the system pressure, ❺.

Characteristic maps are used for the basic stoichiometric setting. The data relating to the engine speed and throttle/load status of the engine enables the optimal operating parameters – such as injected fuel quantity, injection angle and ignition timing – to be selected for each stationary operating point. By contrast, conventional fuel/air mixture systems for hand-held working machines generally have a one-dimensional characteristic curve that sets the ignition timing solely as a function of the engine speed.

The present system, adapts to changing operating conditions (e.g. temperature or geodetic altitude), fuel qualities or wear by means of intelligent map-based pilot controls and closed-loop controllers that determine the required corrective values and adjustments and calculate the basic operating variables. Over the entire product life span, these systems take over the time-consuming task of carburetor adjustment, which otherwise in some cases can require expert knowledge on the part of the user.

During operation, special software functions constantly monitor whether the machine is running at optimal performance and make corrections to indi-

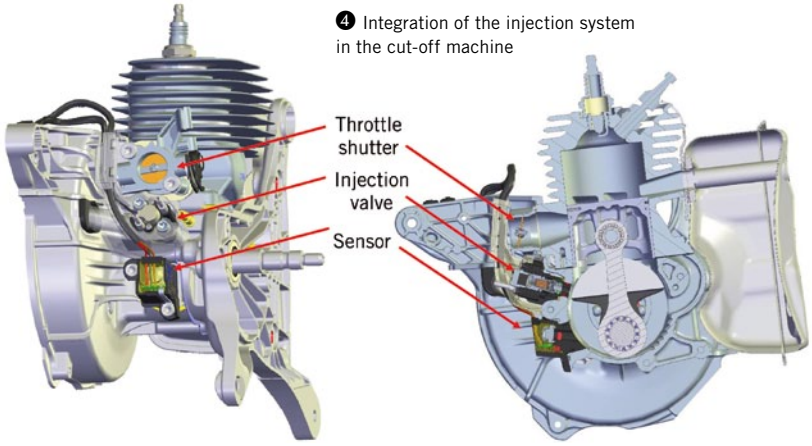

❹ Integration of the injection system in the cut-off machine

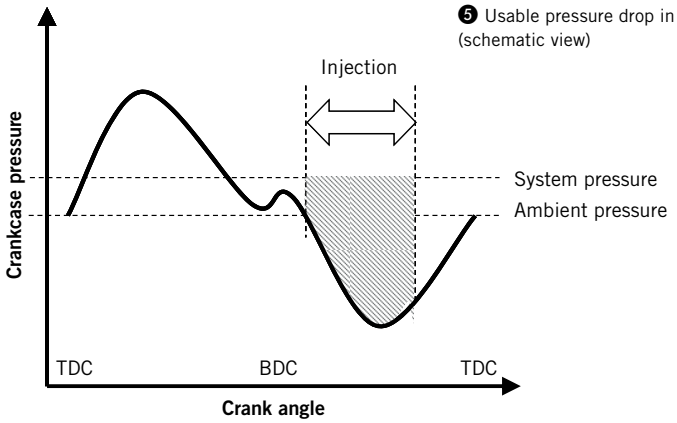

❺ Usable pressure drop in the injection process (schematic view)

vidual operating parameters when necessary. These adjustments can be made in exactly the same way in the wide open throttle range, in engine speed limiting or during machine idling. Correction values are stored at the end of machine operation and are available for the next machine operation. Consequently, long-term adjustments for wear and filter fouling are possible, as well as short-term adjustments to changing ethanol content in the fuel.

The control unit also implements comprehensive diagnostic functions. For example, the control unit performs both an electronic self-diagnosis and a test of the connected components. Each implausible action during operation of the electronic fuel injection system generates an entry in the fault memory. With the aid of a special developed engine diagnostic unit, the fault memory can be read out and failures in the injection components can be detected with the engine at standstill.

SUMMARY AND OUTLOOK

With the presented system, for the first time, an electronically controlled fuel injection system for hand-held working equipment has been developed into a marketable product. All components, including the control unit software, have been specially developed for the specific needs of hand-held machines. The new injection system adapts intelligently to the actual fuel qualities used, the operating altitudes and the fouling levels of the working machine filters. As a batteryless concept, the system can be restarted without special maintenance even after long periods out of use. Since all the benefits of a modern fuel injection system are in operation from the moment the machine is started, starting is extremely simple under all conditions. If required, the system can be expanded with additional sensors and actuators, so that it is ready for all future requirements.

REFERENCES

[1] Gegg, T.: Analyse und Optimierung der Gemischbildung und der Abgasemissionen kleinvolumiger Zweitakt-Ottomotoren. Logos: Berlin, Dissertation, Universität Karlsruhe (TH), 2007
[2] Hehnke, M.; Leufen, H.; Naegele, K.; Bähner, A.: Intelligent Engine Management Systems for Small Handheld Low Emission Engines. SAE Paper 2009-32-019, 2009
[3] Gorenflo, E.; Gegg, T.; Hehnke, M.: Entwicklungstendenzen bei hochdrehenden Kleinmotoren. TAE Esslingen, 2010
[4] Kinnen, A.; Layher, W.; Däschner, H.: Electronically controlled batteryless injection system for small two-stroke SI engines. 12th Stuttgart International Symposium, 2012

ALUMINIUM CONNECTING RODS FOR CAR ENGINES

Within the framework of a research project funded by the Federal Ministry of Economics and Technology (BMWi), Leiber Group GmbH & Co. KG and the University of Stuttgart, Institute for Internal Combustion Engines and Automotive Engineering (IVK) have developed an aluminium connecting rod for a 1.8-l four-cylinder engine. The material-compliant component design made it possible to approximately halve the mass of the new aluminium connecting rod compared to the previous steel version. In a four-cylinder engine, this amounts to a total weight saving of about 1 kg.

AUTHORS

DR.-ING. JAMBOLKA BRAUNER
is Head of Development Materials at the Leiber Group GmbH & Co. KG in Emmingen (Germany).

DR.-ING. ROLF LEIBER
is Managing Director and Head of Development and Sales at the Leiber Group GmbH & Co. KG in Emmingen (Germany).

DR.-ING. ULRICH PHILIPP
is Head of the Engine Acoustics and Mechanics Division at the Research Institute of Automotive Engineering and Vehicle Engines Stuttgart (FKFS) (Germany).

DIPL.-ING. BENJAMIN BURGER
is Research Assistant at the Institute for Internal Combustion Engines and Automotive Engineering (IVK), Chair in Automotive Powertrains, Engine Acoustics and Mechanics Division, at the University of Stuttgart (Germany).

ULTRA HIGH-STRENGTH AND LIGHTWEIGHT MATERIALS FOR CAR CONSTRUCTION

Lightweight construction is one of the key strategies of the automotive industry. The 1990s saw a breakthrough in the use of aluminium in automotive engineering with the launch of the Audi Space Frame. Systematic lightweight design has since established itself at almost all vehicle manufacturers. Material developers are making enormous strides in this regard, opening up new horizons for automotive functions and automotive manufacturing technology with innovative lightweight solutions.

Properties such as high static and dynamic strength, low density, a high degree of thermal conductivity, good machinability and corrosion resistance speak in favour of the use of aluminium. Newly developed, ultra-strong aluminium alloys, for example, have strengths of more than 700 MPa. This opens up new areas of application. Future cars, particularly hybrid and electric cars, will be increasingly dependent on lightweight construction in order to compensate for the additional weight caused by the elaborate drive technology and batteries.

PROGRESS THROUGH INNOVATIVE WROUGHT ALLOYS

Two trimmed materials show the potential in wrought alloys. AluHigh and AluXtrem are based on the alloy EN AW-6082, which is a favoured material for chassis components. The two materials have significantly better strength and expansion properties. The material AluHigh has a 25 % higher strength (Rm and Rp0.2) and at the same time a 40 % higher fracture strain. For AluXtrem (EN AW-6182), the improvements are even 35 % (strength) and 50 % (fracture strain), ❶.

These materials are becoming increasingly interesting for developers. The high fatigue strength (R=-1), ❷, of 170 MPa at room temperature and 90 MPa at 20 °C play a decisive role.

At the moment, a modified Cu-free material based on EN AW-6082 with ultimate tensile strengths of more than 470 MPa (6082 F47) and a fracture strain of > 10 % can be demonstrated on wrought components, ①. And the potential of optimisation is far from exhausted.

Conventional, ultra high-strength aluminium alloys, such as the well-known alloy EN AW-7075, possess maximum utilisable

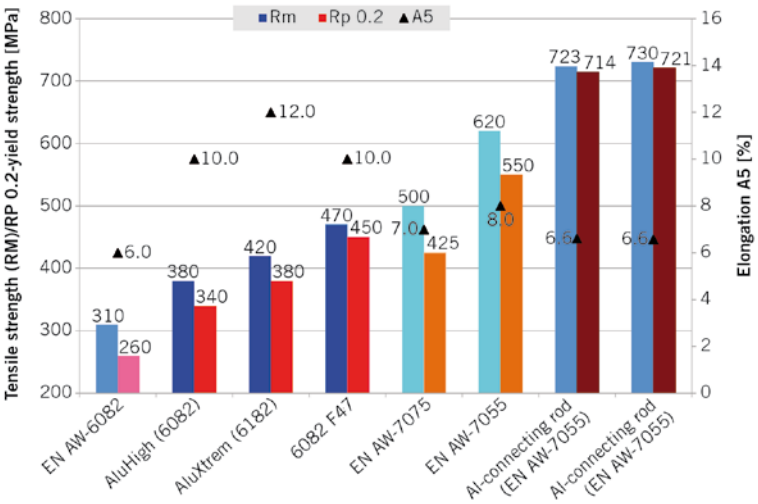

❶ Mechanical data for current aluminium wrought alloys and mechanical data for the aluminium wrought connecting rod

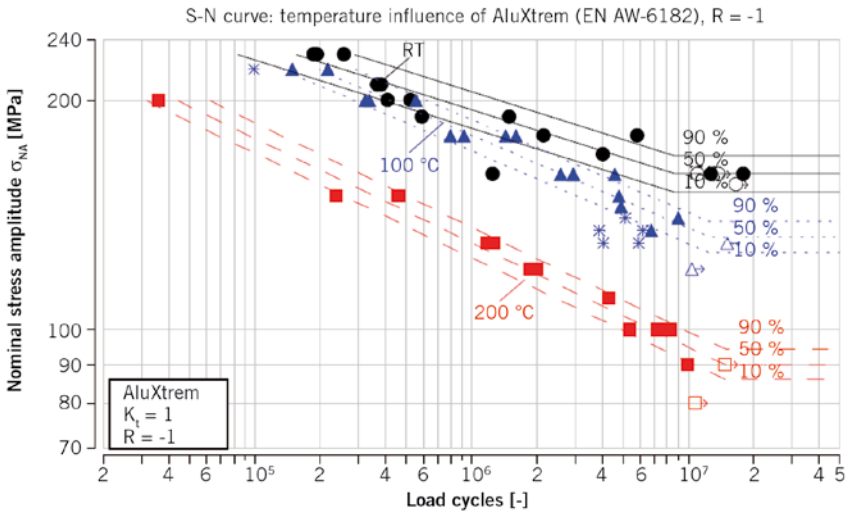

❷ Fatigue strength of AluXtrem material

strengths of around 550 MPa. Derivatives and more modern variants of these alloys, for example EN AW-7055, can display strengths of up to 650 and 700 MPa on the wrought aluminium connecting rod.

Only very few aluminium alloys manufactured in conventional smelting processes display higher strength values. Despite their low weight, these modified aluminium alloys can withstand increasingly higher loadings, as the development of an aluminium connecting rod demonstrates.

LIGHTWEIGHT CONSTRUCTION IN THE CRANK DRIVE

As part of a ZIM Project (Zentrales Innovationsprogramm Mittelstand [Central Innovation Programme for Medium-Sized Companies]) supported by the Federal Ministry of Economics and Technology, Leiber Group GmbH & Co. KG and the University of Stuttgart, Institute for Internal Combustion Engines and Automotive Engineering (IVK) have developed an aluminium connecting rod for a 1.8-l four-cylinder engine, ❸, and subjected it to acoustic and vibration tests on a special engine test stand. The idea behind the project was to advance lightweight construction in areas in which it had previously been unable to compete with steel. While the major connecting rod manufacturers achieve high weight reductions by optimising the geometry of the component in its weight and function [1,2,3], the so-called Aluminium Connecting Rod Project focuses on the ability to optimise the material and a component configuration that takes the specific material into account.

A material and process definition has managed to specifically select the most important component features such as strength, machinability and cracking ability in such a way that a pre-series aluminium connecting rod could be produced. For cracking purposes, the material aluminium requires an optimisation of the various process parameters. It is important to combine brittle fracture behaviour involving separation without plastic deformation and a ductile material behaviour. The bearing shells, bushes and screws for the aluminium connecting rod were taken from a functionally identical series-production steel connecting rod.

As the density of aluminium is only a third that of steel, substitution offers great potential for significantly reducing the mass of the connecting rod. However, significantly greater cross-sections are required to transmit the same load due to the two-thirds lower Young's modulus. The maximum available space for the installation of the connecting rod is therefore one of the limiting factors.

A major influence on the component design is the distribution of mass. In simple terms, because of the combination of rotary and oscillating motion, the connecting rod mass can divided into two parts, the distribution of which is dependent of the centre of gravity. A shifting of the centre of gravity towards the connecting rod small end increases the oscillating percentage of mass and thus also the resulting mass forces. A centre of gravity located in the centre of the crank pin would be ideal for mass compensation, as rotary mass forces are relatively simple to compensate for by means of counterweights on the crankshaft. On a connecting rod made of steel, a centre of gravity close to the centre of the crank pin can be achieved more easily, as the cross-section, above all in the highly loaded area of the connecting rod shaft, can be made smaller due to the material. ③ shows the evolution stages in the design of the aluminium connecting rod.

Development was based on a geometry that utilises the maximum possible installation space, ③ (left). Iterative geometry development in combination with FEM calculations created an optimised ribbing in the connecting rod with regard to homogenous stress characteristics, ③ (centre). This type of geometry is not ideal for the manufacturing and forging process, however. This was why a final stage saw ribbing in the connecting rod

❸ Evolution stages of the aluminium connecting rod

being dispensed with. Therefore, an FEM-aided geometry was developed that constituted an ideal compromise between the forging process and homogenous stress characteristics, ③ (right). Overall, a weight saving potential of around 50 % compared to standard connecting rods made of steel was achieved.

A cylinder pressure profile recorded on a test engine was taken as engine input factors for the connecting rod calculation. The factors of engine speed-dependent mass forces, temperature, heat expansion, screw connection and press fit of the bearing shells or bushing in the small end connecting rod eye were also taken into account in the stress calculations, ❹.

Due to its crank kinematics, in a four-cylinder in-line engine, which is widespread in the car market, rotary and oscillating mass forces of the first order are counter balanced related to the entire engine. On the other hand, the oscillating mass forces of the second and higher orders of all cylinders sum up. In order to verify not only the strength of the vibration and acoustic behaviour of an engine with an aluminium connecting rod, four different build states of a mechanically supercharged four-cylinder internal combustion engine were investigated on a anechoic engine test bench at the Institute for Internal Combustion Engines and Automotive Engineering (IVK) at the University of Stuttgart, ❺.

: steel connecting rod with a Lanchester balancer shaft (base state) (variant 1)
: steel connecting rod without a Lanchester balancer shaft (variant 2)
: aluminium connecting rod without a Lanchester balancer shaft (variant 3)
: aluminium connecting rod with a matched Lanchester balancer shaft (variant 4).

The test bench is fitted with acoustically absorbing wedges on all six roomsides. This configuration absorbs 99 % of all the noise generated by the engine and virtually no reflections occur. Tri-axial acceleration sensors were fitted to the fifth crankshaft main bearing, on the engine mount left/right and on the gear box mount to record vibration and structure-borne noise. Sound pressure measurements on five engine sides at 1 m distance and combustion chamber pressure indicating in cylinder 4 supplemented the range of measurements.

Full load and overrun run-up from 800-4000 rpm for each of the four variants were measured. To protect the aluminium connecting rods, the engine speed was initially limited to 4000 rpm. After completion of the series of measurements, a saw tooth speed profile was run over several hours on variant 4. This involved the engine being accelerated from approximately 1000 to 4000 rpm. Following this, the engine speed limit was raised to 6000 rpm and full load and overrun run-up for variant 4 were measured again. The subsequent visual inspection and measuring of the connecting rods revealed no signs of damage or tolerance deviations.

The acoustic and vibration analyses confirm the expectations derived from the construction. Although the mass of the aluminium connecting rod is about 50 % lower and the oscillating portion is reduced by 38 % compared to the steel connecting rod, this only translates into a reduction of the entire oscillating masses (connecting rod part, piston, bolts and rings) of 8 %. The free mass forces of the second order fall by the same ratio. The aluminium connecting rod therefore not

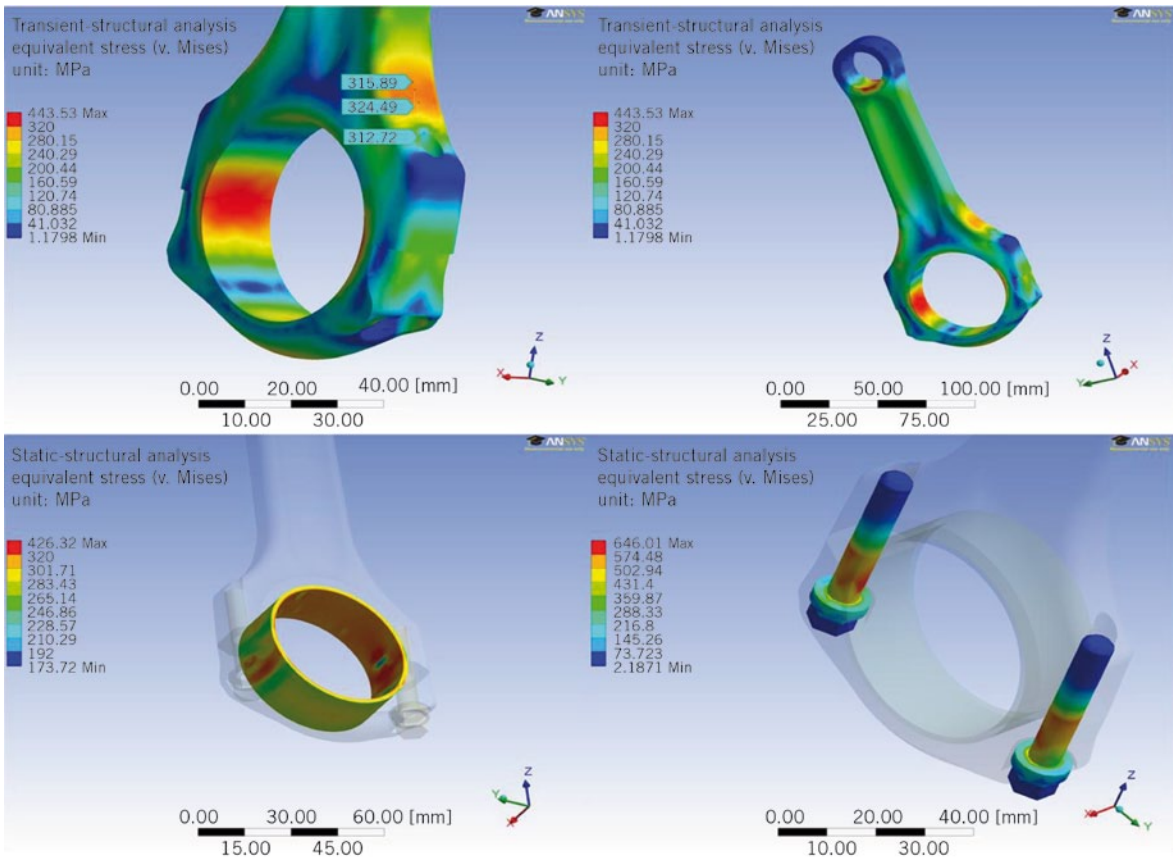

❹ FEM calculation of the aluminium connecting rod

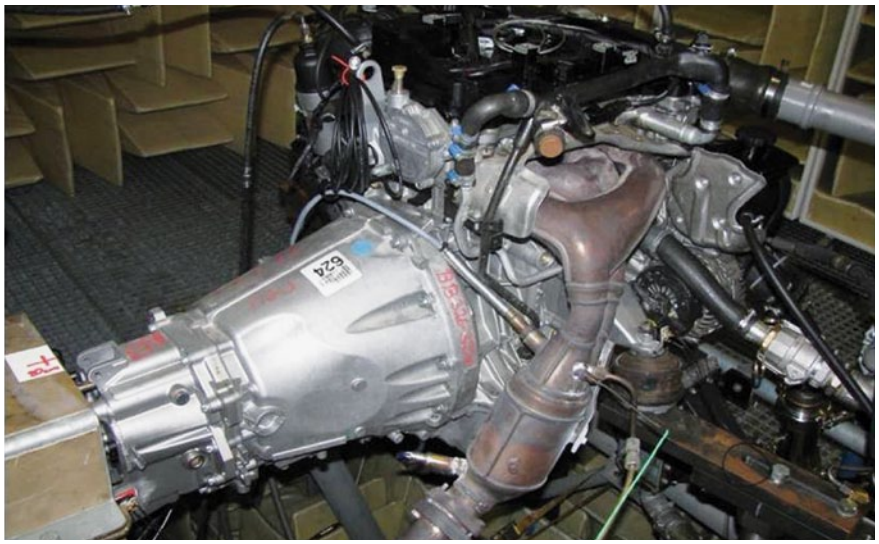

❺ Test setup

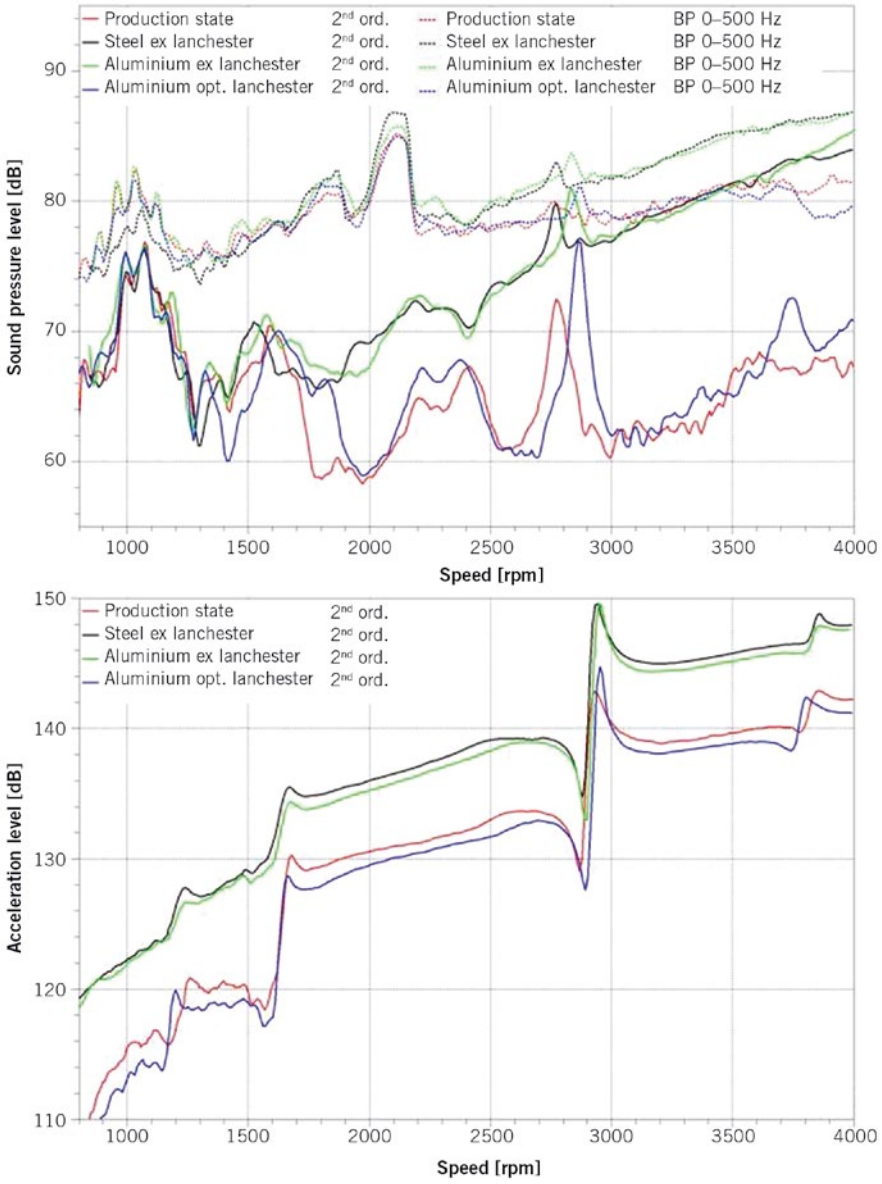

❻ Airborne noise measurement: full load acceleration from 800 to 4000 rpm (top, BP stands for band pass filter) and structure-borne noise measurement: overrun run-up from 800 to 4000 rpm (bottom) (source IVK)

only offers huge weight benefits but also slight acoustic and vibrational advantages compared to the steel connecting rod, ❻. The crankshaft and the balancer shafts can likewise be adapted to the lower oscillating or rotary masses of the lighter connecting rod. Overall, this approach can save 2 kg of moving mass in the crank mechanism.

CONCLUSION

The advantages of a material can be optimally utilised if the "the right material in the right quantity is employed in a form suited to the material in the right place". The new ultra high-strength wrought aluminium alloys as well as innovative technologies and processes allow huge weight-saving potentials to be exploited. Clever component configuration or matching of the fibre direction to the direction of loading in the component have additional optimisation potential. The ZIM research project has demonstrated that the use of aluminium wrought alloys inside the engine shows decisive weight advantages of approximately 2 kg of moving mass compared to the steel variants. Thus, lightweight construction with aluminium is ready to meet the increasing demands in automotive construction in the long term.

REFERENCES

[1] Lipp, K.; Kaufmann, H.: Schmiede- und Sinterschmiedewerkstoffe für Pkw-Pleuel. In: MTZ 72 (2011), No. 5, pp. 416 – 421
[2] Lapp, M.; Hall, C.: Verringerung bewegter Massen durch Leichtbaupleuel. In: Lightweight design, (2011), No. 4, pp. 30 – 36
[3] Lapp, M.: Saving weight saves fuel. In: Automotivedesign.eu.com, (2011), No. 6, pp. 32 – 33

ATZ. A VARIETY IN AUTOMOTIVE KNOWLEDGE.

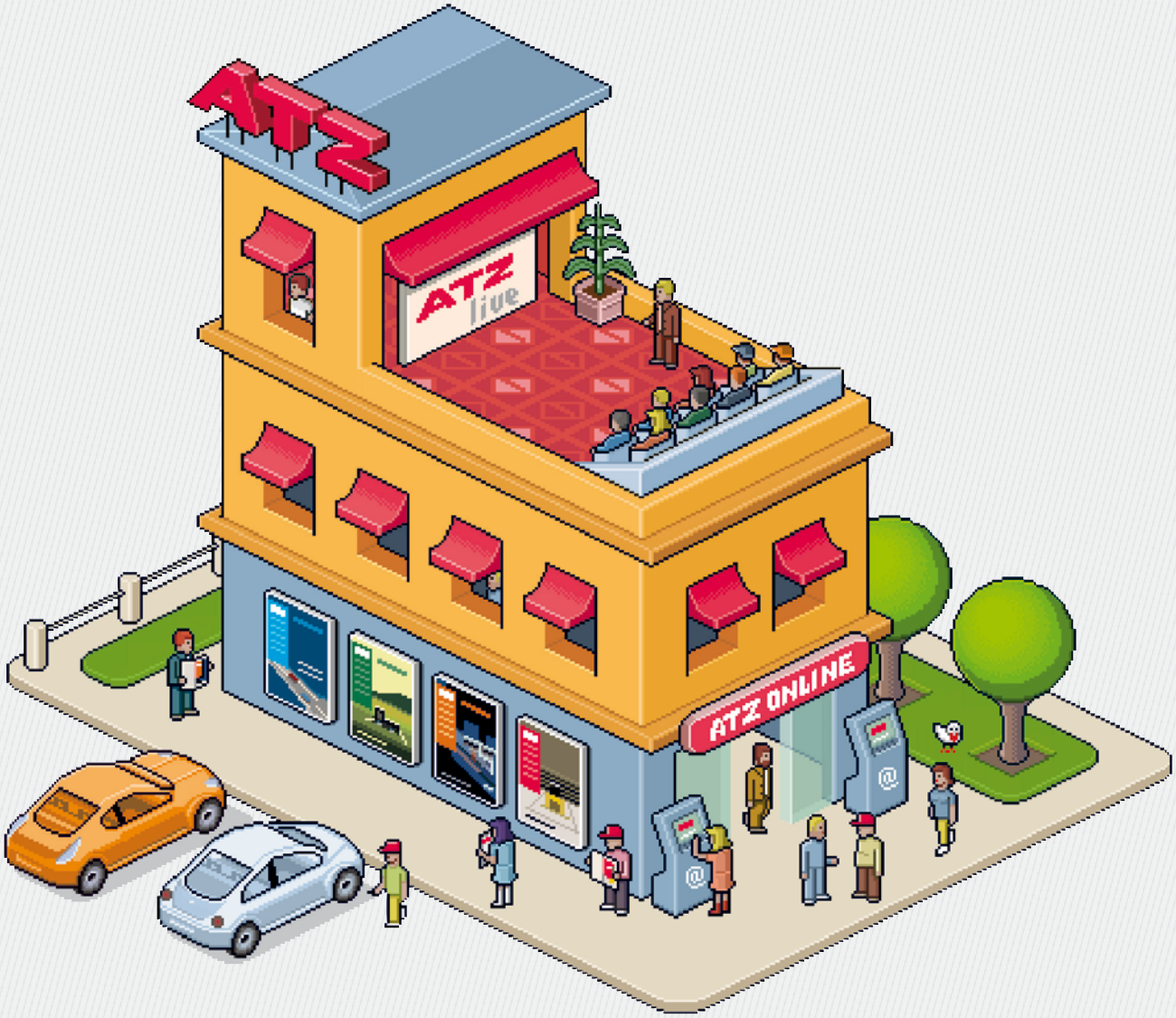

6 TITLES WITH TOPICS FOR EVERY DISCIPLINE.

Up-to-date information, printed and digital formats, advanced training and events: this is **ATZ**. Professional journals for every discipline within the automotive world, with additional digital features like **ATZ online** portal and eMagazines. Plus events, conferences and seminars. One publisher, every bit of information.

See the entire collection at *www.ATZonline.com*

ATZ

DIRECT EXHAUST FLOW MEASUREMENT USING ULTRASONICS UP TO 600 °C

Direct measurement of the exhaust gas volume flow rate is becoming extremely important in the development process due to increasingly shorter vehicle development cycles and successively more stringent emissions standards. These analyses have to begin at a development stage at which, in many cases, it is not yet possible to measure emissions on an exhaust roller dynamometer test bench. The further developed Flowsic150 Carflow measuring device from Sick Maihak GmbH sets new standards in direct ultrasonic volume flow measurement and makes a major contribution towards the development and optimisation of new engine generations.

AUTHORS

DIPL.-ING. SEBASTIAN STOOF
is Product Manager Flow Solutions at the Sick Engineering GmbH in Ottendorf-Okrilla (Germany).

DIPL.-ING. EKKEHARD RIEDEL
is Engineer Research & Development Flow Solutions at the Sick Engineering GmbH in Ottendorf-Okrilla (Germany).

HISTORY

With the Flowsic150 Carflow, Sick has offered an ultrasonic exhaust flow meter for test bench applications for more than ten years. Based on this experience, the device has been comprehensively overhauled in collaboration with leading automobile manufacturers. The focus was to improve metrological properties while expanding its field of application. The advanced ultrasonic technology for industrial flow measurement from Sick has been transferred to the device and its application expanded to exhaust temperatures up to 600 °C.

MEASUREMENT METHOD

Piezoelectric ultrasonic sensors are used at Sick in accordance with the ultrasonic transit time difference method. Ultrasonic signals are transmitted alternatively through the exhaust flow at an angle. Driving and braking effects due to the exhaust flow lead to different transit times of the signals through the flow of exhaust, ❶. This difference in transit time is analysed by the integrated electronics and converted into a flow velocity along the ultrasonic measuring path. A representative area velocity can be determined using four ultrasonic measuring paths arranged across the flow cross-section, Eq. 1. The exhaust volume flow results from computation with the pipe cross-section at the measuring point.

EQ. 1	$v_A = \frac{1}{N} \sum_{i=1}^{N} w_i \cdot v_{P,i}$

v_A stands for the mean area velocity, N for the number of measuring paths, w_i for the weighting factor of a measuring path and v_P for the mean path velocity.

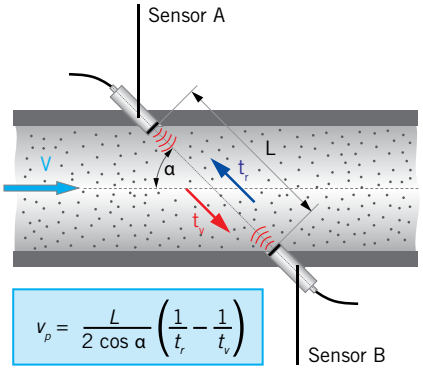

❶ Measuring principle of ultrasonic flow measurement

MEASURED VARIABLES	Volumetric flow (actual), volumetric flow (normalised), gas velocity, speed of sound, gas temperature, gas pressure (barometric)
MEASURING RANGE (ACTUAL VOLUMETRIC FLOW)	0 to 180 l/s [0 to 650 m³/h] as 2,5" device 0 to 500 l/s [0 to 1800 m³/h] as 4" device
MEASURING PRINCIPLE	Four-path ultrasonic transit time difference
ACCURACY	< 0.5 % of reading from 0.05 Q_{max}..Q_{max}
REPEATEABILITY	< 0.2 %
TURN-DOWN RATIO	> 1000:1
EXHAUST TEMPERATURE	maximum 600 °C
PRESSURE DROP	< 12 mbar

❷ Technical data (excerpt)

REQUIREMENTS

The requirements for exhaust flow meters have increased in many ways in recent years: real-time capability, a wide measuring range at high resolution, high temperature capability, low pressure loss, low-maintenance operation and maximum measuring accuracy even under dynamic flow and very low flow rates. The flow condition in the exhaust of internal combustion engines greatly depends on operating conditions and is subject to high dynamics. Pulsations when idling also appear like highly turbulent flows and very low flow velocities.

TECHNOLOGICAL APPROACH

The exhaust velocity is measured in the measurement chamber of the device on four independent ultrasonic measuring paths, whose individual results go into the measurement result weighted. By using this four-path arrangement, disrupted flow profiles that result from less-than-ideal flow from the exhaust pipe can also be accurately measured. Measuring range, measuring accuracy and repeatability are available in ❷.

To reliably capture the dynamics of the exhaust flow and to achieve very high measurement accuracy in all areas, 50 transit time measurements are taken per second on each of the four measuring paths. This guarantees a solid base of data for signal evaluation without extending the response time of the device. ❸ shows a representative step response. The increase here is 30 m/s². The T90 time is approximately 0.9 s.

The individual ultrasonic signals are sampled by the electronics in the MHz range, where a reliable transit time determination is achieved in the ± 5 ns range. This accuracy is particularly critical in the range of low flow velocities, e.g. when idling the engine, because the physical measuring effect is very small here. In addition, adaptive path compensation adjusts faulty measurements to individual paths under dynamic flow conditions and guarantees uninterrupted measurement even for strongly pulsating exhaust. The ratio of the transit time measurements between the individual measuring paths is acquired for uninterrupted measurement and compensated for short-term signal interference. Another advantage of the measurement principle is its independence from the state-dependent sound velocity in the exhaust, thus achieving a degree of independence from the composition of the exhaust, the temperature and the pressure. In addition to the operating volume flow, the measuring instrument also calculates the normalised flow rate through the integrated pressure and temperature measurement, Eq. 2.

EQ. 2 $$\dot{V}_N = \frac{p}{p_0} \cdot \frac{T_0}{T} \cdot \dot{V}_B$$

$\dot{V}_N$ stands for the standard flow, p for the pressure, p_0 for the standard pressure, T_0 for the standard temperature, T for the temperature and $\dot{V}_B$ for the operating flow.

FLOW CONDITIONING

To further improve the metrological properties, innovative flow conditioning is used in the newly developed version of the device to compensate for interrupted flow conditions. Based on experience, ideal inlet conditions are often difficult to achieve when installing the measuring instrument due to the confined spaces. In addition, variable inlet configurations lead to different flow profiles. From the user perspective, the immunity of the device to flow perturbation is therefore of great importance – thus, the actual measurement of the flow velocity becomes independent of the specific flow conditions.

Copper plates in the preheating section of the device cause flow rectification due to their location and support the occurrence of a possible rotationally symmetrical flow profile with minimum pressure loss. In addition, they are welded to the heated pipe wall, whereby heat transfer is optimised for the inflowing exhaust. To keep the temperature gradients between the pipe wall and exhaust as small as possible and to prevent condensation, the entire measurement section of the device is heated throughout. This solution ensures uniform temperature distribution of the exhaust over the entire pipe cross-section, whereby the temperature measurement and subsequent normalisation of the volume flow is carried out with considerably higher accuracy.

SENSOR COOLING

The piezoelectric materials in the ultrasonic sensors lose their piezoelectric properties above the Curie temperature (approximately 280 °C). Alternating thermal stress loads near the Curie tempera-

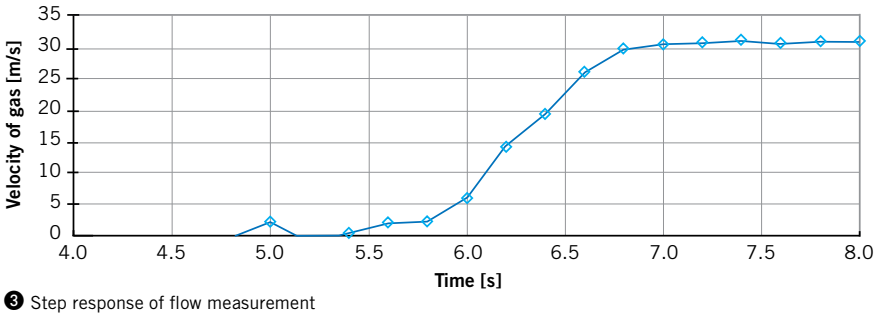

❸ Step response of flow measurement

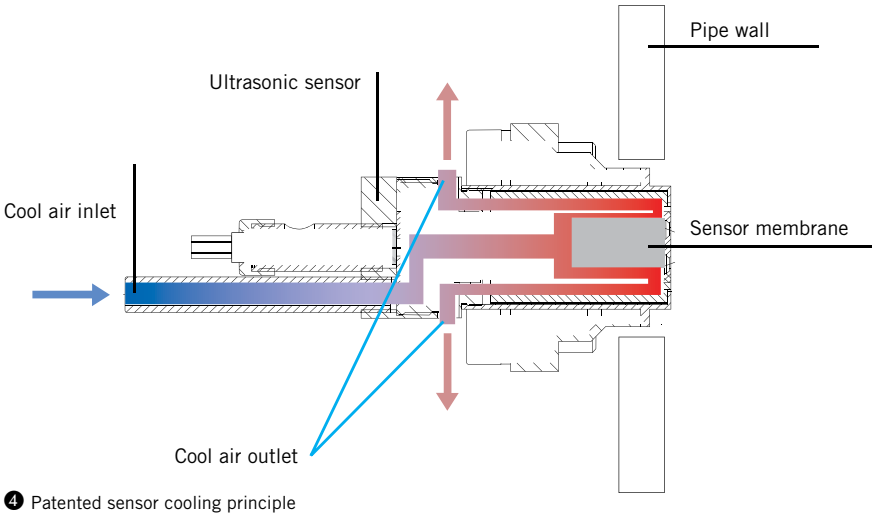

❹ Patented sensor cooling principle

ture also lead to an increased aging effect of the materials, which is why use of the measuring instrument was previously limited to exhaust temperatures below the Curie temperature. To expand the field of application of the device to exhaust temperatures up to 600 °C, patented sensor cooling with ambient air is now used, ❹. Thermal management of the ultrasonic sensors could be decisively improved and the sensor temperature remains safely below the Curie temperature up to 600 °C even when used continuously. In addition, the temperature fluctuations of the sensors could be significantly reduced by cooling, which leads to significantly lower aging behaviour of the sensors.

CALIBRATION

Each device is also calibrated to achieve the highest possible accuracy. Certified test stands are used at the manufacturer in accordance with Measuring Instruments Directive 2004/22/EC. The calibration is performed based on the Reynolds number after Eq. 3. For this purpose, the measuring instrument is installed in the test stand in series connection to a calibrated ultrasonic gas flow meter with eight measuring paths. By testing, the remaining variance from measuring instrument and reference meter is determined as an error curve and recorded in relation to the Reynolds number.

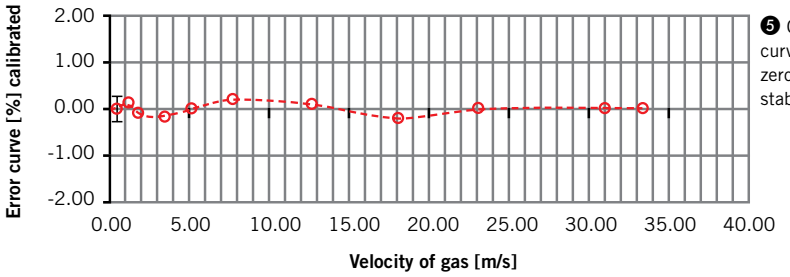

❺ Calibration curve and zero flow stability

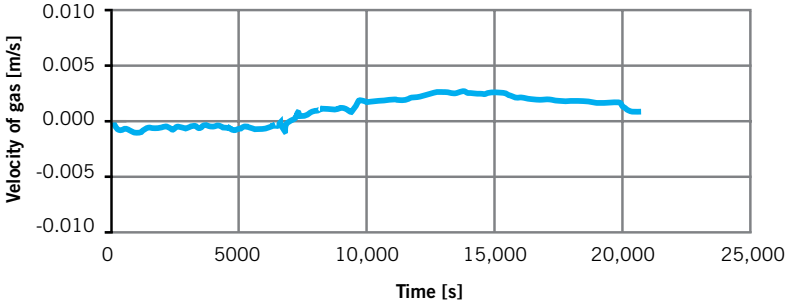

EQ. 3	$Re_{uncorr} = v_A \cdot Di \cdot \frac{\rho}{\eta}$

Re stands for the Reynolds number, ρ for the exhaust density and η for the dynamic viscosity.

Subsequently, a correction of the error is made by a suitable polynomial, whose coefficients can be configured as parameters in the measuring instrument, Eq. 4.

EQ. 4	$k = f(\mathrm{Re}, cc0..cc4)$

k is the correction factor, cc0..cc4 are the polynomial coefficients.

The correction factor is multiplied by the measured area velocity and thus leads to the corrected gas velocity, Eq. 5. In ❺ (top) the results of such a calibration are shown. In addition to the low residual error of max. ± 0.3 %, the repeatability at < 0.2 % is assessed as very good.

EQ. 5	$v_{corr} = k \cdot v_A$

ZERO-POINT STABILITY

The accuracy of flow meters is primarily affected by the zero-point stability at low flow velocities. The minimum quantity range is also of particular interest for the exhaust gas measurement, e.g. in the range near idling. For this reason, the gas velocity of a sealed measuring instrument was recorded over several hours. The results in ⑤ (bottom) show that stability is better than 5 mm/s. The results of zero-point testing with hot gas are in the same range.

APPLICATIONS

Direct exhaust gas flow measurement has significant advantages over the alternative calculation of the exhaust volume flow from other measured values or model approaches. The measuring error increases when calculating from various measured values on the one hand and on the other, model approaches are often limited to specific system environments. Therefore, measurement of the exhaust flow rate represents the simplest, most accurate method and is used in various applications.

DISCRETE EMISSIONS CURVES

Direct exhaust gas flow measurement allows allocation of pollutant concentrations from exhaust analyses to the actual exhaust volume flow with no time-consuming dead time correction. If the exhaust volume flow corrected to standard conditions is used, the emission densities known under standard conditions are used to calculate mass-related emissions, Eq. 6.

EQ. 6	$\dot{m}_i = c_i \cdot \frac{\dot{V}_N}{1\,o^6}\,\rho_{i,N}$

$\dot{m}$ stands for mass flow, c_i for the pollutant concentration, $\dot{V}_N$ for the standard flow and $\rho_{i,N}$ for the pollutant density under normal conditions.

The result is the time curve of the quantity of pollutants. Representative pollutant emissions corresponding to the bag results from CVS systems on chassis dynamometers result from the accumulation of the measured values. This method can also be used on engine test benches to determine discrete pollutant curves and thus allows early and very accurate determination of the results of a CVS measurement to be used.

BAG MINI DILUTER

In addition to the CVS methodology, the Bag Mini Diluter has been certified in the USA by the EPA since 2002 [1]. With this measurement method, vehicle emissions are diluted with synthetic air and directed to the exhaust bag proportional to the exhaust volume flow. The exhaust volume flow of the vehicle is required in real-time as a control factor for the mass flow controller for sampling. Various test results confirm that the volume measurement of exhaust gases by ultrasonics is very well suited for this method [2,3].

SUMMARY

Flow measurement using ultrasonics is ideally suited to meet the diverse requirements of the exhaust gas flow measurement in test bench applications. The test results of the new Flowsic150 Carflow have very high measurement accuracy with a very short response time. With improvements in the area of flow conditioning and by using state-of-the-art sensor technology in the four-path design, independence from the inlet configuration, the zero-point stability and low flow measurement was further optimised. The patented sensor cooling extends the application of the new device to exhaust temperatures up to 600 °C and at the same time, ensures a long service life of the ultrasonic sensors through improved thermal management. Thus, the objectives of the new development were achieved and the new Flowsic150 Carflow is ideally suited for flexible exhaust gas flow measurement on exhaust and chassis dynamometers, not least due to the compact design as a trolley.

REFERENCES

[1] United States Environmental Protection Agency: Dear Manufacturer letter CCD-01-23. December 6, 2001

[2] Guenther, M.; Vaillancourt, M.; Polster, M.: Advancements in Exhaust Flow Measurement Technology. SAE Technical Paper 2003-01-0780, 2003

[3] Yassine, M.; Kirchoff, C.; Laymac, T.; Berndt, R. et al.: Improving Direct Vehicle Exhaust Flow Measurement. SAE Technical Paper 2005-01-0686, 2005

IMPRINT

MTZ

WORLDWIDE

www.MTZonline.com

Founded 1939 by Prof. Dr.-Ing. E. h. Heinrich Buschmann and
Dr.-Ing. E. h. Prosper L'Orange

Organ of the Fachverband Motoren und Systeme im VDMA, Verband Deutscher Maschinen- und Anlagenbau e.V., Frankfurt/Main, for the areas combustion engines and gas turbines
Organ of the Forschungsvereinigung Verbrennungskraftmaschinen e.V. (FVV)
Organ of the Wissenschaftliche Gesellschaft für Kraftfahrzeug- und Motorentechnik e.V. (WKM)
Organ of the Österreichischer Verein für Kraftfahrzeugtechnik (ÖVK)
Cooperation with the STG, Schiffbautechnische Gesellschaft e.V., Hamburg, in the area of ship drives by combustion engine

09 I 2012 _ September 2012 _ Volume 73
Springer Vieweg I Springer Fachmedien Wiesbaden GmbH
P. O. Box 15 46 · 65173 Wiesbaden · Germany I Abraham-Lincoln-Straße 46 · 65189 Wiesbaden · Germany
Amtsgericht Wiesbaden, HRB 9754, USt-IdNr. DE811148419

Managing Directors Dr. Ralf Birkelbach (Chairman), Armin Gross, Albrecht Schirmacher I **Director Corporate Publishing, Corporate Content & Ad Sales** Armin Gross
Director Marketing & Direct Sales Rolf-Günther Hobbeling I **Director Production** Christian Staral

EDITORS IN CHARGE
Dr. Johannes Liebl, Wolfgang Siebenpfeiffer

EDITOR IN CHIEF
Dr. Alexander Heintzel
phone +49 611 7878-342 · fax +49 611 7878-462
alexander.heintzel@springer.com

VICE EDITOR IN CHIEF
Dipl.-Ing. (FH) Richard Backhaus
phone +49 611 5045-982 · fax +49 611 5045-983
richard.backhaus@rb-communications.de

MANAGING EDITOR
Kirsten Beckmann M. A.
phone +49 611 7878-343 · fax +49 611 7878-462
kirsten.beckmann@springer.com

EDITORIAL STAFF
Dipl.-Ing. (FH) Andreas Fuchs
phone +49 6146 837-056 · fax +49 6146 837-058
fuchs@fachjournalist-fuchs.de
Dipl.-Ing. Michael Reichenbach
phone +49 611 7878-341 · fax +49 611 7878-462
michael.reichenbach@springer.com
Stefan Schlott
phone +49 8726 9675-972
redaktion_schlott@gmx.net
Markus Schöttle
phone +49 611 7878-257 · fax +49 611 7878-462
markus.schoettle@springer.com
Martina Schraad
phone +49 611 7878-276 · fax +49 611 7878-462
martina.schraad@springer.com

PERMANENT CONTRIBUTORS
Andreas Burkert, Prof. Dr.-Ing. Stefan Breuer, Hartmut Hammer, Dipl.-Ing. Ulrich Knorra, Prof. Dr.-Ing. Fred Schäfer, Roland Schedel

ENGLISH LANGUAGE CONSULTANT
Paul Willin

ONLINE I ELECTRONIC MEDIA
Portal Manager Automotive
Christiane Brünglinghaus
phone +49 611 7878-136 · fax +49 611 7878-462
christiane.bruenglinghaus@springer.com
Editorial Staff
Katrin Pudenz M. A.
phone +49 6172 301-288 · fax +49 6172 301-299
redaktion@kpz-publishing.com

SPECIAL PROJECTS
Managing Editorial Journalist
Markus Bereszewski
phone +49 611 7878-122 · fax +49 611 7878-462
markus.bereszewski@springer.com

ASSISTANCE
Christiane Imhof
phone +49 611 7878-154 · fax +49 611 7878-462
christiane.imhof@springer.com
Marlena Strugala
phone +49 611 7878-180 · fax +49 611 7878-462
marlena.strugala@springer.com

ADDRESS
Abraham-Lincoln-Straße 46 · 65189 Wiesbaden
P. O. Box 1546 · 65173 Wiesbaden, Germany
redaktion@ATZonline.de

ADVERTISING

HEAD OF KEY ACCOUNT MANAGEMENT
Tanja Pfisterer

HEAD OF SALES MANAGEMENT
Britta Dolch

SALES MANAGEMENT
Volker Hesedenz
phone +49 611 7878-269 · fax +49 611 7878-78269
volker.hesedenz@best-ad-media.de

MEDIA SALES
Frank Nagel
phone +49 611 7878-395 · fax +49 611 7878-78395
frank.nagel@best-ad-media.de

KEY ACCOUNT MANAGEMENT
Rouwen Bastian
phone +49 611 7878-399 · fax +49 611 7878-78399
rouwen.bastian@best-ad-media.de

DISPLAY AD MANAGER
Petra Steffen-Munsberg
phone +49 611 7878-164 · fax +49 611 7878-443
petra.steffen-munsberg@best-ad-media.de

AD PRICES
Advertising ratecard from October 2011

MARKETING I OFFPRINTS

PRODUCT MANAGEMENT AUTOMOTIVE MEDIA
Sabrina Brokopp
phone +49 611 7878-192 · fax +49 611 7878-407
sabrina.brokopp@springer.com

OFFPRINTS
Martin Leopold
phone +49 2642 907-596 · fax +49 2642 907-597
leopold@medien-kontor.de

PRODUCTION I LAYOUT
Heiko Köllner
phone +49 611 7878-177 · fax +49 611 7878-78177
heiko.koellner@springer.com

SUBSCRIPTIONS
Springer Customer Service Center GmbH
Haberstraße 7 · 69126 Heidelberg · Germany
phone +49 6221 3454-303 · fax +49 6221 3454-229
Monday to Friday, 8 a.m. to 6 p.m.
springervieweg-service@springer.com

SUBSCRIPTION CONDITIONS
The eMagazine appears 11 times a year at an annual subscription rate 199 € for private persons and 299 € for companies. Special rate for students on proof of status in the form of current registration certificate 98 €. Special rate for VDI/ÖVK members on proof of status in the form of current member certificate 172 €. Special rate for studying VDI members on proof of status in the form of current registration and member certificate 71 €. Annual subscription rate for combination MTZworldwide (eMagazine) and MTZ (print) 398 €. All prices include VAT at 7%. Every subscription comes with access to the ATZonline archive. However, access is only available for the individual subscription holder. To obtain access for your entire company/library/organisation, please contact Rüdiger Schwenk (ruediger.schwenk@springer.com or phone +49 611 7878-357).

YOUR HOTLINE TO MTZ

Editorial Staff
☎ +49 611 5045982
Customer Service
☎ +49 6221 3454-303
Advertising
☎ +49 611 7878-395

The subscription can be cancelled in written form at any time with effect from the next available issue.

HINTS FOR AUTHORS
All manuscripts should be sent directly to the editors. By submitting photographs and drawings the sender releases the publishers from claims by third parties. Only works not yet published in Germany or abroad can generally be accepted for publication. The manuscripts must not be offered for publication to other journals simultaneously. In accepting the manuscript the publisher acquires the right to produce royalty-free offprints. The journal and all articles and figures are protected by copyright. Any utilisation beyond the strict limits of the copyright law without permission of the publisher is illegal. This applies particularly to duplications, translations, microfilming and storage and processing in electronic systems.

Springer Vieweg is a brand of Springer DE.
Springer DE is part of Springer Science+Business Media.

Springer Vieweg

PEER REVIEW

PEER REVIEW PROCESS FOR RESEARCH ARTICLES IN ATZ, MTZ AND ATZ ELEKTRONIK

STEERING COMMITTEE

Prof. Dr.-Ing. Lutz Eckstein	RWTH Aachen University	Institut für Kraftfahrzeuge Aachen
Prof. Dipl.-Des. Wolfgang Kraus	HAW Hamburg	Department Fahrzeugtechnik und Flugzeugbau
Prof. Dr.-Ing. Ferit Küçükay	Technische Universität Braunschweig	Institut für Fahrzeugtechnik
Prof. Dr.-Ing. Stefan Pischinger	RWTH Aachen University	Lehrstuhl für Verbrennungskraftmaschinen
Prof. Dr.-Ing. Hans-Christian Reuss	Universität Stuttgart	Institut für Verbrennungsmotoren und Kraftfahrwesen
Prof. Dr.-Ing. Ulrich Spicher	Karlsruher Institut für Technologie	Institut für Kolbenmaschinen
Prof. Dr.-Ing. Hans Zellbeck	Technische Universität Dresden	Lehrstuhl für Verbrennungsmotoren

ADVISORY BOARD

Prof. Dr.-Ing. Klaus Augsburg	Prof. Dr. rer. nat. Uli Lemmer
Prof. Dr.-Ing. Michael Bargende	Dr. Malte Lewerenz
Prof. Dipl.-Ing. Dr. techn. Christian Beidl	Prof. Dr.-Ing. Markus Lienkamp
Prof. Dr. sc. techn. Konstantinos Boulouchos	Prof. Dr. rer. nat. habil. Ulrich Maas
Prof. Dr. Dr. h.c. Manfred Broy	Prof. Dr.-Ing. Markus Maurer
Prof. Dr.-Ing. Ralph Bruder	Prof. Dr.-Ing. Martin Meywerk
Dr. Gerhard Bruner	Prof. Dr.-Ing. Klaus D. Müller-Glaser
Prof. Dr. rer. nat. Heiner Bubb	Dr. techn. Reinhard Mundl
Prof. Dr. rer. nat. habil. Olaf Deutschmann	Prof. Dr. rer. nat. Peter Neugebauer
Prof. Dr.-Ing. Klaus Dietmayer	Prof. Dr. rer. nat. Cornelius Neumann
Dr. techn. Arno Eichberger	Prof. Dr.-Ing. Nejila Parspour
Prof. Dr. techn. Helmut Eichlseder	Prof. Dr.-Ing. Peter Pelz
Prof. Dr. Wilfried Eichlseder	Prof. Dr. techn. Ernst Pucher
Dr.-Ing. Gerald Eifler	Dr. Jochen Rauh
Prof. Dr.-Ing. Wolfgang Eifler	Prof. Dr.-Ing. Konrad Reif
Prof. Dr. rer. nat. Frank Gauterin	Prof. Dr.-Ing. Stephan Rinderknecht
Prof. Dr. techn. Bernhard Geringer	Prof. Dr.-Ing. Jörg Roth-Stielow
Prof. Dr.-Ing. Uwe Dieter Grebe	Dr.-Ing. Swen Schaub
Dr. mont. Christoph Guster	Prof. Dr. sc. nat. Christoph Schierz
Prof. Dr.-Ing. Holger Hanselka	Prof. Dr. rer. nat. Christof Schulz
Prof. Dr.-Ing. Horst Harndorf	Prof. Dr. rer. nat. Andy Schürr
Prof. Dr. techn. Wolfgang Hirschberg	Prof. Dr.-Ing. Ulrich Seiffert
Univ.-Doz. Dr. techn. Peter Hofmann	Prof. Dr.-Ing. Hermann J. Stadtfeld
Prof. Dr.-Ing. Bernd-Robert Höhn	Prof. Dr. techn. Hermann Steffan
Prof. Dr. rer. nat. Peter Holstein	Prof. Dr.-Ing. Wolfgang Steiger
Prof. Dr.-Ing. Volker von Holt	Prof. Dr.-Ing. Peter Steinberg
Dr. techn. Heidelinde Holzer	Dr.-Ing. Peter Stommel
Prof. Dr.-Ing. habil. Werner Hufenbach	Dr.-Ing. Ralph Sundermeier
Prof. Dr.-Ing. Armin Huß	Prof. Dr.-Ing. Wolfgang Thiemann
Prof. Dr.-Ing. Roland Kasper	Prof. Dr.-Ing. Dr. h.c. Helmut Tschöke
Prof. Dr.-Ing. Tran Quoc Khanh	Prof. Dr.-Ing. Georg Wachtmeister
Dr. Philip Köhn	Prof. Dr.-Ing. Jochen Wiedemann
Prof. Dr.-Ing. Ulrich Konigorski	Prof. Dr. techn. Andreas Wimmer
Dr. Oliver Kröcher	Prof. Dr. rer. nat. Hermann Winner
Prof. Dr.-Ing. Peter Krug	Prof. Dr. med. habil. Hartmut Witte
Dr. Christian Krüger	Dr.-Ing. Michael Wittler
Univ.-Ass. Dr. techn. Thomas Lauer	

Scientific articles of universities in ATZ Automobiltechnische Zeitschrift, MTZ Motortechnische Zeitschrift and ATZelektronik are subject to a proofing method, the so-called peer review process. Articles accepted by the editors are reviewed by experts from research and industry before publication. For the reader, the peer review process further enhances the quality of the magazines' content on a national and international level. For authors in the institutes, it provides a scientifically recognised publication platform.

In the Peer Review Process, once the editors has received an article, it is reviewed by two experts from the Advisory Board. If these experts do not reach a unanimous agreement, a member of the Steering Committee acts as an arbitrator. Following the experts' recommended corrections and subsequent editing by the author, the article is accepted.

In 2008, the peer review process utilised by ATZ and MTZ was presented by the WKM (Wissenschaftliche Gesellschaft für Kraftfahrzeug- und Motorentechnik e. V./German Professional Association for Automotive and Motor Engineering) to the DFG (Deutsche Forschungsgemeinschaft/German Research Foundation) for official recognition. ATZelektronik participates in the Peer Review since 2011.

AUTHORS

DIPL.-PHYS. SAMUEL VOGEL
is Senior Manager of the Department Predevelopment, Methods and Analytics of DIF Die Ideenfabrik GmbH in Tettnang (Germany).

DIPL.-ING. BERND DANCKERT
is CEO and Managing Partner of DIF Die Ideenfabrik GmbH in Tettnang (Germany).

PD DR.-ING. STEPHAN RUDOLPH
is Head of the Similarity Mechanics Group at the Institute for Statics and Dynamics of Aerospace Structures of the University of Stuttgart (Germany).

KNOWLEDGE-BASED DESIGN OF SCR SYSTEMS USING GRAPH-BASED DESIGN LANGUAGES

The ability to cope with different applications and system variants is a big challenge when designing exhaust aftertreatment systems. Especially in the off-highway application area designers are faced with many different vehicle variants featuring lots of different load profiles. In addition, the future emission legislation makes an external exhaust gas aftertreatment necessary. To meet these challenges a graph-based design language is developed at the Die Ideenfabrik and the University of Stuttgart as a new design method for the design of SCR systems.

RECEIVED 2011-12-15
REVIEWED 2012-02-03
ACCEPTED 2012-06-01

1 INTRODUCTION

1.1 NECESSITY

Graph-based design languages are a kind of formalised rule-based expert systems [1]. They provide a complete formal representation and an automatic iterative product development process [17]. Design languages represent hereby a new point of view of the problem of product design that leans on languages spoken by humans like German or French, in which vocabulary and rules make up a grammar that specifies the format and structure of syntactically valid sentences. The meaning of design languages in this interpretation is that every valid sentence is a legal combination of vocabulary representing a valid specific product design.

1.2 DESIGN LANGUAGES

The system terms, parts and assemblies of the product to be designed build up the vocabulary. Combination rules are defined on vocabulary and form thus a grammar. Based on given requirements (called axiom) the rules can be (re-) executed to assemble the vocabulary to a valid product design of the system [12]. The sequence of rules that combines the vocabulary is called production system. A graph-based representation of rules and vocabulary is particularly beneficial for the human understanding of a design language [12]. The method has already been used in the design of complex aircrafts and satellites [4, 19].

Modelling languages like the Unified Modelling Language (UML) provide an internationally standardised and manufacturer independent representation of design data [14, 15]. This simplifies the portability and reusability of the engineering know-how embedded in the design language. The generated universal and digital master model of the product is processed in a design compiler [10, 22]. The design compiler automatically generates domain specific models for analysing in downstream process chains: computer-aided design (CAD), structural analysis (FEM), computational fluid dynamics (CFD), enterprise resource planning (ERP), product lifecycle management (PLM) etc. The validity and accuracy of the results mainly depend on the abilities of the analysis software used and do not differ from conventional design methods. The design compiler offers an internal constraint processing mechanism that is able to process and solve the design constraints for the predimensioning of the originating product [18]. Transferring the analysis results back into the design language leads to a realisation of a closed-loop optimisation scenario, ❶. Precondition for this optimisation is an automatic evaluation of the generated designs. This design evaluation [16, 17] is preferably implemented using dimensionless numbers of similarity mechanics [5].

2 DESIGN LANGUAGE FOR THE SCR SYSTEM DESIGN

2.1 VOCABULARY

The SCR system is topologically decomposed to its elementary parts and terms and its parametrical description (such as pipe elements, pre-/post-chamber, catalyst, components of the dosing system, engine data, installation room etc.). These vocabulary correspond classes in the UML. The classes and their relations (associations) formed by edges between classes make up the class diagram, ❷. Data and information are exchanged along the edges of the class diagram between the classes.

2.2 RULES

Graph transformations and programme code form the rules to build-up and modify the virtual model. The rule-based composi-

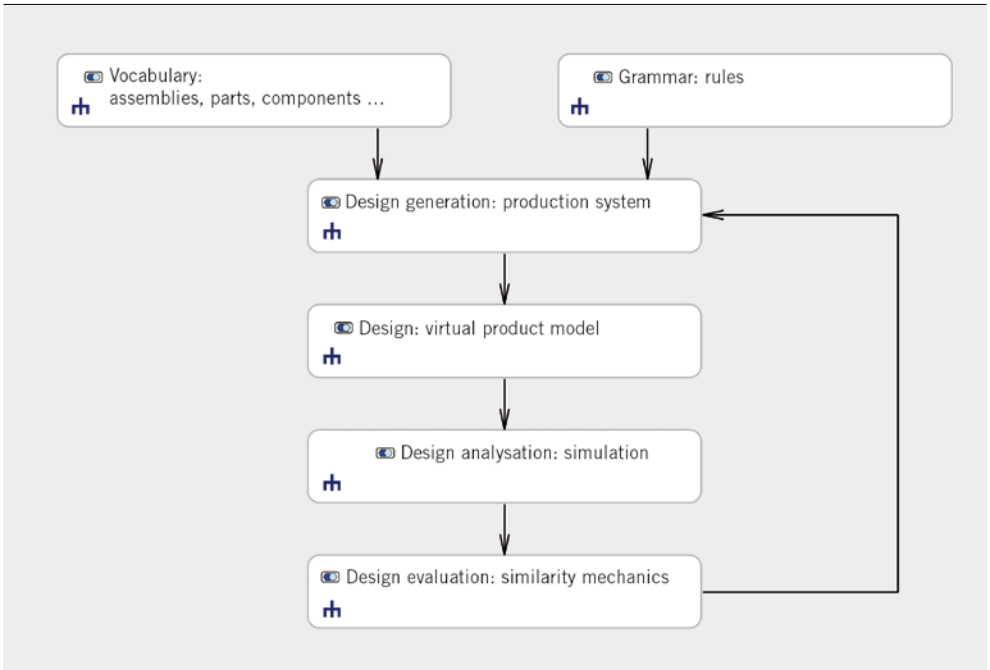

❶ Schematic design process using design languages

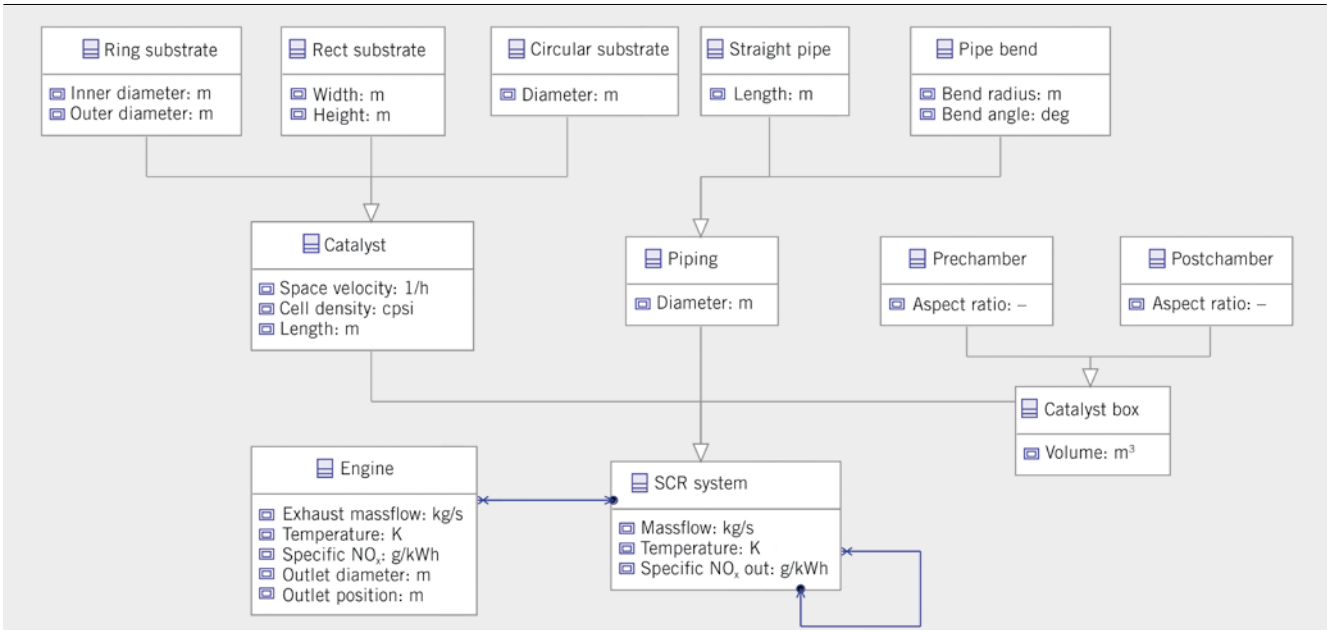

❷ Detail of a class diagram of a SCR system

tion of the virtual design ensures a complete algorithmic storage of design knowledge. The graphically formulated rules are made-up according to an "if-then"-scheme. The scheme is split into the "if"-side of the rule that contains the graph pattern that is searched in the model and into the "then"-side containing the final modified state of the looked-up graph pattern. ❸ shows a rule that attaches a prechamber of a catalyst box to a straight pipe element. Rules to manipulate the product model are automatically executed within the design compiler. The first rule of the production system is called the axiom. The axiom contains fixed requirements and given boundary conditions. The successive rules compose a virtual product design that is compatible with the previously given requirements and boundary conditions.

2.3 PRODUCTION SYSTEM

The production system contains the sequence of rules that determines the incremental build-up of the final design graph. It comprises hierarchical sub-programmes and decision nodes. The decision nodes allow a selective call of rules and sub-programmes based on the state of the current design graph. By using decision nodes, the conventionally manual decision making process is reproduced digitally in the production system. The diamonds in the UML activ-

❸ Graphical rules to build-up the virtual product model

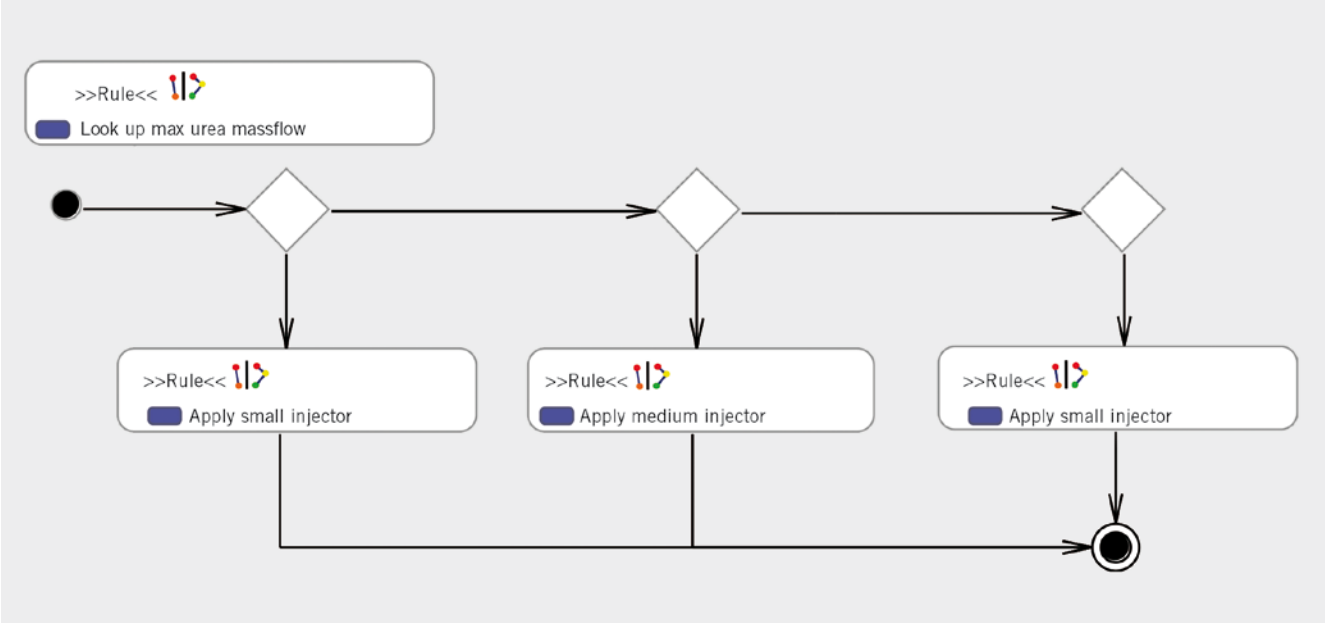

❹ Sub-programme using decision nodes (diamond) to choose a fitting urea injector

ity diagram, ❹, represent such decision nodes. In the example an appropriate urea injector is selected by the decision nodes and finally is built-in by calling the proper rule (small-, medium- or large-sized). The rules and decision nodes allow the graphical implementation of the well-known control flow states from programming (such as if, then, else, for, while). This leads to an integrated and complete digital representation of the design knowledge that is easily (re-) executable and reusable even in a different design context.

❺ shows the implemented design cycle for the development of a SCR system. The design cycle starts with a coarse analytic dimensioning of the catalyst size and the pipe diameter [3, 11]. On the basis of these geometric dimensions an automated packaging and routing procedure is conducted using the digitally predefined installation space. This results in a CAD model that is finally simulated using numerical CFD techniques to obtain the expected efficiency of the system.

2.4 PROCESS CHAIN

2.4.1 PACKAGING

Based on the system dimensions, determined in the analytic predimensioning, the target installation position of the SCR box is determined within the given CAD model of the installation space. This is done by a discretisation of the installation room followed

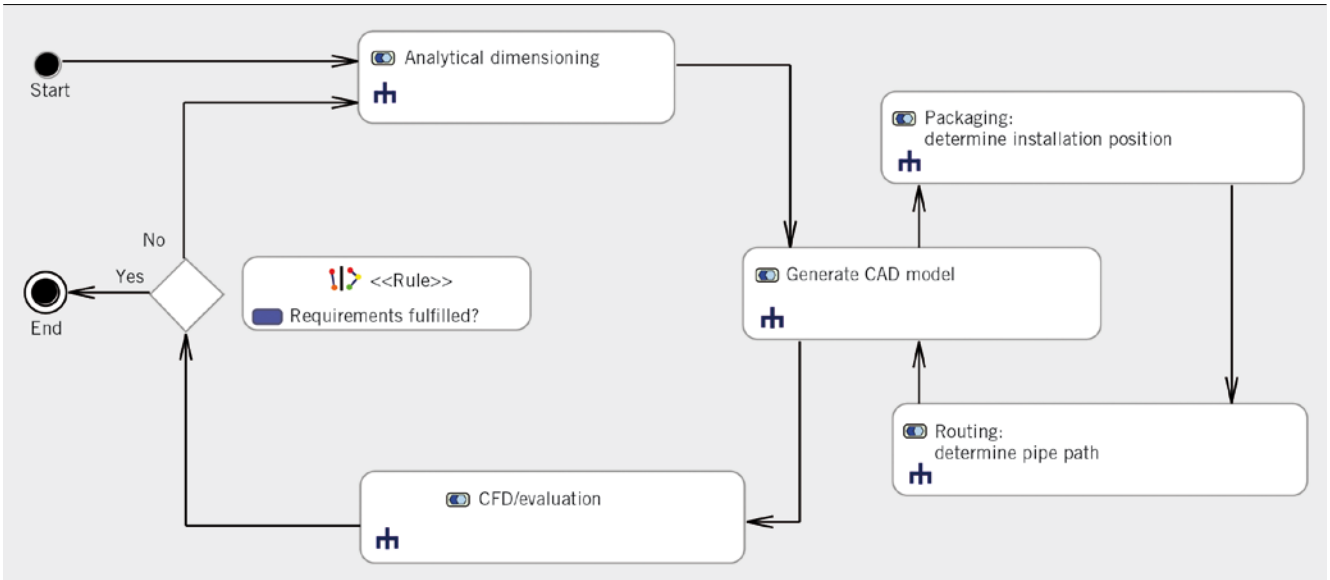

❺ Schematic design cycle

by the execution of appropriate algorithms [9, 20] within the design compiler to find the best fitting installation position under the given requirements and boundary conditions.

2.4.2 ROUTING

The routing module of the design compiler calculates the path routes from the engine to the SCR box and from the SCR box to the environment following the previous identification of the SCR box position. This is done again by a discretisation of the installation room and by executing a path search algorithm [13]. Different smoothing and path finding options (such as paths with maximised wall distances) are available. The found path is stored then as polygonal line in the design language. After that, the polygonal line is rule-based transformed onto the (CAD) model of pipework optionally with a constant bend radius or with arbitrary bend radii.

2.4.3 CAD

The geometric information is extracted from the model by the CAD plug-in provided in the design compiler framework. These information is processed and a CAD model of the SCR system is generated. ❻ schematically shows the sequence of the presented design compiler plug-ins (packaging, routing and CAD). Topologically different SCR box designs are generated by recombining different prechamber, postchamber and catalyst geometries, ❼. The models remain stable [7] as the whole design language is re-executed from the beginning after performing a topological modification.

2.4.4 CFD

After the geometry generation the CFD simulation model (Euler/Lagrange two-phase) is created in the appropriate plug-in of the design compiler [8]. Using a standardised generation of the simulation models leads to a good comparability of the simulation results. The simulation of the wall-film formation is omitted in the conceptual design stage. The urea mass flow impacting on the wall is calculated instead. The urea mass flow *j(i)* impacting the wall at cell *i* is calculated according to Eq. 1

EQ. 1

$$j(i) = \sum_{t} \frac{\dot{m}_{wall}\,(i,\,t)}{A_i}$$

With $\dot{m}_{wall}$ = urea mass flow impacting on the wall, t = time and A_i = cell area.

The urea flow density can be compared with empirical data to get a first estimation if the wall contact is subcritical or supercritical with regard to the deposit formation. The CFD process chain automatically calculates the uniformity indexes *Ui* (Uniformity-Indexes) [2] at the critical flow cross sections (such as catalyst entry).

The uniformity indexes of the gaseous and liquid components are calculated. For the calculation of the liquid components uniformity index the cross section is equidistantly discretised and the droplet masses m_j (droplet index j) of the droplet track j are summed up at the nearest grid points (grid point index i) to m_i. Based on the summed-up masses the uniformity index is calcu-

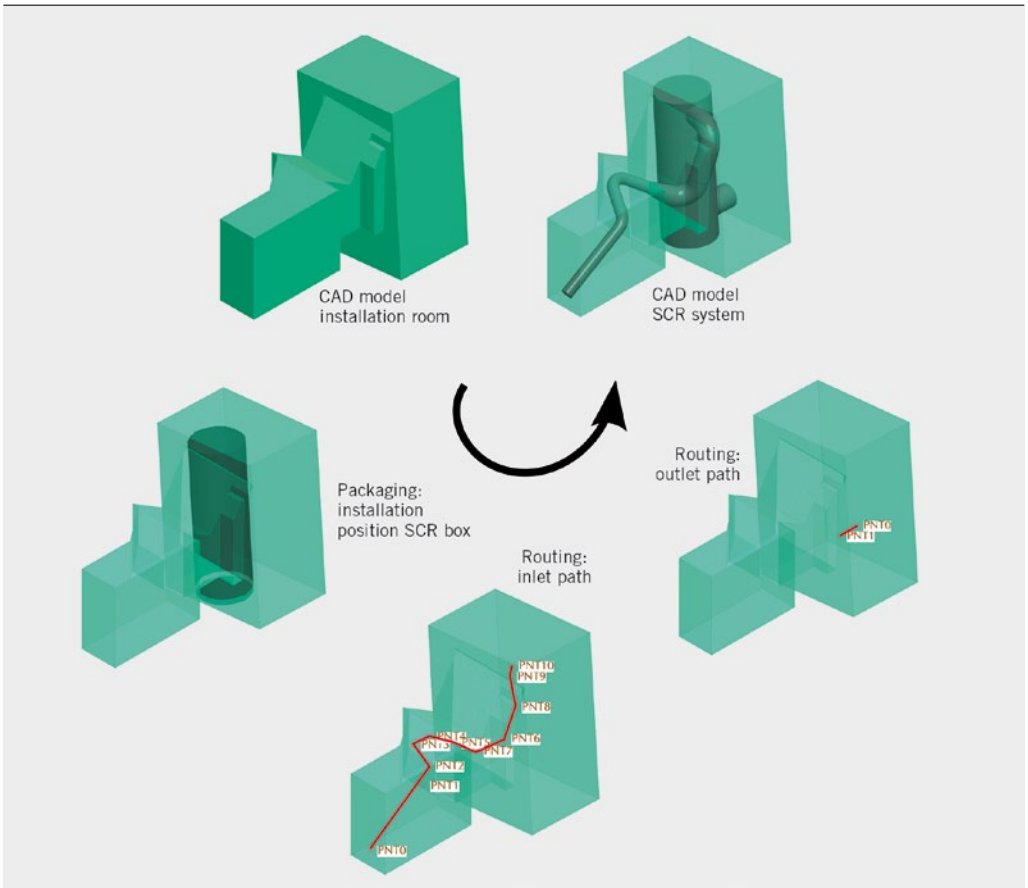

❻ From the installation space to the CAD model (schematic)

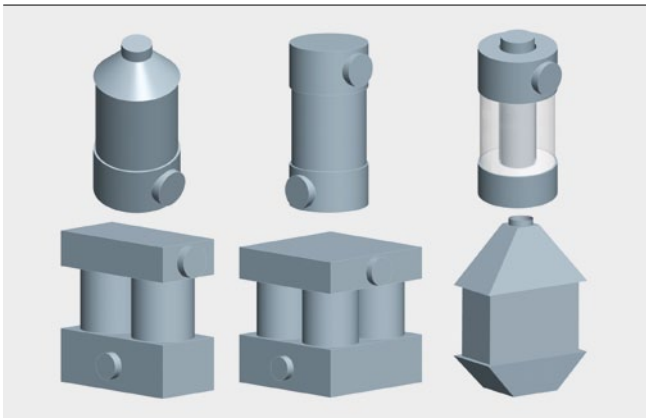

❼ Topological variants of SCR boxes (CAD models)

lated [2]. The dimensionless uniformity indexes allow an objective evaluation of the generated SCR systems.

2.5 EXPLORING THE DESIGN SPACE

Besides the project-specific application in the field of critical project parameters the design language can be used in the predevelopment for a computational exploration of the design space [17]. The whole syntactical variety of topological and parametric variants that can be combinatorially built from the class diagram of the design language spans the design space. This design space can be computationally scanned and systematically evaluated.

3 SIMULATION RESULTS

In terms of exploring the design space three different prechamber designs of SCR systems were generated and evaluated exemplarily. ❽ shows the evaluated prechamber geometries (d_{pipe} = 100 mm, d_{cat} = 350 mm). Each of the variants is processed with two different substrate types (high and low backpressure substrates). The plane for the calculation of the uniformity indexes is marked black. A dimensionless quality number for the evaluation of the prechamber is defined, Eq. 3. The quality should scale down with an increasing pressure loss and scale up with an increasing uniformity index of the gas phase. Therefore the pressure loss is expressed as dimensionless Euler number Eu (Eq. 2).

EQ. 2	$Eu = \frac{\Delta p}{p \cdot v^2}$

EQ. 3	$G = \frac{Ui}{Eu}$

The results, ❾, show that the prechamber configuration with radial entry is dominant. For smaller Reynolds numbers the configuration with lower substrate backpressure results in a higher prechamber quality. For lack of space this short result presentation with results limited to the gas phase shall be sufficient as these results should primarily serve to show the usage and application of design languages.

4 METHODOLOGY RESULTS

The design language execution takes less than ten minutes (on a medium-class desktop PC) for one run through the proposed design cycle (excluding CFD calculation). The CFD simulation duration can be cut down swapping it to an external computer cluster. The practical experiences in using design languages have not shown so far a deterioration of the result quality compared with the manual approach. This is ensured by the fact that not only the design know-how is stored in the design language but also the know-how of the simulation engineer can be stored in the rules within the design language and the associated process chains.

5 SUMMARY AND OUTLOOK

Graph-based design languages turn out to be a suitable methodology to completely automatise recurring design tasks that increases significantly the efficiency of the design process (of SCR

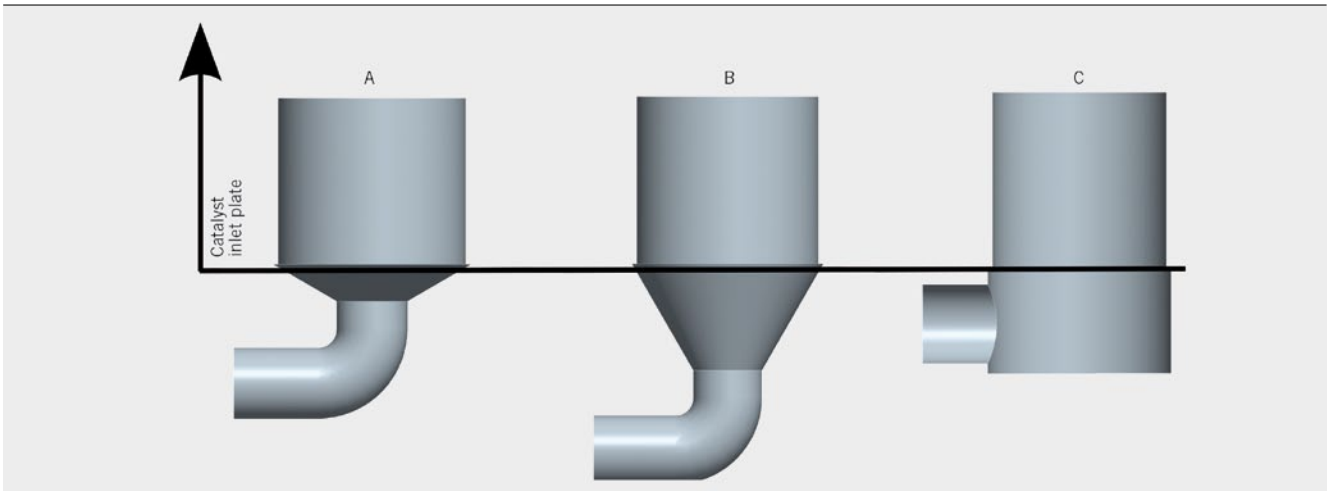

❽ Evaluated geometries: variant A (60° cone), variant B (30° cone), variant C

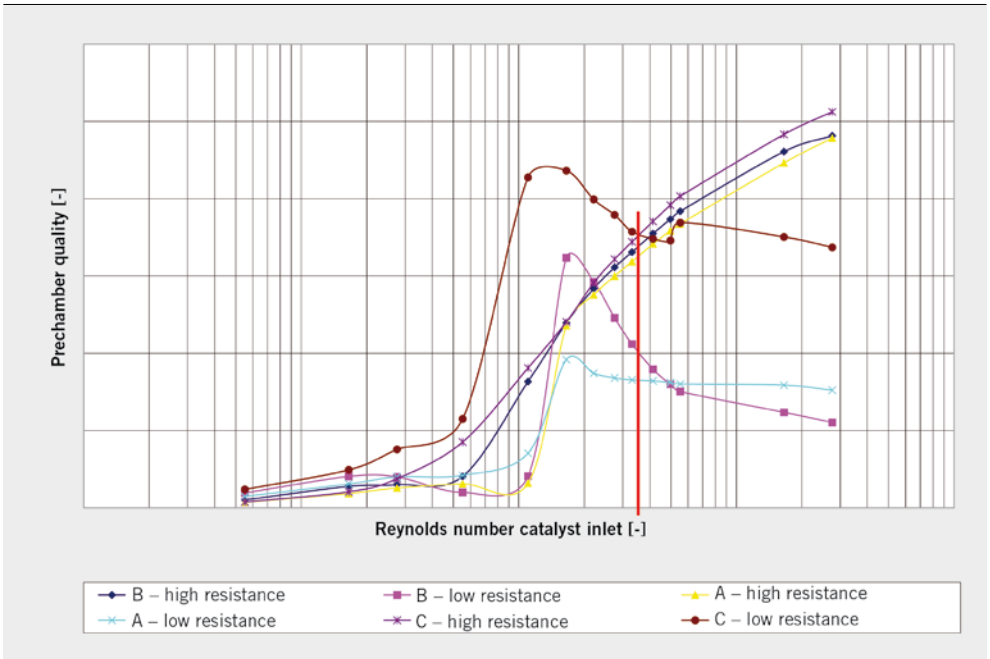

9 Prechamber quality depending on the Reynolds number measured at catalyst entry

systems). The increased one-time effort implementing a design language is compensated many times through the efficiency gain in the actual design process.

The integration of evolutionary or DoE (Design of Experiments) optimisation algorithms will be one task for the future to lead a design iteratively to its optimum. In parallel conducted projects design languages are developed to generate the "Digital Factory" belonging to a product, that is engineered using design languages. Following this research direction makes it possible to optimise and design a product not only in regard to its functionality, as demonstrated with this work, but also in the interwoven context of design and manufacturing constraints.

REFERENCES

[1] Antonsson, E. (ed.); Cagan, J. (ed.): Formal Engineering Design Synthesis. Cambridge University Press, 2001
[2] Birkhold, F.; Meingast, U.; Wassermann, P.; Deutschmann, O.: Modelling and simulation of the injection of urea-water-solution for automotive SCR DeNO$_x$-systems. In: Applied Catalysis B: Environmental 70 (2007), No. 1-4, pp. 119 – 127
[3] Bogdanic, M.: Simulation von Autoabgasanlagen. Dissertation, TU Berlin, 2007
[4] Böhnke, D.; Reichwein, A.; Rudolph, S.: Design Language for Airplane Geometries using the Unified Modelling Language. In: ASME Proceedings of Design Engineering Technical Conferences, San Diego, CA, August 30 to September 2, 2009
[5] Buckingham, E.: On physically similar systems – Illustrations of the use of dimensional equations. In: Phys. Rev. 4 (1914), pp. 345 – 376
[6] Danckert, B.; Huonker, M.; Vogel, S.: Implementierung und Erprobung eines kombinierten SCR/CUC-Abgasnachbehandlungssystems für Marinefahrzeuge der Luxusklasse zur Erfüllung zukünftiger Emissionsgesetzgebungen. In: MTZ Konferenz Heavy Duty Engines, Köln/Bonn, 2008
[7] Dungs, S.: Wissensbasierte Geometriemodelle zur Strukturanalyse. Dissertation, Uni Duisburg-Essen, 2008
[8] Gruenwald, J.: Verbesserung der Reduktionsmitteldispersion und -verdunstung in SCR-Anlagen. Dissertation TU München, 2007
[9] Hu, M.-K.: Visual pattern recognition by moment invariants. In: Information Theory, IRE Transactions on 8 (2007), pp. 179 – 187
[10] www.iils.de: The Design Compiler 43. IILS Ingenieurgesellschaft für Intelligente Lösungen und Systeme mbH, 2007
[11] Kaiser, R.; Stadler, F.; Pace, L.; Presti, M.: Simulationsmodell von Drei-Wege-Katalysatoren mit perforierten Folien. In: MTZ 68 (2007), No. 5, pp. 374 ff.
[12] Kröplin, B.; Rudolph, S.: Entwurfsgrammatiken – Ein Paradigmenwechsel? In: Der Prüfingenieur 26 (2005), pp. 34 – 43
[13] Lee, C. Y.: An Algorithm for Path Connections and Its Applications. In: IRE Transactions on Electronic Computers EC-10 2 (1961), pp. 346 – 365
[14] www.uml.org: Unified Modelling Language. OMG Object Management Group (ed.), 2011
[15] Reichwein, A.: Application-specific UML Profiles for Multidisciplinary Product Data Integration. Dissertation, Universität Stuttgart, 2010
[16] Rudolph, S.: Eine Methodik zur systematischen Bewertung von Konstruktionen. Dissertation, Universität Stuttgart, 1995
[17] Rudolph, S.: Übertragung von Ähnlichkeitsbegriffen. Habilitationsschrift, Universität Stuttgart, 2002
[18] Rudolph, S.; Bölling, M.: Constraint-based conceptual design and automated sensitivity analysis for airship concept studies. In: Aerospace Science and Technology 8 (2004), pp. 333 – 345
[19] Schaefer, J.; Rudolph, S.: Satellite Design by Design Grammars. In: Aerospace Science and Technology 9 (2005), pp. 81 – 91
[20] Schrijver, A.: Combinatorial Optimization. Springer-Verlag, 2004
[21] Vogel, S.; Danckert, B.; Rudolph, S.: Entwicklung von Abgasnachbehandlungssystemen auf Basis einer graphenbasierten Entwurfssprache. In: MTZ-Konferenz Heavy-Duty, On- und Off-Highway-Motoren, Mannheim, 2010
[22] Ward, A.; Seering, W.: Quantitative Inference in a Mechanical Design Compiler. In: Proceedings 1st DTM Conference, Montreal, Canada, 1989

Heavy-Duty, On- and Off-Highway Engines

Efficiency and emissions –
how to optimize both?

7th International MTZ Conference
6 and 7 November 2012
Nuremberg | Germany

CLEAN AND FUEL-EFFICIENT DIESEL AND GAS ENGINES
New powertrains for commercial vehicles and off-highway, marine and stationary applications

EMISSIONS REDUCTION
Solutions inside and outside the engine

SUPERCHARGING, FUEL INJECTION AND COMBUSTION PROCESSES
Innovative concepts and systems

/// FACTORY TOUR
MAN Nuremberg Engine Plant

/// KINDLY SUPPORTED BY

RICARDO

ATZ live
Abraham-Lincoln-Straße 46
65189 Wiesbaden | Germany

Phone +49 (0)611 / 7878 – 131
Fax +49 (0)611 / 7878 – 452
ATZlive@springer.com

PROGRAM AND REGISTRATION
www.ATZlive.com

DEPOSITION MECHANISMS IN EXHAUST HEAT EXCHANGERS

The recirculation of cooled exhaust gas is seen as an effective means of meeting the legal limits for NO_x emissions in modern diesel engines. During exhaust-gas recirculation (EGR) in diesel engines, there are often cooling performance losses in the EGR cooler due to the admission of engine-out emissions. These losses are mainly due to the condensation of high boiling soot-hydrocarbon agglomerates, which are responsible for forming an insulating layer of deposits. The TU München studied the formation of deposits in EGR coolers within the framework of the FVV projects No. 966 and 1048.

AUTHORS

DIPL.-ING. PETER VÖLK
is Scientific Assistant at the Institute for Internal Combustion Engines of the TU München (Germany).

PROF. DR.-ING. GEORG WACHTMEISTER
is Head of the Institute for Internal Combustion Engines at the TU München (Germany).

DIPL.-ING. GABRIELE HÖRNIG
was Scientific Assistant at the Institute of Hydrochemistry and Chemical Balneology of the TU München (Germany).

PROF. DR.-ING. REINHARD NIESSNER
is Head of the Institute of Hydrochemistry and the Chair for Analytical Chemistry at the TU München (Germany).

THE SEAL OF APPROVAL FOR SCIENTIFIC ARTICLES IN MTZ.
MTZ PEER REVIEW
RECEIVED 2012-04-16
REVIEWED 2012-05-16
ACCEPTED 2012-06-04
REVIEWED BY EXPERTS FROM RESEARCH AND INDUSTRY.

1 INTRODUCTION

EGR has proven itself as an effective means of reducing NO_x emissions, which will be limited to 0.4 g/kWh for trucks and buses with the introduction of Euro VI in 2014. Compared to the limitations of Euro V, this means a decrease by 80 %. Due to the possibility to reach high ballast gas fractions with moderate temperatures at the start of combustion, cooled exhaust-gas recirculation is very effective, although the buildup of deposits is problematical. Contamination (sooting) of the exhaust heat exchanger by the formation of a deposit layer consisting of highly adhesive particle agglomerates (soot, hydrocarbons, sulphur) on the exhaust side results in a decrease of cooling performance by 20 to 30 % compared to the clean cooler. These deposition mechanisms were analysed within the framework of the FVV projects No. 966 and 1048 and possible measures for reducing the formation of a deposit layer or for removing existing deposit layers were derived.

2 EXPERIMENTAL SETUP AND BOUNDARY CONDITIONS

A BMW six-cylinder Diesel engine (type M57D30 TU2) produced the required exhaust gas. Some engine data are shown in ❶. For further technical specifications [1]. The fouling experiments were accomplished with a custom double-pipe heat exchanger, which was made of aluminium (tube length: 160 mm; inner diameter: 10 mm; wall thickness: 1 mm) that replaced the OEM heat exchanger. ❷ shows a schematic diagram of the experimental setup. The counter-flow heat exchanger was displaced from the exhaust manifold by an offset of 60 cm to facilitate additional exhaust-gas conditioning (heating up of exhaust gas, sampling locations for gas analysis). The thickness of deposition in the EGR tubes was measured by the non-destructive use of neutron radiography. This is one reason why a custom aluminium EGR is used instead of the stainless steel OEM version, as aluminium, in comparison to steel, is almost transparent for neutron beam/transmission. Furthermore, the thermal conductivity of aluminium is many times higher than steel allowing thicker pipe walls to ease the

❶ Data of the BMW engine

Bore	84 mm
Stroke	90 mm
Displacement	2993 cm³
Performance	170 kW at 4000 rpm
Maximum torque	500 Nm at 2000 rpm
Maximum common rail pressure at full load	1600 bar

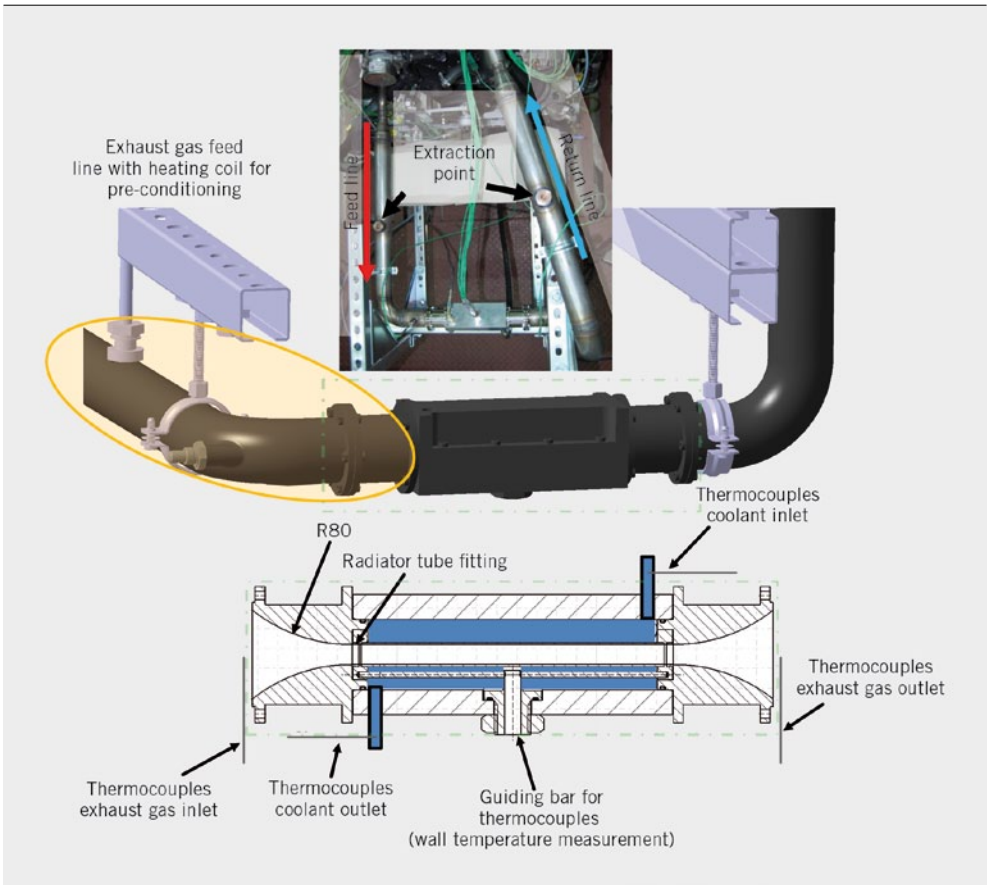

❷ Schematic of the experimental setup at the engine test bench

placement/integration of thermocouples. These are glued into minute blind holes located on the outside of the pipe's wall. This specific design of measuring local temperatures extremely close to the inner pipe surface not only preserve the initial fluid flow and convection states, but also makes it possible to detect the build-up of insulating layers by drops in temperature inside the wall pipes. In addition to the cooling water and exhaust-gas temperatures at the respective inlet and outlet also a rough space-resolved indication of the deposit growth could be derived.

The deposition enhancing components in the original raw exhaust gas were too low to induce any noteworthy fouling. Therefore, the engine's operating strategy was modified by activating the post injection depending on the EGR rate. The total amount of hydrocarbons was increased from 350 to 450 ppm while the particle mass-flow increased from 91.15 to 575.3 mg/hr. The double-pipe heat exchanger was operated with exhaust mass flows of 4.5, 9 and 15 kg/h and the exhaust-gas inlet temperatures ranged between 200 and 400 °C. The coolant temperatures were varied between 20 and 80 °C, to induce condensations effects. For better interpretation of the dynamic exhaust-gas impingement has been waived. Instead, long-term experiments were performed in stationary mode.

3 DEPOSITION STUDIES AT THE EGR COOLER

The non-destructive neutron radiographies of the deposits thicknesses were carried out at the Neutron Source Forschungs-Neutronenquelle Heinz Maier-Leibnitz (FRM II) of TU München. The detailed configuration of the equipment can be obtained from [10]. ❸ (top) shows a diagram of the test arrangement, ③ (bottom) the typical deviation of the neutron beam's attenuation, which was normalised with the intensity of the unopposed beam. A scintillator consisting of Gd_2O_2S and doped with Terbium is encouraged by the weakened beam and emits photons, which are detected by a chargecoupled device.

Light elements like carbon or hydrocarbon have a stronger weakening effect on the neutrons than heavier elements like Aluminium [8, 9]. This is reflected by the materials characteristically distinct grey levels of the two-dimensional sections recorded by the camera. Thus the deposits can be clearly separated from the aluminium tube as they show significantly darker shades of gray. By rotating the sample several planes of the heat exchanger tube could be analysed and due to the uniform appearance of deposits in circumference direction a dependence of gravity could be excluded as influence force of deposition build-up.

As a result of this method, the development of the deposits thickness along the tube could be derived. Alongside the measured wall temperatures which are both time and space-resolved conclusions about the development of thermal conductivity and the topmost temperature of the soot layer were made. Thus, the thermophoretic deposition efficiency could be estimated as well as the surface forces upon the deposited layer. Therefore a force balance model (developed by Phillips [7]) among adhesive and removing forces was used.

Correlations of surface structures with different coolant temperatures were subject for further examinations. For these investigations, a closed-loop coolant circuit was setup that independently controlled the coolant temperature. After each long-term steady-state experiment, an endoscopy analysis showed the different surface structures on the pipes inner walls. There is an increasing embrittlement of the deposits with decreasing coolant

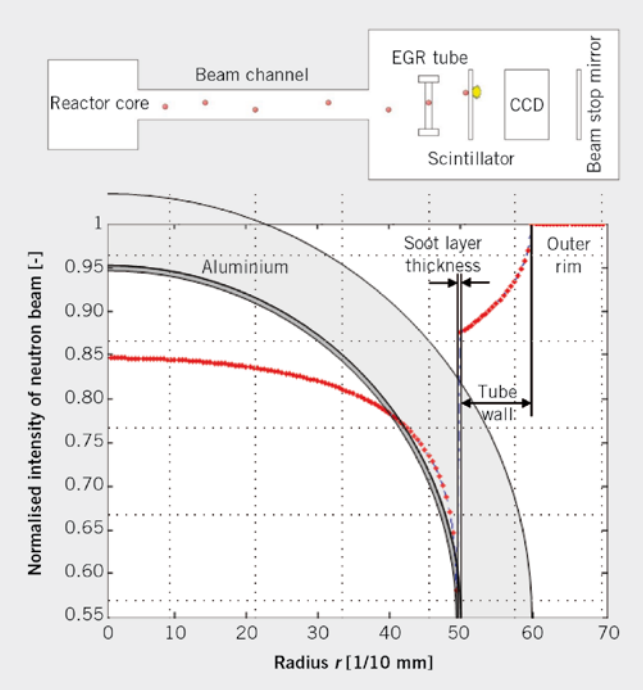

❸ Diagram of experimental setup [10] (top); attenuation of the neutron beam when passing a contaminated pipe (bottom)

temperature. As shown in ❹ flaking or wash out effects can be the results of water condensation which also has a good side effect of cleaning the cooler. Increasing the Reynolds number results in smoother topmost layers followed by higher resistance against sporadic flaking. This is because of the higher wall temperatures due to the enhanced convective heat transmission.

Inducing water condensation for the purpose of cleaning the wall can be evaluated critically, as a closed film of water can not be realised. Wash out effects can only be detected downstream of the cooler's gas side, whereas the entrance area is not affected. With advancing time of cooler operation, the zone of condensation is moved towards the outlet of the gas, which leads to the build-up of a closed soot layer. A continuous cleaning of the completely cooler surface, however, could not be achieved. Cleaning the cooler by inducing water condensation can be assessed as an ineffective way as the development of a uniform film condensation is not feasible.

4 DEPOSIT FORMATION AND MECHANISMS OF POLLUTION

As part of the FVV project No. 1048 calculations were carried out to describe the EGR cooler fouling. These calculations are based on measurements made in project No. 966 which also include the determination of the deposits thickness in response of the tube length and test time, ❺. ❻ shows, that the deposited layer's growth gradient increases at the beginning of the fouling process together with an increase in mass flow (increasing Re numbers in the heat exchanger but same engine operation point) of exhaust gas. This can be explained by the higher through put of condensing components and particles. In combination with high Reynolds numbers which support abrasion, the initial high growth gradient decreases quickly after a short space of time. The behaviour at low Reynolds

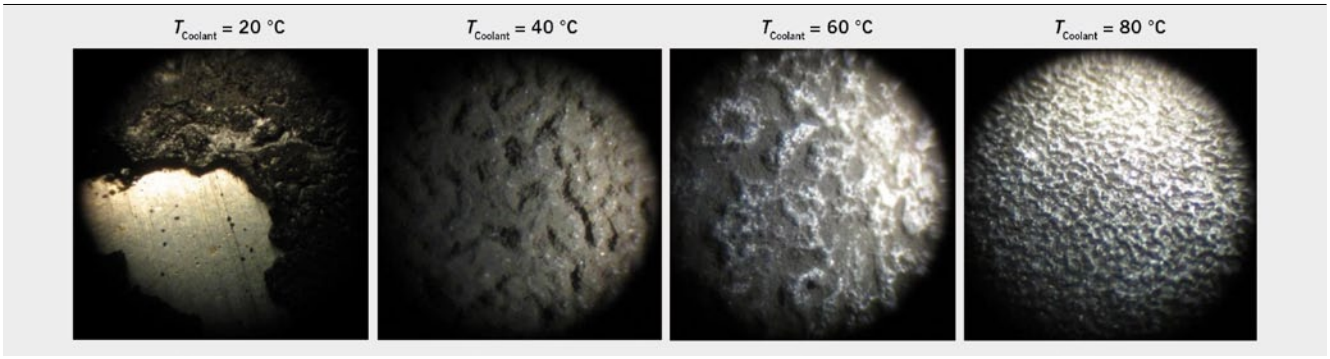

❹ Endoscopy of the cooler deposits at different coolant temperatures but otherwise equal conditions (longitudinal coordinate: x/L = 2/3) [2]

numbers is vice versa. At low Reynolds numbers the deposit growth gradient at the beginning is a lot lower and only decreases gradually over time. In ❼ it becomes apparent that the best heat transfer can be achieved with high Reynolds numbers. The curves shown are based on calculations of the respective deposit growth, taking into account the measured layer thickness after 1, 2, 4 and 8 h. In this connection both the convective heat transfer and the development of the deposit thicknesses of the different operation points were considered. Especially the layer thickness is the governing factor of influence for the heat transfer coefficient. Additionally the compression of the topmost layer at high flow velocity amplifies this tendency as proved in [5].

5 DEVELOPMENT OF THE THERMOPHORETIC DEPOSITION

The thermophoretic deposition efficiency was calculated using several approaches from literature sources. All known approaches are based on the assumption of ideal conditions, such as dry synthetic air. These assumptions are not directly transferable to diesel exhaust gas, especially due to the high amount of water and hydrocarbons with different boiling temperatures. However, the calculation allows an assessment of the thermophoretic deposition efficiency under the influence of thermal and fluid dynamic conditions.

❽ shows the thickness of the deposition over time in hours (with the appropriate base layer, which has been formed until then). ⑧ (left) shows the average layer thickness over five sections of the tube, ⑧ (right) the according calculation of the thermophoretic deposition efficiency as suggested by [6] whereat both the alteration of the surface temperature of the topmost soot layer and the flow velocity were regarded. These calculations are also based on measured layer thicknesses after 1, 2, 4 and 8 h. The increase of the exhaust flow velocity by reason of cross-section reduction was also taken into account. Due to the decrease of the exhaust gases' kinematic viscosity and its internal friction induced by falling temperatures along the tube, the thermophoretic deposition efficiency increases from the inlet of the exhaust gas to the outlet. This at first seems implausible as the observed deposition thickness from the inlet towards the outlet decreases but the efficiency is not the only decisive factor. Furthermore, an additional updraft is effective which was postulated by Phillips [7]. This force is increasing with cooling exhaust gas and seems to be dominant in comparison

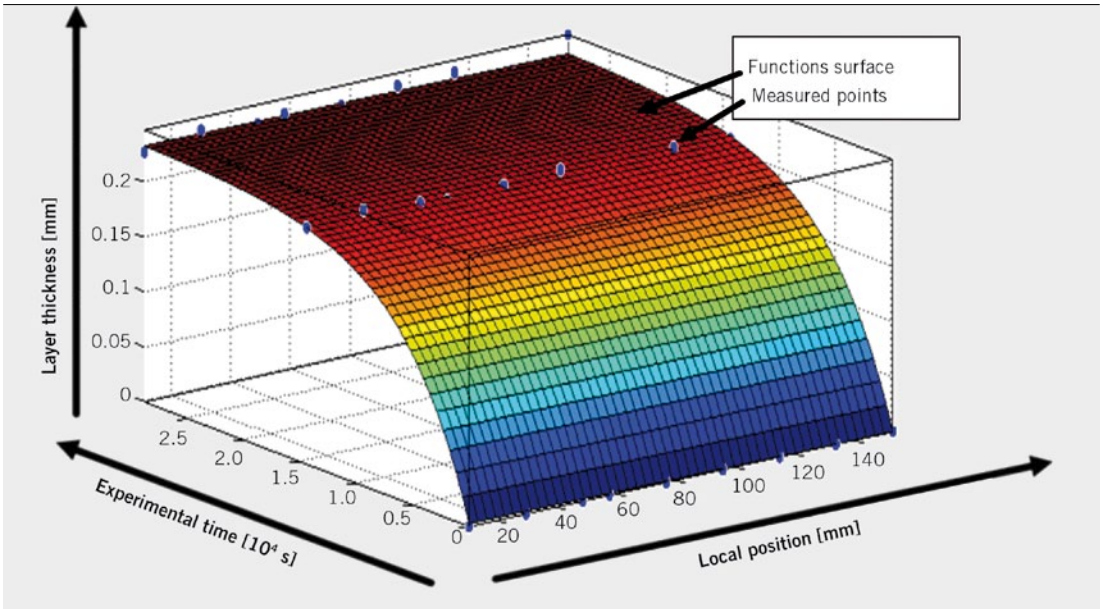

❺ Example of layer thickness in local and temporal dependency [3]

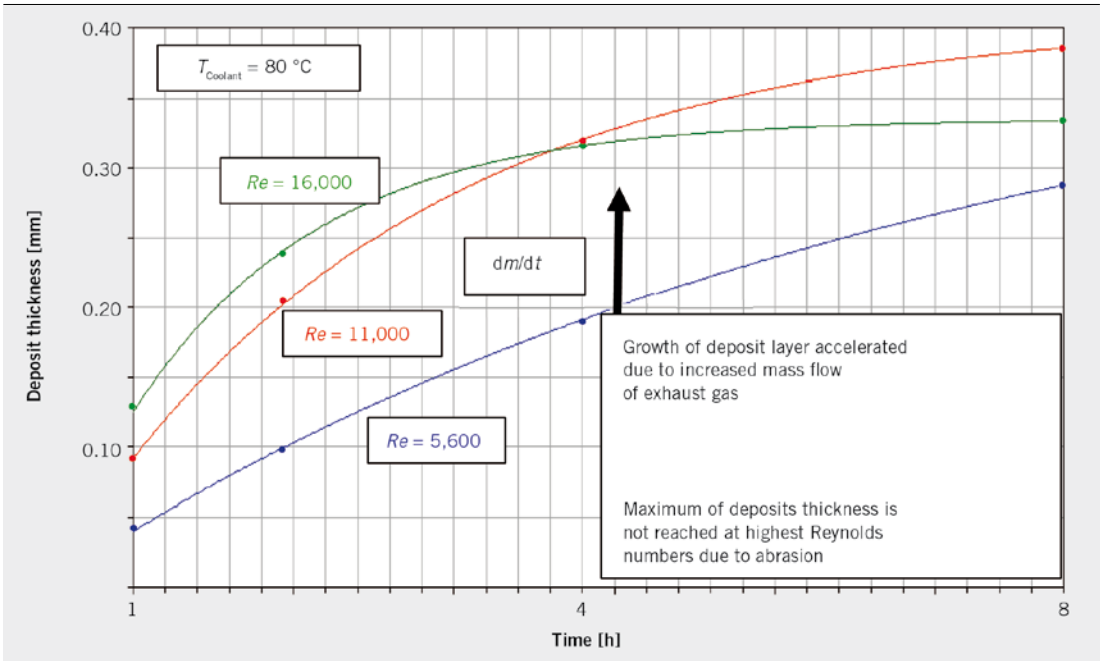

❻ Varying rates of deposit growth at the beginning of the fouling tests are subject to different flow rates

with the thermophoretic deposition whereby a decreasing layer thickness along the tube is the result.

6 FORCE BALANCE MODEL AND STATE OF EQUILIBRIUM

❾ and ❿ exemplify the prediction of the equilibrium state with the aid of Phillips's force balance model [7]. Based on measured values for the deposition thickness the development of the adhesion and updraft is calculated to determine the final thickness. Phillips distinguishes four different forces, which act on particles. The parameters regarded are particle diameter, its distance from the wall and the ratio of particle size to boundary layer thickness. Collectively two adhesive and two flaking forces account for the balance and can act upon a deposited particle under certain conditions. It is of great importance to mention the influence of a particle's net weight

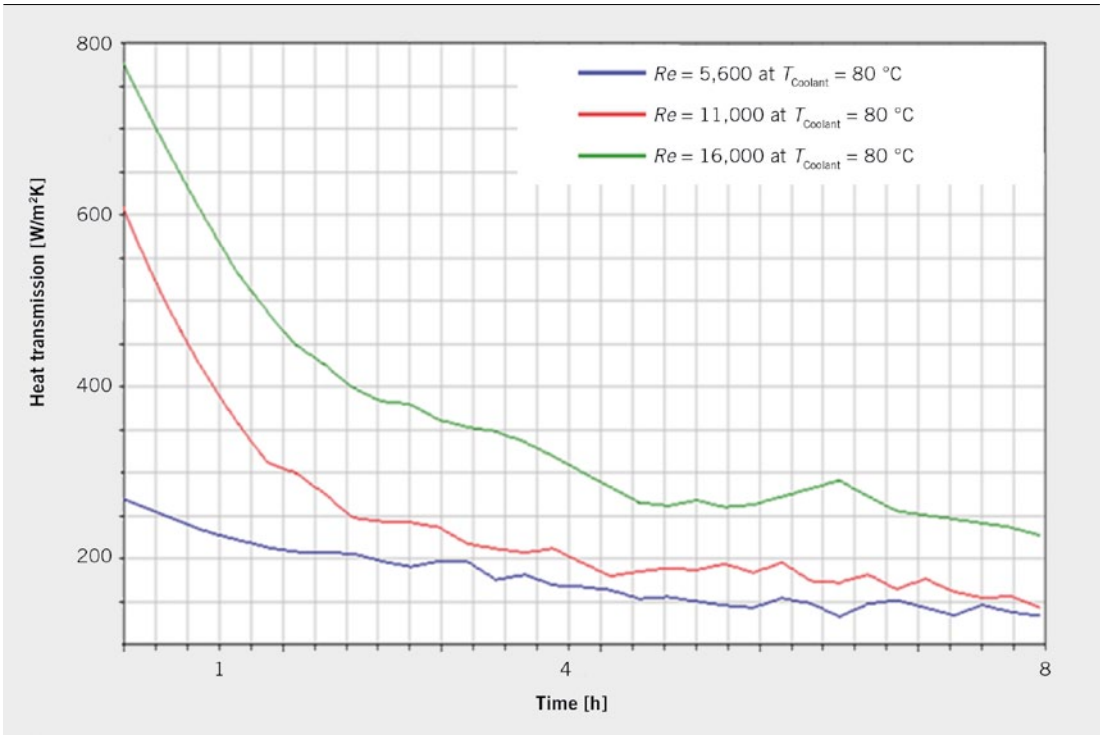

❼ Comparison of the periodic change of the locally averaged heat transfer coefficient at different EGR mass flows

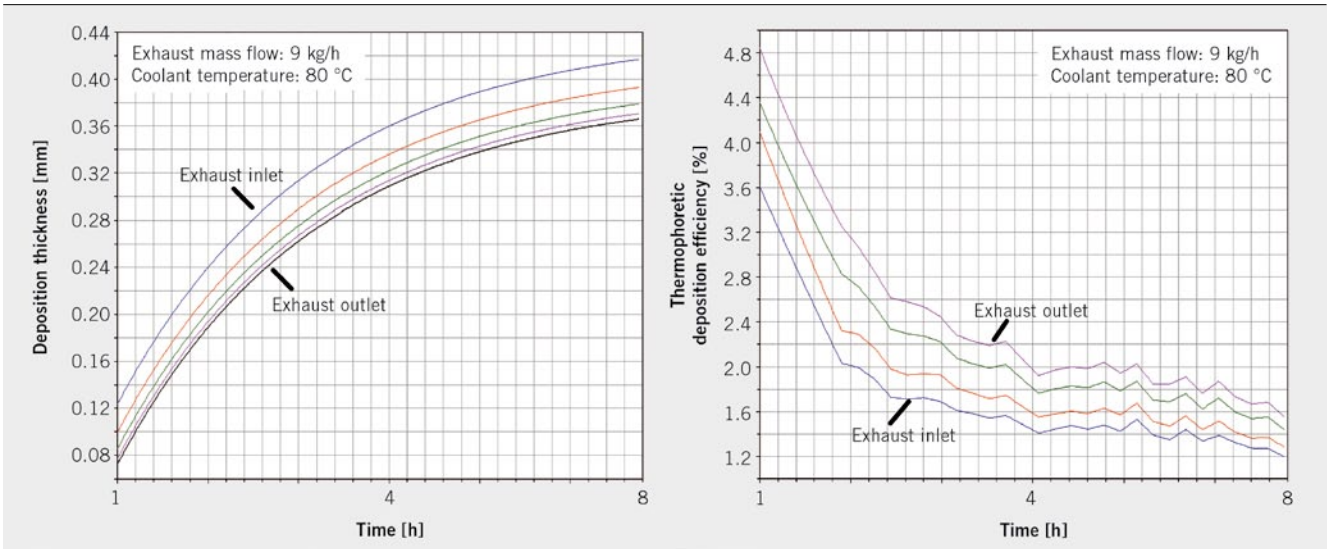

❽ Comparison of layer growth (left) and deposition efficiency (exhaust mass flow: 9 kg/h, exhaust-gas temperature at heat exchanger inlet: 300 °C, coolant temperature: 80 °C)

when they exceed a diameter of 100 µm, otherwise it is negligible. The adhesive force, however, already is an important effect for particles less than 10 µm in diameter. In the FVV project No. 966 theparticle sizes in exhaust gas were classified in the range of 10 nm to 1000 nm using a SMPS. Neutron radiography results proved that net weight in these magnitudes is negligible due to the fact that a homogenous distribution of the deposition thickness in circumferential direction could be observed. Hence, the adhesion is the only relevant holding force for the force balance.

On the other side, the hydrodynamic drag and the updraft under a burst are mentioned as lifting forces in [7]. While the latter is dominant for those particles whose diameter is small enough to be within the flow boundary layer, drag forces become important, when particles protrude the boundary layer, which does not occur within the given particle dimensions. Thus, the constraints for a force balance as postulated in [7] are achieved, when adhesion and updraft are of identical value. Since only air and water were taken into account as carrier medium for the particles, both the calculations of force balance and the thermophoretic deposition were calculated under idealised conditions. However, the magnitudes of the layer thicknesses, which arise from the state of balance and the curves of forces, are within a reasonable context as shown in the figures below, ⑨ and ⑩.

⑨ shows that an increase of the layer thicknesses can be expected for lower coolant temperatures (in this case $T_{Coolant}$ = 60 and 80 °C were compared). At the same time, a higher lifting force is required

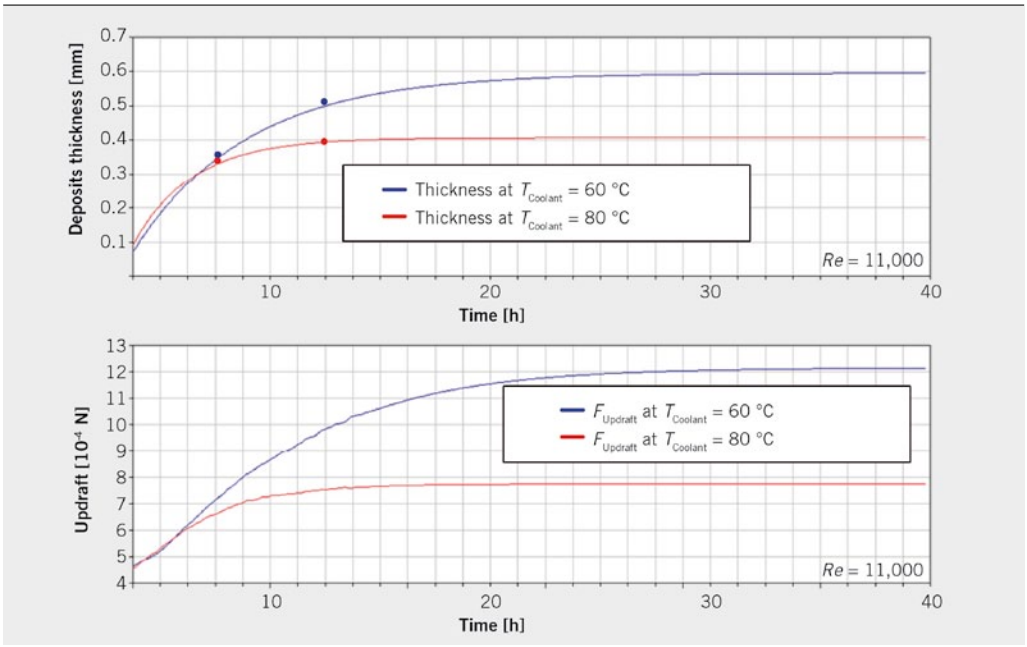

❾ Progress of deposit thickness and lifting force at Re = 11,000 on the gas side of the EGR cooler when operated at different coolant temperatures

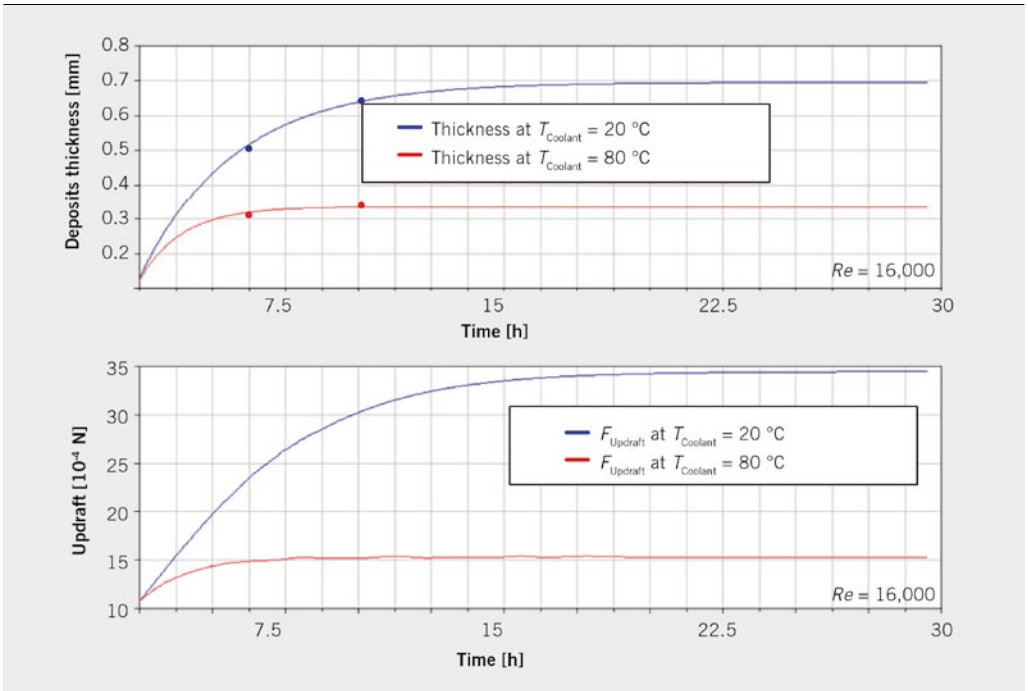

❿ Progress of deposit thickness and lifting force at $Re = 16{,}000$ on the gas side of the EGR cooler when operated at different coolant temperatures

in balanced conditions. Comparing ❾ and ❿ at equal coolant temperatures of $T_{Coolant} = 80$ °C it becomes clear that increasing the flow velocities leads to an increase of lifting forces which results in thinner deposit layers when the state of balance is reached which occurs in less time than with smaller flow velocities.

7 CONCLUSION

Based on the measurements and calculation results of the FVV project No. 966 and 1048 the following recommendations were derived to abate the fouling of EGR coolers.

- Coolant-side optimisation: It has been shown that low coolant temperatures, especially if no washing is induced by condensate, enhances the layer growth significantly. Using high condensation rates to clean the cooler through wash out is no recipe for success as it does not persistently work throughout the heat exchanger. When the EGR cooler is directly coupled with the engine cooling system, exhaust gas should not be passed through before the operating temperature is reached. Especially during the engine warm up phase and when idling the EGR cooler should be bypassed as high hydrocarbon concentrations promote the build-up of an adhesive primary layer.
- Gas-side optimisation: In conventional designs of EGR systems, the heat exchanger is combined with an EGR valve to control the amount of recirculated exhaust. Since the creation of high flow velocities is beneficial to reduce deposit formation a proposed method would be to adjust gas-side Reynolds numbers for all operating states. Due to the high deviation of EGR rates this cannot be realised with the conventional radiator valve combination. However one approach would be to integrate the restrictor directly into the radiator such as using blinds that cover currently redundant flow channels keeping the flow velocity at higher levels, promoting the abrasive effect and thereby reducing fouling.

REFERENCES

[1] Mattes, W.; Mayr, K.; Neuhauser, W.; Steinparzer, F.: BMW-Sechszylinder-Dieselmotor mit Euro-4-Technik. In: MTZ 65 (2004), No. 7/8, pp. 540 – 550

[2] Hörnig, G.; Völk, P.; Nießner, R.; Wachtmeister, G.: Untersuchung der Ablagerungsmechanismen auf der gasseitigen Oberfläche von Abgaswärmeaustauschern und die Entwicklung von Lösungsansätzen zu ihrer Vermeidung und zum Ablösen der Ablagerung. Abschlussbericht, FVV-Vorhaben No. 966

[3] Hörnig, G.; Völk, P.; Nießner, R.; Wachtmeister, G.: Modellbildung zum Verständnis der an der Ablagerungsbildung im AGR-Kühler beteiligten Mechanismen inklusive experimenteller Bestätigung. Abschlussbericht, FVV-Vorhaben No. 1048

[4] VDI-Wärmeatlas: Berechnungsblätter für den Wärmeübergang. VDI-Verlag, 7. erweiterte Auflage, 1994

[5] Weber, O.: Ursachen der Ablagerungsbildung in Abgaswärmeübertragern von Verbrennungsmotoren. Aachen, TechnischeHochschule, Dissertation, 1990

[6] Romay, F.; Takagaki, S.; Pui, D.; Liu, B.: Thermophoretic Deposition of Aerosol Particles in Turbulent Pipe Flow. Journal of Aerosol Science, 29 : 943 – 959, 1998

[7] Phillips, M.: A force balance model for particle entrainment into a fluid stream. Journal of Physics D: Applied Physics, Volume 13, Issue 2, 1980, pp. 221 – 233

[8] Domanus, J.C.: Practical Neutron Radiography; Kluwer Academic Publishers, Dordrecht, The Netherlands, 1992

[9] Harms, A.A.: Mathematics and Physics of Neutron Radiography, D. Reidel Publishing Company, Dordrecht, The Netherlands, 1986

[10] Grünauer, F.: Design, Optimization, and Implementation of the New Neutron Radiography Facility at FRM-II; Dissertation, TU München, 2005

THANKS

This work,as part of the projects No. 966 and 1048, was enabled by the support of the Forschungsvereinigung Verbrennungskraftmaschinen e. V. (FVV). In this context the participating research facilities want to express their deep gratefulness to the FVV, the working group and especially the Chairman Dr.-Ing Frank Kraemer.